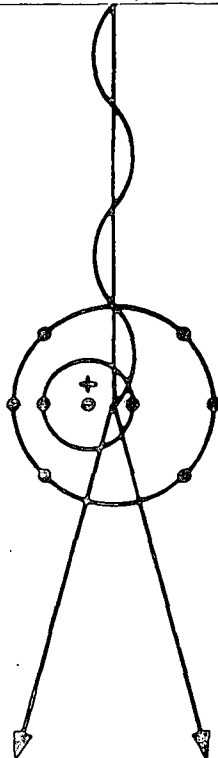


WORKSHOP ON  
**COSMOGENIC NUCLIDES**

(NASA-CR-176886) WORKSHOP ON COSMOGENIC  
NUCLIDES (Lunar and Planetary Inst.) 82 p  
CSCL 03B  
N86-32348  
THRU  
N86-32371  
Unclas  
G3/88 42958



**WORKSHOP ON  
COSMOGENIC NUCLIDES**

**Edited by  
Robert C. Reedy  
and  
Peter Englert**

**Sponsored by  
The Lunar and Planetary Institute  
The Los Alamos National Laboratory**

**A Lunar and Planetary Institute Workshop  
Los Alamos, New Mexico,  
July 26-27, 1984**

**Lunar and Planetary Institute 3303 NASA Road 1 Houston, Texas 77058-4399**

**LPI Technical Report 86-06**

Compiled in 1986 by the  
LUNAR AND PLANETARY INSTITUTE

The Institute is operated by Universities Space Research Association under Contract NASW-4066 with the National Aeronautics and Space Administration.

Material in this document may be copied without restraint for library, abstract service, educational or personal research purposes; however, republication of any portion requires the written permission of the authors as well as appropriate acknowledgment of this publication.

This report may be cited as:

Reedy R. C. and Englert P. (1986) *Workshop on Cosmogenic Nuclides*. LPI Tech. Rpt. 86-06. Lunar and Planetary Institute, Houston. 80 pp.

Papers in this report may be cited as:

Author A. A. (1986) Title of paper. In *Workshop on Cosmogenic Nuclides*. (R. C. Reedy and P. Englert, eds.), pp. xx-yy. LPI Tech Rpt. 86-06. Lunar and Planetary Institute, Houston.

This report is distributed by:

LIBRARY/INFORMATION CENTER  
Lunar and Planetary Institute  
3303 NASA Road 1  
Houston, TX 77058-4399

*Mail order requestors will be invoiced for the cost of postage and handling.*

# Contents

<b>Introduction</b>	<b>1</b>
<b>Program</b>	<b>5</b>
<b>Discussion of Cosmogenic Nuclides</b>	<b>7</b>
<b>Abstracts</b>	<b>23</b>
<i>Nuclide production in (very) small meteorites</i> J. R. Arnold and K. Nishiizumi	25
<i>Simulation experiments for gamma-ray mapping of planetary surfaces: Scattering of high-energy neutrons</i> J. Brückner, P. Englert, R. C. Reedy, and H. Wänke	26
<i>Precompaction irradiation effects: Particles from an early active sun?</i> M. W. Caffee, J. N. Goswami, C. M. Hohenberg, and T. D. Swindle	29
<i>Determination of Ca-41, I-129, and Os-187 in the Rochester tandem accelerator and some applications of these isotopes</i> U. Fehn, D. Elmore, H. E. Gove, P. Kubik, R. Teng, and L. Tubbs	31
<i>Solar modulation of galactic cosmic rays: Contemporary observations and theories</i> M. A. Forman	34
<i>Evolution of gas-rich meteorites: Clues from cosmogenic nuclides</i> J. N. Goswami	36
<i>The exposure history of Jilin and production rates of cosmogenic nuclides</i> G. Heusser	38
<i>Radionuclide measurements by accelerator mass spectrometry at Arizona</i> A. J. T. Jull, D. J. Donahue, and T. H. Zabel	41
<i>Cosmic ray interactions in the ground: Temporal variations in cosmic ray intensities and geophysical studies</i> D. Lal	43
<i>Production rates of neon and xenon by energetic neutrons</i> D. A. Leich, R. J. Borg, and V. B. Lanier	46
<i>Live <sup>129</sup>I-<sup>129</sup>Xe dating</i> K. Marti	49
<i>Production of radionuclides in artificial meteorites irradiated isotropically with 600 MeV protons</i> R. Michel, P. Dragovitsch, P. Englert, and U. Herpers	52
<i>Resonance ionization mass spectrometry for isotopic abundance measurements</i> C. M. Miller	56
<i>Compilation of cosmogenic radionuclides in meteorites</i> K. Nishiizumi	58
<i>Redetermination of parameters for semi-empirical model for spallogenic He and Ne in chondrites</i> L. E. Nyquist and A. F. McDowell	59
<i>Calculations of cosmogenic nuclide production rates in the earth's atmosphere and their inventories</i> K. O'Brien	60

<i><sup>10</sup>Be contents of SNC meteorites</i>	62
D. K. Pal, C. Tuniz, R. K. Moniot, W. Savin, S. Vajda, T. Kruse, and G. F. Herzog	
<i>Studies on cosmogenic nuclides in meteorites with regard to an application as potential depth indicators</i>	64
R. Sarafin, U. Herpers, P. Englert, R. Wieler, P. Signer, G. Bonani, H. J. Hofmann, E. Morenzoni, M. Nessi, M. Suter, and W. Wölfli	
<i>The production rate of cosmogenic <sup>21</sup>Ne in chondrites deduced from <sup>81</sup>Kr measurements</i>	67
L. Schultz and M. Freundel	
<i>A direct time series comparison between the La Jolla and Belfast radiocarbon records</i>	69
C. P. Sonett and H. E. Suess	
<i>Neutron capture production rates of cosmogenic <sup>60</sup>Co, <sup>59</sup>Ni and <sup>36</sup>Cl in stony meteorites</i>	71
M. S. Spergel, R. C. Reedy, O. W. Lazareth, and P. W. Levy	
<i>Simulation of cosmic irradiation conditions in thick target arrangements</i>	74
S. Theis, P. Englert, R. C. Reedy, and J. R. Arnold	
<i>Cosmogenic rare gases and <sup>10</sup>Be in a cross section of Knyahinya</i>	77
R. Wieler, P. Signer, U. Herpers, R. Sarafin, G. Bonani, H. J. Hofmann, E. Morenzoni, M. Nessi, M. Suter, and W. Wölfli	
<b>List of Registered Attendees</b>	<b>78</b>

# Introduction

The Workshop on Cosmogenic Nuclides was held July 26-27, 1984, at the Los Alamos National Laboratory, Los Alamos, New Mexico. It was co-sponsored by the Lunar and Planetary Institute and the Los Alamos National Laboratory. The co-conveners were Dr. Robert C. Reedy of the Los Alamos National Laboratory and Dr. Peter Englert of the Department of Nuclear Chemistry of the University of Cologne (presently at San Jose State University). Studies of the nuclides made by the cosmic rays in terrestrial and extraterrestrial matter have been done for almost 40 years. New ultra-sensitive measurement techniques (such as accelerator mass spectrometry) are revolutionizing the field; additional types of samples (such as Antarctic meteorites or volcanic rocks), improved models (like those for cosmogenic-nuclide production rates or the modulation of galactic cosmic rays), recent laboratory experiments (some simulating cosmic-ray bombardments of meteorites), and new questions (such as the possible martian origins of certain meteorites) has also increased the interest in cosmogenic nuclides. In addition to renewed activities from fields that have traditionally used cosmogenic nuclides (for example, meteoritics and radiocarbon dating), other research areas (such as volcanology and glaciology) are now interested in cosmogenic nuclides. The workshop allowed researchers who represented varied disciplines to discuss a range of topics related to cosmogenic nuclides.

There were 39 participants at the Workshop on Cosmogenic Nuclides, including 16 attendees from five foreign countries. Talks based on the 20 abstracts submitted prior to the meeting were presented along with eight additional papers by other workshop participants. Ten of the 28 presentations were given by foreigners, illustrating the worldwide effort on cosmogenic-nuclide research. Many of the results given at the Workshop were obtained by consortia of researchers from different institutions and included a wide range of cosmogenic products, not just a few isotopes. Comprehensive results from such collaborations are making significant contributions to this research area. Simulation experiments, cross-section measurements, and improved models for calculating production rates are improving our understanding of how nuclides are made by cosmic rays in solar system matter. The use of the new measurement techniques, such as accelerator mass spectrometry, allows the investigation in simulation experiments of the same long-lived radionuclides studied in

natural samples. Cosmogenic nuclides continue to provide information on past variations in cosmic-ray fluxes, including now possible records from the beginning of the solar system. A major emphasis now is more quantitative and accurate results for the exposure histories of meteorites, such as Jilin's complex history and the recent records in space of the shergottites, nakhlites, and chassignites (the SNC meteorites), which possibly came from Mars.

The use of lasers to selectively ionize only one element (resonance ionization) in the source of a regular mass spectrometer was presented as a technique to avoid isobaric interferences. Many of the measurements of long-lived cosmogenic nuclides reported at the workshop were done with a fairly new technique, accelerator mass spectrometry (AMS). The advantage of AMS is that the atoms of a radioactive nuclide are counted rather than the decay products, and very small samples can now be used to determine concentrations of long-lived radionuclides, such as  $^{14}\text{C}$  and  $^{10}\text{Be}$ . With small sample sizes, a number of different analyses can now be made from one main sample.

Calculations with a diffusion model for the modulation of the cosmic rays by solar activity were compared with contemporary observations. Our understanding of solar modulation is improving, but there are many things that are not yet understood. Cosmogenic  $^{14}\text{C}$  in tree rings show wiggles with 200-year periodicities that are real and that represent phenomena that we presently don't understand well.

Calculated production rates of nuclides made in the Earth's atmosphere generally agreed well with measurements. The use of AMS to measure low concentrations of cosmogenic nuclides in terrestrial material was considered as a method to study possible cosmic-ray variations and to date young volcanic rocks. Accelerator bombardments of various targets are being used to simulate and better understand the cosmic-ray irradiation of extraterrestrial objects. The gamma rays emitted from several targets exposed to fast neutrons were reported. Such gamma-ray measurements are being done to plan for future remote-sensing planetary experiments, such as the Mars Observer. One bombardment showed that very large thick targets are needed to contain the whole cascade of secondary particles. Irradiations of stone spheres at an accelerator showed that secondary particles are important even for radii as small as 5 cm. Two sets of calculations were presented that have improved abilities to

predict the production rates of several cosmogenic nuclides in stony meteorites.

Most of the cosmogenic-nuclide results were reported for meteorites. Cosmogenic nuclides in meteoritic grains that had been irradiated prior to compaction into gas-rich meteorites are providing clues on the evolution of these meteorites and on the early sun. Very small meteorites are rare, possibly because it is difficult to use cosmogenic nuclides to identify meteorites that were very small objects in space. Methods to determine a meteorite's size and a sample's depth were presented using suites of data for different meteorites or for many samples of one meteorite. These data show that production rates of cosmogenic nuclides can vary considerably and that spallogenic nuclides are often not very good indicators of a sample's shielding conditions. The use of additional cosmogenic products, such as nuclides made by neutron-capture reactions or tracks made by heavy cosmic-ray nuclei, can help to unfold the exposure histories of meteorites. Measurements of many cosmogenic nuclides from a suite of samples were presented for several meteorites. Such results for Jilin clearly showed its complex cosmic-ray exposure history in space. Exposure ages were reported for several eucrites using  $^{81}\text{Kr}$ -Kr measurements and used to get  $^{38}\text{Ar}$  production rates. The production rates of  $^{21}\text{Ne}$  inferred from the  $^{38}\text{Ar}$  results are low, like other recent results. Complex histories could be more common than believed and could be the cause of the high  $^{21}\text{Ne}$  production rates determined for meteorites with short exposure ages inferred from  $^{26}\text{Al}$  activities. A method was proposed to get exposure ages using 16-million-year  $^{129}\text{I}$  determined by AMS and its decay product  $^{129}\text{Xe}$ .

Two presentations discussed the cosmic-ray exposure histories of the shergottites, nakhlites, and chassignites (the SNC meteorites), which some scientists think came from Mars. The  $^{10}\text{Be}$  contents of the eight SNC meteorites are consistent with the three groups of exposure ages inferred from concentrations of cosmogenic noble-gas isotopes. These meteorites did not have complex exposure histories, and the cosmogenic radionuclides were made in objects similar in size to those for other types of meteorites. Activities of radionuclides in the Antarctic shergottite EETA79001 showed that it had a fairly short terrestrial residence time and that it had to be ejected from a large parent body much later than the other three shergottites. Although not making the ultimate source of the SNC meteorites any clearer, the

cosmogenic radionuclides in the SNC meteorites are being useful in determining their recent histories. A compilation of the cosmogenic radionuclides measured in meteorites is being prepared. One problem with the large number of measurements being made of cosmogenic nuclides or of cross sections for the reactions that make such nuclides is that it is sometimes hard to publish the large number of results and to keep track of all the reported measurements.

# Program

Informal presentations are given in parentheses. An asterisk is present beside each speaker's name.

Thursday, 26 July 1984

8:45 a.m.

## Opening Activities

- R. C. Reedy  
*General comments about the workshop*
- D. C. Hoffman  
*(Division Leader, Isotope and Nuclear Chemistry Division), Welcome*
- J. R. Arnold  
*A review of the history of cosmogenic nuclides*

9:30 a.m.

## New Techniques for Measuring Cosmogenic Nuclides

- D. Rokop\*  
*Measuring a small number of atoms - the pitfall of isobaric impurities*
- C. M. Miller\*  
*Resonance ionization mass spectrometry for isotopic abundance measurements*
- U. Fehn\*, D. Elmore, H. E. Gove, P. Kubik, R. Teng, and L. Tubbs  
*Determination of Ca-41, I-129 and OS-187 in the Rochester tandem accelerator and some applications of these isotopes.*
- A. J. T. Jull\*, D. J. Donahue, and T. H. Zabel  
*Radionuclide measurements by accelerator mass spectrometry at Arizona*

1:00 p.m.

## Solar Modulation

- M. A. Forman (presented by R. Zwickl\*)  
*Solar modulation of galactic cosmic rays: contemporary observations and theories*
- (C. P. Sonett\* and H. E. Suess)  
*A direct time series comparison between the La Jolla and Belfast radiocarbon records*

1:45 p.m.

## Terrestrial Studies

- K. O'Brien\*  
*Calculations of cosmogenic nuclide production rates in the Earth's atmosphere and their inventories*
- D. Lal (presented by J. Goswami\*)  
*Cosmic ray interactions in the ground: temporal variations in cosmic ray intensities and geophysical studies*
- (B. Leavy\*)  
*Dating of young volcanic rocks by in-situ production of  $^{36}\text{Cl}$*

3:00 p.m.

## Simulations and Cross Sections

- J. Brückner\*, P. Englert, R. C. Reedy, and H. Wänke  
*Simulation experiments for gamma-ray mapping of planetary surfaces: Scattering of high-energy neutrons*
- S. Theis, P. Englert\*, R. C. Reedy, and J. R. Arnold  
*Simulation of cosmic irradiation conditions in thick target arrangements*
- R. Michel, P. Dragovitsch, P. Englert, and U. Herpers\*  
*Production of radionuclides in artificial meteorites irradiated isotropically with 600 MeV protons*

D. A. Leich\*, R. J. Borg, and V. B. Lanier  
*Production rates of neon and xenon isotopes by energetic neutrons.*

Friday, 27 July 1984  
 8:30 a.m.

**Production-Rate Calculations for Extraterrestrial Matter**

M. S. Spergel\*, R. C. Reedy, O. W. Lazareth, and P. W. Levy  
*Neutron capture production rates of cosmogenic Co-60, Ni-59 and Cl-36 in stony meteorites*

L. E. Nyquist\* and A. F. McDowell  
*Redetermination of parameters for semi-empirical model for spallogenic He and Ne in chondrites*

9:45 p.m.

**Meteorites**

M. W. Caffee\*, J. N. Goswami, C. M. Hohenberg, and T. D. Swindle  
*Precompaction irradiation effects: Particles from an early active sun?*

J. N. Goswami\*  
*Evolution of gas-rich meteorites: Clues from cosmogenic nuclides*

(R. O. Pepin\*)  
*Early irradiations of lunar breccia 79035*

J. R. Arnold\* and K. Nishiizumi  
*Nuclide production in (very) small meteorites*

R. Sarafin\*, U. Herpers, P. Englert, R. Wieler, P. Signer, G. Bonani, M. Nessi, M. Suter, and W. Wölfli  
*Studies on cosmogenic nuclides in meteorites with regard to an application as potential depth indicators*

1:00 p.m.

**Meteorites (continued)**

R. Wieler\*, P. Signer, U. Herpers, R. Sarafin, G. Bonani, H. J. Hofmann, E. Morenzoni, M. Nessi, M. Suter, and W. Wölfli  
*Spallogenic nuclides in a cross section of Knyahinya*

G. Heusser\*  
*The exposure history of Jilin and production rates of cosmogenic nuclides*

L. Schultz\* and M. Freundel  
*The production rate of cosmogenic  $^{21}\text{Ne}$  in chondrites deduced from  $^{81}\text{Kr}$  measurements*

(K. Marti\*)  
*Live  $^{129}\text{I}$ - $^{129}\text{Xe}$  dating*

D. K. Pal, C. Tuniz, R. K. Moniot, W. Savin, S. Vajda, T. Kruse, and G. F. Herzog\*  
*Be-10 contents of SNC meteorites*

(R. Sarafin\*)  
*Cosmogenic radionuclides in EETA 79001*

K. Nishiizumi\*  
*Compilation of cosmogenic radionuclides in meteorites*

# Discussion of Cosmogenic Nuclides

P. Englert and R. C. Reedy

Cosmogenic nuclides are all products, stable or radioactive, of nuclear reactions induced by the solar or galactic cosmic radiation in matter. They are produced either directly by the primary cosmic-ray particles or by the induced cascade of secondaries. The importance of such a nuclide for a particular field of science depends on its half-life and the target element from which it is produced. For terrestrial applications in the field of glaciology, for example, long-lived radionuclides such as  $^{10}\text{Be}$ ,  $^{14}\text{C}$ ,  $^{26}\text{Al}$ ,  $^{36}\text{Cl}$ , as well as the comparatively short-lived isotope  $^{32}\text{Si}$ , are of importance. Their main target elements are the constituents of the Earth's atmosphere: nitrogen, oxygen, and argon. In meteorites or in the surface of the moon or Earth, other target elements are more abundant and, therefore, other nuclides become more important. Table 1 lists cosmogenic nuclides that are or might be important for extraterrestrial and terrestrial studies, regardless of whether they can be determined easily by any existing methods or not. Mentioning some of the "difficult" nuclides may stimulate improvement of the detection methods.

TABLE 1. Cosmogenic Nuclides Frequently Measured.

Nuclide	Half-life <sup>a</sup> (years)	Main Targets <sup>b</sup>	Particles <sup>c</sup>
$^3\text{H}$	12.3	O, Mg, Si, Fe, (N, O)	GCR, SCR
$^3\text{He}$ , $^4\text{He}$	S	O, Mg, Si, Fe	GCR, SCR
$^7\text{Be}$	53 day	O, Mg, Si, Fe, (N, O)	GCR
$^{10}\text{Be}$	$1.6 \times 10^6$	O, Mg, Si, Fe, (N, O)	GCR
$^{14}\text{C}$	5730	O, Mg, Si, Fe, (N)	GCR, SCR
$^{20}\text{Ne}$ , $^{21}\text{Ne}$ , $^{22}\text{Ne}$	S	Mg, Al, Si, Fe	GCR, SCR
$^{22}\text{Na}$	2.6	Mg, Al, Si, Fe, (Ar)	SCR, GCR
$^{26}\text{Al}$	$7.1 \times 10^5$	Si, Al, Fe, (Ar)	SCR, GCR
$^{32}\text{Si}$	105	(Ar)	GCR
$^{36}\text{Cl}$	$3.0 \times 10^5$	Fe, Ca, K, Cl, (Ar)	GCR
$^{36}\text{Ar}$ , $^{38}\text{Ar}$	S	Fe, Ca, K	GCR
$^{37}\text{Ar}$	35 days	Fe, Ca, K, (Ar)	GCR
$^{39}\text{Ar}$	269	Fe, Ca, K, (Ar)	GCR
$^{40}\text{K}$	$1.3 \times 10^9$	Fe	GCR
$^{39}\text{K}$ , $^{41}\text{K}$	S	Fe	GCR
$^{41}\text{Ca}$	$1.0 \times 10^5$	Ca, Fe	GCR
$^{46}\text{Sc}$	84 days	Fe	GCR
$^{48}\text{V}$	16 days	Fe, Ti	GCR, SCR
$^{53}\text{Mn}$	$3.7 \times 10^6$	Fe	SCR, GCR
$^{54}\text{Mn}$	312 days	Fe	SCR, GCR
$^{55}\text{Fe}$	2.7	Fe	SCR, GCR
$^{56}\text{Co}$	79 days	Fe	SCR
$^{59}\text{Ni}$	$7.6 \times 10^4$	Ni, Fe	GCR, SCR
$^{60}\text{Fe}$	$1.5 \times 10^6$	Ni	GCR
$^{60}\text{Co}$	5.27	Co, Ni	GCR
$^{81}\text{Kr}$	$2.1 \times 10^5$	Rb, Sr, Zr, (Kr)	GCR, SCR
$^{78}\text{Kr}$ , $^{80}\text{Kr}$ , $^{82}\text{Kr}$ , $^{83}\text{Kr}$	S	Rb, Sr, Zr	GCR, SCR
$^{129}\text{I}$	$1.6 \times 10^7$	Te, Ba, La, Ce, (Xe)	GCR
$^{124-132}\text{Xe}$	S	Te, Ba, La, Ce, I	GCR

<sup>a</sup> S denotes that the nuclide is stable.

<sup>b</sup> Elements from which most production occurs; those in parentheses are for the Earth's atmosphere.

<sup>c</sup> Type(s) of cosmic-ray particles producing significant amounts: GCR = galactic cosmic rays, SCR = solar cosmic rays.

## Historical Review

The present status of cosmogenic nuclide research has been documented in a recent review article (Reedy *et al.*, 1983). Some reflections on the early development of cosmogenic nuclide research were made at the beginning of the workshop by Prof. James Arnold. References cited below cover the more historical aspects of the field that are not included in the most recent review (Reedy *et al.*, 1983). Though by no means complete, these references should provide the reader with a good introduction to the history of cosmogenic nuclide research.

The beginnings of the field of cosmogenic nuclide research were at the time of the rapid development of nuclear chemistry and nuclear physics (Batzel *et al.*, 1951). In the late 1940s, W. Libby and co-workers (Libby, 1955) used radiocarbon, the cosmogenic  $^{14}\text{C}$  made in the Earth's atmosphere, for a number of studies. At about the same time, several researchers (such as Bauer, 1947) proposed that the helium observed in iron meteorites was not radiogenic but was made by cosmic rays. The rapid development of cosmogenic nuclide research in meteorites started after Paneth's detection of spallation-produced  $^3\text{He}$  in iron meteorites (Paneth *et al.*, 1952, 1953), followed by the subsequent detection of heavier spallogenic noble-gas isotopes in stony and iron meteorites (Gerling and Levsky, 1956; Gentner and Zaehring, 1955). Extensive work on stable cosmogenic isotopes then followed (Gentner and Zaehring, 1957; Eberhardt and Hess, 1960; Kirsten *et al.*, 1963; Hintenberger *et al.*, 1964), leading to the first attempts to search also for short- and long-lived cosmogenic radioisotopes in meteorites after previous attempts had failed (Chackett *et al.*, 1950). One of the first cosmogenic radionuclides to be determined in meteorites was  $^3\text{H}$  ( $T = 12.3$  a) (Fireman and Schwarzer, 1957; Begemann *et al.*, 1957). Aluminum-26,  $^{10}\text{Be}$ , and  $^{60}\text{Co}$  were observed soon thereafter (Ehmann, 1957; Ehmann and Kohman, 1958a,b). Radioactive and stable cosmogenic nuclides were used for exposure-age determinations (Begemann *et al.*, 1957; Eberhardt and Geiss, 1961). There were intensive studies of freshly fallen iron and stony meteorites, such as Yardymly (then called Aroos) and Bruderheim (Honda *et al.*, 1961a,b; Honda and Arnold, 1961, 1964, 1967).

New techniques to measure cosmogenic nuclides were developed. At Los Alamos (the host for this workshop), non-destructive gamma-ray spectroscopy was used to measure natural and cosmogenic radioactivities in meteorites (Van Dilla *et al.*, 1960). Studies of cosmogenic nuclides in large suites of meteorites became routine. The trends for measured ratios of the cosmogenic noble-gas isotopes were established by workers in Bern (Eberhardt *et al.*, 1966). Exposure ages were determined for many meteorites, usually with pairs of radioactive/stable nuclides. The exposure ages of iron meteorites determined with  $^{40}\text{K}/\text{K}$  disagreed with those determined using shorter-lived radionuclides and implied that the intensities of cosmic rays were lower in the past (Voshage, 1962). Spatial variations of the galactic cosmic rays in the inner solar system were investigated using  $^{37}\text{Ar}/^{39}\text{Ar}$  ratios measured in the metal phases of meteorite falls (Fireman and Goebel, 1970). It was not until about 1975, with the Pioneers 10 and 11 and, later, the Voyager spacecrafts, that direct measurements were made of the spatial variations of the cosmic rays.

In parallel with the rapid growth in cosmogenic nuclide measurements, a number of theoretical models were developed. Simple models, in which the primary cosmic-ray particles were exponentially attenuated and secondary particles produced and removed, were used by several investigators, such as Signer and Nier (1960), who applied such a model to their noble-gas data for the Grant iron meteorite. Other models for the production of cosmogenic nuclides were developed (Arnold *et al.*, 1961). Bombardments of thin and thick targets at accelerators helped to establish production ratios and profiles for cosmogenic nuclides (Honda and Arnold, 1964, 1967). Researchers in the cosmogenic nuclide community discovered and/or characterized a number of long-lived radionuclides, such as  $^{26}\text{Al}$  and  $^{53}\text{Mn}$ .

During the 1960s, additional measurements were made, and the ideas used to interpret the observations were refined. Measurement techniques for the tracks produced in certain minerals by heavy nuclei were developed and applied to meteorites (Fleischer *et al.*, 1967). Some meteorites, those with high concentrations of trapped gases and tracks, were realized to have been exposed to energetic solar particles on the surface of some parent object (Goswami *et al.*, 1984). The orbits of three stony meteorites, Pribram, Lost City, and Innisfree, were accurately determined by several photographic networks, and all had aphelia in the asteroid belt and perihelia near 1 AU. In the early 1970s, investigators were busy studying lunar samples. Some new methods for measuring cosmogenic nuclides were perfected using lunar samples. The lunar sample studies confirmed meteoritic results about the galactic cosmic rays and greatly expanded our knowledge about cosmogenic nuclides produced by the solar cosmic rays (SCR) and about temporal variations of the SCR (Reedy, 1980). In the late 1970s, interest in the studies of meteorites increased, especially for stones. Cosmogenic nuclides were being measured in samples much smaller than previously possible because of the use of improved or new measurement techniques (like accelerator mass spectrometry). New types of samples were also being investigated, such as cosmic spherules and dust. By the mid-1980s, the study of the cosmogenic nuclides was a mature field with gradual but steady advances in all of its aspects.

### Some Recent Trends

The early measurements of radionuclides were usually based on radiochemical separation in combination with low-level counting of the characteristic decay radiation of the respective radionuclides. One of the nuclides,  $^{53}\text{Mn}$ , which was then thought to have a long half-life of 2 million years (Kaye and Cressy, 1965), exhibited unusual nuclear properties, in particular, a very high cross section for thermal neutron capture (Millard, 1965). This reaction changes  $^{53}\text{Mn}$  to  $^{54}\text{Mn}$ , which has a half-life of 312 days and is readily measured. Manganese-53 soon became a favorite radionuclide to be determined because only small samples were required (Herpers *et al.*, 1967, 1969; Imamura *et al.*, 1969; Nishiizumi, 1978; Englert and Herr, 1978). The increase in information on cosmogenic nuclides in meteorites and lunar samples soon led to model considerations on the depth and size dependence of cosmogenic nuclide production in meteorites and planetary surfaces (Signer and Nier, 1960; Arnold *et al.*, 1961; Reedy and Arnold, 1972). With the increasingly well-developed techniques, cosmogenic stable and radioactive isotopes were studied intensively in a joint effort of the entire community of meteorite researchers in the exciting meteorite falls St. Severin\* and Jilin (Ouyang and Xiaoxia, 1979) and, of course, in lunar samples (Fruchter *et al.*, 1978; Shedlovsky *et al.*, 1970). Present trends in cosmogenic nuclide analyses of meteorites were presented in several workshop contributions (Arnold and Nishiizumi, Heusser, Jull *et al.*, Pal *et al.*, Sarafin *et al.*, Schultz and Freundel, Wieler *et al.*), including many results using accelerator mass spectrometry.

Analysis of stable and radioactive isotopes in meteorites soon stimulated experiments to simulate the interaction of galactic cosmic radiation (GCR) with matter (Fireman and Rowland, 1955; Fireman, 1955). The study of close-to-realistic conditions with so-called "thick target arrangements" stood in the foreground. Kohman and Bender (1967) give an extensive review on these efforts through 1967. A more recent paper covers a series of experiments until 1974 (Michel *et al.*, 1974). Tables 2-5 give all of the thick-target simulation experiments with energetic protons performed to date that studied cosmogenic nuclide production. The target set-up and dimensions, their chemical compositions, the proton energies, and the reaction products observed are listed. One reason for this extensive compilation is to demonstrate the advances made in recent experiments simulating  $2\pi$  and  $4\pi$  irradiation conditions in space (Theis *et al.*, 1984; Michel *et al.*, 1984). The first accurate simulation of a  $4\pi$  irradiation of stony meteorites (Michel *et al.*, 1984) and the first results from an irradiation of a spherical object of the preatmospheric size of St. Severin (diameter 50 cm) (Michel *et al.*) were reported at the workshop. The use of the complex

TABLE 2. Early Thick Target Experiments (before 1962).

Matrix	Energy (GeV)	Length (cm)	Width (cm)	Targets	Radioactive Products	References
H <sub>2</sub> O	2.2	22.7	4.4 (Cyl)	H <sub>2</sub> O	H-3, n	T1
NH <sub>3</sub>	2.2	16.4	4.4 (Cyl)	NH <sub>3</sub>	H-3, n	T1
Fe	2.2	4.6	2.5, 10	Fe	H-3	T2
Diverse	0.45	< 1	2	Matrix	H-3	T3
Fe	2.05	2.8	2.5, 5.8	Fe	H-3	T3
Diverse	2.05	<1.4	2.5, 5.8	Matrix	H-3	T3
Fe	0.16	6.3	1.9	Fe	H-3, Ar-37	T4
Fe	1.0	23	2.5, 3.8	Fe	H-3, Ar-37	T4
Fe	3.0	23	2.5, 2.8	Fe	H-3	T4
Fe	6.2	21	(?)	Fe	H-3, Ar-37	T4
Bronze	0.44	ca.18	ca.10	Fe(*)	$\beta^-$	T5
Steel	0.44	ca.23	ca.10	Steel	$\beta^-$	T5
Steel	0.44	ca.13	ca.10	Zn	$\beta^-$ , Cu-64	T5
Al	0.44	ca.40	ca.10	S	$\beta^-$ , P-32	T5
Steel	0.44	ca.22	15	Fe	V-48, Cr-51, Mn-52, Mn-54, Co-56	T6

(\*) Stainless steel.

\*See references concerning St. Severin in: *Meteorite Research*, P. M. Millman, ed., D. Reidel, Dordrecht (1969).

particle spectra around accelerator beam stops to unravel the role that high-energy secondary neutrons play in the production of cosmogenic nuclides was also reported (Theis *et al.*, 1984; also see Englert *et al.*, 1983). For the first time, the longer-lived species, such as  $^{10}\text{Be}$  (Englert *et al.*, 1984) and  $^{26}\text{Al}$ , were also determined in samples from these simulation experiments by means of AMS or other methods (Theis *et al.*, 1984). More long-lived radioisotopes will be available soon. The progress of these experiments should help to understand the role energetic secondary particles, especially neutrons, play in the production of cosmogenic nuclides.

TABLE 3. Irradiations of Thick Targets of Various Composition.

Matrix	Energy (GeV)	Length (cm)	Width (cm)	Targets	Radioactive Products	References
Cu	0.45	26.5	30	Cu	Zn-65 Mn-54	T16 T17
Plexiglass	1.00	25	30	Al	F-18, Na-24	T12, T13, T14
Plexiglass	2.20	25	30	Al	F-18, Na-24	T14
Plexiglass	2.90	25	30	Al	F-18, Na-24	T14

TABLE 4. Irradiations of Thick Metal Targets (Since 1962).

Energy (GeV)	Length (cm)	Width (cm)	Targets	Radioactive Products	References
0.10	10	10	Al	Na-22, Na-24	T7
			Fe	V-48, Cr-51, Mn-52, Mn-54, Co-56	T8
0.45	34	15	Al	Na-22, Na-24	T9
			Fe	Na-24, P-32, Sc-48, V-48, Cr-51, Mn-52, Mn-54	T8
0.50	160	100	Al	Na-24	T10
			Fe	V-48, Mn-52, Mn-54, Mn-56, Co-56	T10
			Cu	Co-58	T10
			Au	Au-198	T10
0.66 Sphere (R=10 cm)			Al	Na-24	T11
			Fe	Al-26, V-48, Sc-44m, Ca-47, Sc-47	T11
1.0	94	30	Al	F-18, Na-24	T12, T13, T14
			Fe	Be-7, Na-24, P-32, Sc-46, V-48, Cr-51, Mn-52, Mn-54, Co-56	T15
			Cu	Zn-65 Mn-54	T16 T17
3.0	92	30	Al	F-18, Na-24	T12, T13, T14
			Fe	Ar-37	T18
			Fe	Na-24, P-32, Sc-44m, V-48, Cr-51, Mn-54, Fe-55	T19
			Ni	Co-56, Co-57, Co-58	T19
			Fe	Be-7, P-32, V-48, Cr-51, Mn-52, Mn-54, Co-56, Co-58	T15
			Fe	C-14, Si-32	T20
			Cu	Zn-65 Mn-54	T16 T17
6.1	80	15	CH <sub>2</sub>	Be-7	T21
			Mg, Al	Na-22, Na-24	T21
			Fe	Be-7, Na-24, P-32, Sc-44m, Sc-47, V-48, Cr-51, Mn-52, Mn-54, Co-56	T21
			Ni	Co-56, Co-57	T21

For a long time, the analysis of long-lived cosmogenic radionuclides in geological media suffered from the low level of induced activities, despite their enormous potential for solving geophysical and geochemical problems, as pointed out in workshop contributions. Though attempts have been made to determine nuclides such as  $^{10}\text{Be}$ ,  $^{14}\text{C}$ ,  $^{26}\text{Al}$ ,  $^{36}\text{Cl}$ ,  $^{53}\text{Mn}$ , and  $^{129}\text{I}$ , which were produced by the cosmic radiation in terrestrial material or transported from production zones in the atmosphere to geological and biological formations,

there were many experimental difficulties in generating a large data base. A selected number of references (not complete), which show results of cosmogenic nuclide determinations in terrestrial surface material, is given (Davis and Schaeffer, 1955; Imamura *et al.*, 1979; Elmore *et al.*, 1979; Litherland and Rucklidge, 1981; Arnold, 1956; Lal *et al.*, 1960; Lal and Peters, 1962; Edwards and Rey, 1968; Bibron *et al.*, 1973; Takagi *et al.*, 1974; Hampel *et al.*, 1975; Kirsten and Hampel, 1975; Reyss *et al.*, 1976; Yokoyama *et al.*, 1977), including a brief historical review of the chemical techniques and methods applied in the mid-fifties (Davis and Schaeffer, 1955). With the exception of  $^{14}\text{C}$  measurements, most other nuclides were difficult to separate from the large amounts of material from which they had to be chemically removed in order to collect a sufficiently large amount of radioactive atoms. In order to increase the specific activity of the separated radionuclides, mass separation of the isotope considered was required (Imamura *et al.*, 1979). The technique of AMS improved the detection limits by orders of magnitude, thus overcoming many of the above mentioned difficulties (Elmore *et al.*, 1979; Litherland and Rucklidge, 1981). Two contributions of the workshop (Fehn *et al.* and Jull *et al.*) dealt with the application of various accelerators for cosmogenic nuclide determinations in extraterrestrial and terrestrial samples.

TABLE 5. Irradiations of Thick Silicate Targets (Since 1962).

Energy (GeV)	Length (cm)	Width (cm)	Targets	Radioactive Products	References
0.10	10	10	C <sub>2</sub> H <sub>2</sub> , CH <sub>2</sub> O	Be-7	T22
			Mg, Al, Glass	Na-22, Na-24	T22
			Si	Na-22	T22
			Fe	V-48, Cr-51, Mn-54, Co-56	T22
			Ag	Ag-105	T22
			Pb	Bi-205	T22
			C <sub>2</sub> H <sub>2</sub> , CH <sub>2</sub> O	Be-7	T23
0.44	30	20	Mg, Glass	Be-7, Na-22, Na-24	T23
			Fe	Na-24, Sc-44m, Sc-46, Sc-47, V-48, Cr-48, Cr-51, Mn-52, Mn-54	T23
			Al	Be-7, Na-22, Na-24	T24-T27
0.60	250	30	Quartz	Be-7, Na-22, Na-24	T24-T27
			Fe	Sc-44m, Sc-46, Sc-47, V-48, Cr-51, Mn-52, Mn-54, Co-56	T24-T27
			Co	Sc-46, V-48, Cr-51, Mn-52, Mn-54, Co-56, Co-57, Co-58	T24-T27
			Ni	Sc-44m, Sc-46, Sc-47, V-48, Cr-51, Mn-52, Mn-54, Co-56, Co-57, Co-58, Co-60, Ni-57	T24-T2
			(*)	Be-7, Sc-44m, Sc-46, Sc-47, V-48, Cr-51, Mn-52, Mn-54, Co-56	T24-T27
			Co	Co-60	T28
			Cu	Cu-64	T28
			W	W-187	T28
			Ir	Ir-192	T28
			Au	Au-198	T28
			Al	F-18, Na-24,	T12, T13, T14
			C <sub>2</sub> H <sub>2</sub> , CH <sub>2</sub> O	Be-7	T29
			Mg, Glass	Be-7, Na-22, Na-24	T29
			Fe	Na-24, Sc-44m, Sc-46, Sc-47, V-48, Cr-51, Mn-52, Mn-54	T29
3.0	87	45	Al	F-18, Na-24	T12, T13
			C <sub>2</sub> H <sub>2</sub> , CH <sub>2</sub> O	Be-7	T29
			Fe	Na-24, Sc-44m, Sc-46, Sc-47, V-48, Cr-48, Cr-51, Mn-52, Mn-54	T29
			Mg, Glass	H-3, Be-7, Na-22, Na-24	T30

\*Artificial lunar regolith (see T24).

References for Tables 2 through 5:

[T1] E. L. Fireman, Tritium production by 2.2-BeV protons on iron and its relation to cosmic radiation, *Phys. Rev.* 97, 1303-1304 (1955).

- [T2] E. L. Fireman and F. S. Rowland, Tritium and neutron production by 2.2-BeV protons on nitrogen and oxygen, *Phys. Rev.* 97, 780-782 (1955).
- [T3] L. A. Currie, W. F. Libby, and R. L. Wolfgang, Tritium production by high energy protons, *Phys. Rev.* 101, 1557-1563 (1956).
- [T4] E. L. Fireman and J. Zaehring, Depth variation of tritium and argon-37 produced by high energy protons in iron, *Phys. Rev.* 107, 1695-1698 (1957).
- [T5] P. S. Goel, in *Nuclear Chemistry Research 1956-1960*, Carnegie Institute of Technology, Pittsburgh, PA, p. 36 (1960).
- [T6] J. P. Shedlovsky, in *Nuclear Chemistry Research 1960-1961*, Carnegie Institute of Technology, Pittsburgh, PA, p. 74 (1961).
- [T7] G. V. S. Rayudu, in *Nuclear Chemistry Research 1962-1963*, Carnegie Institute of Technology, Pittsburgh, PA, p. 15 (1963).
- [T8] G. V. S. Rayudu, in *Nuclear Chemistry Research 1965-1966*, Carnegie Institute of Technology, Pittsburgh, PA, p. 45 (1966).
- [T9] G. V. S. Rayudu, in *Nuclear Chemistry Research 1962-1963*, Carnegie Institute of Technology, Pittsburgh, PA, p. 20 (1963).
- [T10] T. Arakita, H. Hirayama, T. Inagaki, and M. Miyajima, Study of an iron beam stop for 500 MeV protons, *Nucl. Instrum. & Methods*, 164, 255-265 (1979).
- [T11] A. K. Lavrukina, G. K. Ustinova, V. V. Malyshev, and L. M. Satarova, Modeling nuclear reactions in an isotopically irradiated thick target, *Atomnaya Energiya* 34, 23-28 (1973).
- [T12] B. S. P. Shen, Some experiments on the passage of high-energy protons in dense matter, *Proc. Symp. on Protection Against Radiation Hazards in Space*, USAEC Report TID-7652, pp. 852-865 (1962).
- [T13] B. S. P. Shen, Nuclear problems in radiation shielding in space, *Astronaut. Acta* 9, 211-274 (1963).
- [T14] B. S. P. Shen, Some experimental data on the nuclear cascade in thick absorbers, In *Second Symposium on Protection Against Radiations in Space*, NASA Report SP-71, p. 357-362 (1965).
- [T15] J. P. Shedlovsky and G. V. S. Rayudu, Radionuclide productions in thick iron targets bombarded with 1-GeV and 3-GeV protons, *J. Geophys. Res.* 69, 2231-2242 (1964).
- [T16] A. J. M. Van Ginneken, Studies on Internuclear Cascades, Ph.D. Thesis, University of Chicago (1966).
- [T17] A. J. M. Van Ginneken and A. Turkevich, Production of manganese-54 and zinc-65 from copper in thick targets by 0.45 GeV, 1.0 GeV, and 3.0 GeV protons, *J. Geophys. Res.* 75, 5121-5137 (1970).
- [T18] R. Davis, Jr. and R. W. Stoenner, A study of the production of <sup>37</sup>Ar by 3-BeV protons in a thick sample of iron, *J. Geophys. Res.* 67, 3552 (1962).
- [T19] M. Honda, Spallation products distributed in a thick iron target bombarded by 3-BeV protons, *J. Geophys. Res.* 67, 4847-4858 (1962).
- [T20] P. S. Goel and J. P. Shedlovsky, in *Nuclear Chemistry Research 1961-1962*, Carnegie Institute of Technology, Pittsburgh, PA, p. 11 (1962).
- [T21] G. V. S. Rayudu, in *Nuclear Chemistry Research 1963-1964*, Carnegie Institute of Technology, Pittsburgh, PA, p. 7 (1964).
- [T22] G. V. S. Rayudu, in *Nuclear Chemistry Research 1963-1964*, Carnegie Institute of Technology, Pittsburgh, PA, p. 10 (1964).
- [T23] G. V. S. Rayudu, in *Nuclear Chemistry Research 1962-1963*, Carnegie Institute of Technology, Pittsburgh, PA, pp. 30-31 (1963).
- [T24] H. Weigel, R. Michel, U. Herpers, and W. Herr, Simulation of the interaction of cosmic rays with the lunar surface by proton bombardment of a 'thick target'. Part II: Proton induced effects, *Radiochim. Acta* 21, 179-190 (1974).
- [T25] K. Baer and W. Herr, Studies of the thermoluminescence depth profile produced by 600 MeV protons in artificial lunar soil, *Earth Planet. Sci. Lett.* 22., 188-195 (1974).
- [T26] W. A. Kaiser, G. Damm, U. Herpers, W. Herr, H. Kulus, R. Michel, K. P. Roesner, K. Thiel, and H. Weigel, 600 MeV proton bombardment of an artificial lunar soil core: Some implications for the situation on the lunar surface, *Proc. Lunar Sci. Conf. 6th*, pp. 1927-1951 (1975).
- [T27] G. Damm, K. Thiel, and W. Herr, Cosmic-ray-induced fission of the heavier nuclides: Possible Influence on apparent U-238-fission track ages of extraterrestrial samples, *Earth Planet. Sci. Lett.* 40, 439-444 (1978).
- [T28] R. Michel, H. Weigel, H. Kulus, and W. Herr, Simulation of the interaction of cosmic rays with the lunar surface by proton bombardment of a 'thick target.' Part I: Reactions of low energy neutrons, *Radiochim. Acta* 21, 169-178 (1974).
- [T29] G. V. S. Rayudu and J. P. Shedlovsky, in *Nuclear Chemistry Research 1962-1963*, Carnegie Institute of Technology, Pittsburgh, PA, pp. 33-37 (1963).
- [T30] B. M. P. Trivedi and P. S. Goel, Production of Na-22 and H-3 in a thick silicate target and its application to meteorites, *J. Geophys. Res.* 74, 3909-3917 (1969).

## Workshop Presentations

### *Mass Spectrometry and Accelerator Mass Spectrometry and Their Application to Geochemical and Cosmochemical Problems*

Developments in conventional mass spectrometry using thermal and laser resonance ionization sources have considerably improved the measurements of small number of atoms (as discussed by Miller and Rokop at the workshop). Here molecular and isobaric interferences can disturb the correct measurement of isotope ratios considerably. Especially in the case of thermal ionization, isobaric interferences seem to be the limiting factor in improvement of the sensitivity. In the case of the neutron monitors such as  $^{209}\text{Bi}$  and  $^{159}\text{Tb}$  and their multiple (n,xn) products, the importance of careful and elaborate chemical procedures in removing the above-mentioned interferences were demonstrated, so that isotope ratios could be determined routinely with accuracies of  $3 \times 10^{-3}$ . Considerable improvement is expected to be achieved using resonance ionization with lasers (presented by Miller; also see Miller *et al.*, 1982). Applications of isotope determinations of lutetium, thorium, bismuth, uranium, and plutonium were presented by Rokop. The resonance ionization method is applicable to all elements except helium and neon, which do not have suitable transition levels for ionization. The good degree of accuracy obtained with laser resonance ionization is, for example,  $4.4 \times 10^{-7}$  for the  $^{173}\text{Lu}/^{174}\text{Lu}$  isotope ratio as compared with  $3.36 \times 10^{-3}$  for a thermal ion source. This isotope dynamic ratio could be sufficient to determine the solar neutrino capture-produced  $^{98}\text{Tc}$  in molybdenum ores via a two-color-three-photon ionization efficiency sufficient (as discussed by both Miller and Rokop) to measure  $10^7$   $^{98}\text{Tc}$  atoms, the limit presently set by the separation chemistry (Wolfsberg *et al.*, 1985). A considerable improvement of  $^{98}\text{Tc}$  detection is expected by the application of AMS (Kutschera, 1984).

In addition to general description of the capability of AMS to determined rare nuclides and cosmogenic radionuclides, AMS contributions to the workshop concentrated on the applications of these isotopes on specific problems. Though the terrestrial concentrations of  $^{129}\text{I}$  expressed via the  $^{129}\text{I}/^{127}\text{I}$  ratio are as low as  $6 \times 10^{-13}$  in oceans and atmosphere and  $4 \times 10^{-13}$  and  $4 \times 10^{-12}$  in sediments and igneous rocks, respectively, the present limit of detection of  $1 \times 10^{-13}$  of AMS as well as the expected future one of  $1 \times 10^{-14}$  may render  $^{129}\text{I}$  a suitable tracer for hydrothermal convection at locations such as the mid-oceanic ridges (discussed by Fehn *et al.*). Applications of  $^{14}\text{C}$  determinations to archeological, sedimentological, and meteoritical problems as well as results of non-cosmogenic  $^{14}\text{C}$  in uranium ores were presented by Jull *et al.* It is expected that one member of the  $^{235}\text{U}$  decay chain,  $^{223}\text{Ra}$ , also decays to a very small degree by  $^{14}\text{C}$  emission. The measured  $^{14}\text{C}/\text{U}$  ratio in the study presented is  $5.3 \times 10^{-15}$ , which corresponds to a  $^{14}\text{C}/\alpha$  decay branching ratio of  $8.5 \times 10^{-10}$  for  $^{223}\text{Ra}$  (as discussed by Jull *et al.*) Though not a topic of the workshop, but of considerable interest for cosmochemists, was the use of AMS spectrometers for trace elemental analysis (considered by Fehn *et al.*; see also Chew *et al.*, 1984). In addition to the elemental concentrations, one receives information on the isotopical composition of an element in case no stable isobars are present in the sample. The determination of osmium and osmium-isotopes to study the admixture of extraterrestrial material to terrestrial matter such as Suevitflaedi from the Ries crater event were discussed by Fehn *et al.* Even  $10^4$  by mass of extraterrestrial material should be detectable there. Such analyses would be the only way to characterize the extraterrestrial part of very old crater ejecta. This technique could become more sensitive than the determination of cosmogenic nuclides in recent ejecta, which have been used to characterize the lower limit of extraterrestrial components therein (Englert *et al.*, 1984). Additionally, trace element analysis of phosphorous, boron, and chromium in high-purity silicon were discussed by Jull *et al.*

### *The Galactic Cosmic Radiation*

As preparation for discussions of cosmogenic nuclides in extraterrestrial and terrestrial matter, a summary of recent knowledge about the composition, energy spectra, spatial distribution, and modulation of the galactic cosmic radiation was given. Experimental evidence from direct (satellite) and terrestrial observation was compiled and compared with model calculations by Forman. Sonett and Suess demonstrated, by comparing the La Jolla and Belfast  $^{14}\text{C}$  tree ring data, a close global relation of the trends in analyzed  $\Delta^{14}\text{C}$  values. The congruencies of the observed variations of these values with time suggest that the  $\Delta^{14}\text{C}$  record is that of a real interplanetary modulation of the cosmic ray source leading to the nuclide's production in the atmosphere with periodicities of 200, 300, or even 1000 years.

### *Cosmogenic Nuclide Production in the Earth's Atmosphere and Surface*

On the basis of recent knowledge of the GCR modulation, a model of the production of cosmogenic nuclides in the Earth's atmosphere as a function of time and geomagnetic latitude was presented by O'Brien, and the total inventory of such radionuclides in the atmosphere was derived. Such considerations can be improved by comparison to actual measurements of the variation of cosmogenic nuclides in, for example, Greenland ice cores, as is presently being studied by the Bern-Zurich AMS collaboration (Beer *et al.*, 1983a,b; Berner *et al.*, 1980). However, the production of cosmogenic nuclides in terrestrial rocks by the more penetrating part of the cosmic radiation has also been of interest for some time (Kirsten and Hampel, 1975). Some of the work was done on samples exposed at high altitude (Takagi *et al.*, 1974; Hampel *et al.*, 1975; Yokoyama *et al.*, 1977), due to the steep gradient of galactic cosmic radiation in the atmosphere.

D. Lal compiled a number of possible research tasks in geochemistry using terrestrial-surface-produced cosmogenic nuclides. The still unsolved problems of the constancy of the galactic cosmic ray flux over the past million years (Nishiizumi *et al.*, 1980) could be studied by analyzing cosmogenic radionuclides in rocks that were exposed at the surface for a known time; they could either be taken from archeological monuments or well-dated volcanic surface rocks. Because of the strong altitude dependence of cosmogenic nuclide production, uplift velocities could become the subject of serious studies, as could erosion rates of terrestrial formations, assuming no significant temporal variations in the galactic cosmic flux. An ongoing experiment to date young volcanic rocks via both  $^{36}\text{Cl}$  and  $^{10}\text{Be}$  measurements was presented by B. Leavy. The possible contamination source of  $^{36}\text{Cl}$  from weapons tests was discussed. Other experiments with terrestrial rocks are presently in progress at Rutgers University and La Jolla. Cosmogenic nuclide research in terrestrial material has received much emphasis as a result of the improvement of detection methods.

#### *Simulation Experiments*

If primary cosmic radiation strikes an extraterrestrial object of any size, various nuclear interactions will lead to the production of cosmogenic nuclides with a wide range of half lives. The action of the primary as well as the secondary cascade particles is generally understood. However, data interpretation sometimes suffers from the lack of knowledge of many details about these interactions. Ways to fill this gap are through cross-section determinations (discussed by Leich *et al.*; also see Reedy, *et al.*, 1979; Michel and Brinkman, 1980; Michel and Stueck, 1983) or simulation experiments, which simplify the number of conditions considerably—as compared to the extraterrestrial reality—but are close enough to allow direct comparisons.

Both prompt gamma rays and cosmogenic nuclides are produced mainly by secondary neutrons. Several workshop contributions (Brückner *et al.*, Michel *et al.*, and Theis *et al.*) presented the recent progress in experiments that simulated such effects. Phenomena related to cosmogenic nuclide production, the prompt scattering and capture gamma rays from planetary surfaces, are tools for the determination of the chemical surface composition of a planetary or cometary object (Reedy, 1978). In order to study the effect of neutrons of different energies on the production of prompt gamma radiation, single element targets and simple chemical compounds were exposed to neutron fluxes of various spectral shapes and maximum energies (presented at the workshop by Brückner *et al.*; also see Brückner *et al.*, 1984). As expected, the ratio of neutron-capture/neutron-scattering gamma-ray lines measured online changed most drastically going from a thermalized spectrum to one with a neutron maximum energy of approximately 20 MeV, and remained fairly constant up to a maximum energy of 39 MeV. This result gains some significance with a simulation of  $2\pi$  irradiation conditions of an extremely extended target with high-energy protons (Theis *et al.*, 1984). Secondary low-energy neutron fluxes were measured in this case as a function of depth within a massive target with  $1 \times 1 \times 2$  m outer dimensions (note other target dimensions in Tables 2 through 5). In contrast to previous experiments, but in accordance with theory and observation in meteorites and the lunar surface, the maximum of the secondary low-energy neutron fluxes was found to be at 250 to 300 g/cm<sup>2</sup>. From this depth we expect to see a reduced contribution from neutron-capture to the surface gamma ray fluxes (Englert *et al.*, 1983). Calculations show that, if hydrogen were to be added to the thick target, the thermal neutron flux maximum would shift to a considerably shallower depth. This makes the neutron-capture/neutron-scattering ratio of observed gamma ray lines a possible tool to estimate hydrogen concentrations on planetary surfaces, as discussed by Brückner *et al.*

The first attempt to simulate the  $4\pi$  irradiation conditions of stony spherical objects in space was presented by Michel *et al.* (also see Michel *et al.*, 1984). Homogeneous irradiation in a 600-MeV proton beam was achieved. Elemental foils and simple chemicals were exposed in cores through the center of an artificial meteorite made of granodiorite. Neutron-capture as well as spallation-produced reaction products were determined in the exposed targets. The most significant result here is that especially the low-energy spallation products and the neutron-capture products show a significant increase of their production rates from the surface to the center of the meteorite models. This was expected for the large spherical object of 50-cm diameter (St. Severin size) but was also found (surprisingly) for the small 10-cm diameter object. This strongly indicates the development and action of the low-energy secondary particle fluxes even in small meteorites. A  $^{10}\text{Be}$  depth profile from spallation in aluminum was also measured for the small sphere (Englert *et al.*, 1984) and determinations of other long-lived radionuclides are in progress.

In order to better understand the action of high-energy secondary neutrons, elemental targets and simple chemicals were also exposed to particle fields of different spectral shapes at the Los Alamos Meson Physics Facility beam stop (presented by Theis *et al.*). The neutron-to-proton ratio in the experimental area was  $>100$ . In principle, irradiation conditions as they occur deep in planetary surfaces ( $>200 \text{ g/cm}^2$ ) could be simulated (Theis *et al.*, 1984; Englert *et al.*, 1983). There is evidence that production rates of many radionuclides via high-energy neutrons are considerably different than those expected for protons of the same energy (Theis *et al.*, 1984). This, however, has to be supported by cross-section measurements at medium and high neutron energies for key cosmogenic nuclides. Measurements of 14-MeV neutron cross sections leading to the production of stable and radioactive products from targets such as sodium, magnesium, cesium, and barium were reported by Leich *et al.* Though similar measurements are very difficult at higher neutron energies, attempts should be made to determine them.

#### *Pre-irradiation Histories of Extraterrestrial Material*

The scenario that parts of meteorites were exposed to radiation before they were compacted to the final object that reached the Earth was addressed by two contributions (Caffee *et al.* and Goswami). The presence of unusual noble-gas contents in so-called gas-rich meteorites was discussed as a precompaction effect in the very early stage of the solar system, where an active sun might have been the source of a high flux of more energetic charged particles than it is presently (Caffee *et al.*). Model considerations of preirradiation processes of gas-rich grains in an asteroidal regolith were also presented, suggesting the use of long-lived cosmogenic radionuclides to obtain more information about regolith dynamics (Goswami). Similar effects were also reported for nitrogen isotopes and noble gases in a lunar breccia (discussed by Pepin).

#### *Cosmogenic Nuclides in Extraterrestrial Material*

*Calculated production rates.* Three different contributions presented model considerations for the production of cosmogenic nuclides to be expected in meteorites of different sizes (Arnold and Nishiizumi, Nyquist and McDowell, and Spergel *et al.*). Arnold and Nishiizumi considered expected production rates of cosmogenic nuclides in very small meteorites ( $R < 3 \text{ cm}$ ). At such small sizes, secondary particles should not play a significant role, so that only GCR and SCR primary particles effectively produce cosmogenic nuclides. Using  $^{26}\text{Al}$  as a model isotope (whose activity in normal-sized meteorites is 60 dpm/kg) it could be shown by combining reasonable assumptions about meteorite orbits and the SCR flux that the expected activity should be lower than or equal to 60 dpm/kg. As a result, the combined primary SCR and GCR will not cause unusual nuclide production rates in most small meteorites.

Calculated production rates for a wider meteorite size range including St. Severin and Jilin were reported for neutron-capture-produced nuclides by Spergel *et al.* Results were reported for several types of stony meteorites, including ordinary chondrites, hydrogen-rich C-chondrites, and iron-poor aubrites. The neutron-capture calculations demonstrated a significant influence of the chemical composition on the low-energy neutron flux distributions within meteorites and the calculated depth profiles for  $^{60}\text{Co}$ ,  $^{59}\text{Ni}$ , and  $^{36}\text{Cl}$ . Aubrites, with only 1% iron, exhibited the highest production rates for neutron-capture products (normalized to the target nuclide) as an effect of the enhanced neutron down-scattering before the neutron is captured.

For the production of cosmogenic helium and neon in chondrites, a model based on the one developed by Signer and Nier (1960) for iron meteorites was shown by Nyquist and McDowell to reproduce depth-

dependent noble-gas trends (also see Nyquist, 1984). The basic model gave the Bern trend line for  $^3\text{He}/^{21}\text{Ne}$  versus  $^{22}\text{Ne}/^{21}\text{Ne}$  ratios measured in different meteorites (Eberhardt *et al.*, 1966) but couldn't give the different series of lines observed for such data from the St. Severin and Keyes cores. To get a series of lines, Nyquist added a parameter to the model that varied with distance from the sun. This revised version of the model gave a family of curves for the  $^3\text{He}/^{21}\text{Ne}$  versus  $^{22}\text{Ne}/^{21}\text{Ne}$  ratios that were like the measurements for St. Severin and Keyes. However, this parameter varied by about 14%/AU, much greater than the cosmic-ray variations (~3%/AU) observed by satellites during the last decade, as discussed by Forman. Maybe shape-dependent effects are important in the relative production rates of cosmogenic nuclides in meteorites.

**Meteorite data.** A series of contributions were dedicated to the measurement of cosmogenic nuclides in meteorites and their application to cosmochemical problems. Topics such as the depth and size dependence of cosmogenic-nuclide production, complex irradiation histories, the determination of average noble-gas production rates, the use of new isotopes such as  $^{129}\text{I}$  for exposure age determinations, the exposure history of SNC meteorites, and a project to compile the increasing number of cosmogenic nuclide measurements from meteorites were discussed.

Though the depth and size dependent production rates of cosmogenic nuclides have been investigated carefully in the past, the few meteorites for which depth profiles were available (Schultz and Signer, 1976; Englert and Herr, 1980; Tuniz *et al.*, 1984) and the recent advances in AMS invite more detailed depth profile analyses and the search for relationships between the different radionuclides and stable isotopes that could be used to establish depth correction relations (discussed by Heusser and Wieler *et al.*). Recently,  $^{10}\text{Be}$  was determined in addition to  $^{53}\text{Mn}$ ,  $^{26}\text{Al}$ , noble gases, and tracks in a number of meteorite samples. Light noble gases and  $^{10}\text{Be}$  were obtained from a cross section of the Knyahinya meteorite (presented by Sarafin *et al.* and Wieler *et al.*). Whereas for the Knyahinya samples the  $^{10}\text{Be}$  versus  $^{22}\text{Ne}/^{21}\text{Ne}$  trendline (the usual way to establish shielding depth relations) shows a significant anticorrelation comparable to that obtained by Tuniz *et al.* (1984) for St. Severin, individual samples from other meteorites have considerably lower  $^{10}\text{Be}$  concentrations and do not seem to exhibit a noticeable depth or size sensitivity over the same  $^{22}\text{Ne}/^{21}\text{Ne}$  range as in Knyahinya, as discussed by Sarafin *et al.* Similar observations were made earlier for a  $^{26}\text{Al}$  depth profile in Keyes and various individual samples (Cressy, 1975; Herzog and Cressy, 1974).

The complex irradiation history of Jilin, with a first  $2\pi$  exposure stage of ~10 Ma and a second one of 400,000 years as a large sphere was discussed in the light of new data, including also results from the drill cores taken from the main mass of this H-chondrite (discussed at the workshop by Heusser; see also Osadnik *et al.*, 1981; Heusser *et al.*, 1985; Honda *et al.*, 1982). Here the unique opportunity of studying more than eight different short-lived, long-lived, and stable cosmogenic nuclides in aliquots of many individual samples over wide depth ranges will render Jilin a model meteorite for both the  $4\pi$  irradiation of a large sphere and a  $2\pi$  irradiation to considerable depths (Heusser *et al.*, 1985). The lunar surface is usually poor for studies of  $2\pi$  irradiation because of gardening (Arnold, 1975; Langevin *et al.*, 1982) and the limited depths available in lunar cores.

Of the two contributions considering improvements of exposure-age determination methods, one added to the ongoing discussion about the correct noble gas production rates (Schultz and Freundel). Based on depth and size independent  $^{81}\text{Kr}$ -Kr exposure ages determined in a number of achondrites, a  $^{38}\text{Ar}$  production rate of  $0.142 \times 10^8 \text{ cm}^3 \text{ STP/g Ma}$  was obtained. Using the measured  $^{21}\text{Ne}/^{38}\text{Ar}$  ratios and adjusting to L-chondrite chemistry, this results in a  $^{21}\text{Ne}$  production rate of  $0.33 (\pm 0.04) \times 10^8 \text{ cm}^3 \text{ STP/g Ma}$ , in agreement with the production rates recently derived by Nishiizumi *et al.* (1980), Mueller *et al.* (1982), and Englert (1979). The average  $^{21}\text{Ne}$  production rate for typical shielding conditions thus seems to be well established between  $0.30$  and  $0.37 \times 10^8 \text{ cm}^3 \text{ STP/g Ma}$ . This might not yet be sufficiently precise for the unraveling of complex irradiation histories, and one hopes that, in connection with more depth profiles to be analyzed, a more precise estimation will be possible for both typical and unusual shielding conditions.

As a result of the progress in instrumental development, a new exposure age determination method was suggested on the basis of the  $^{129}\text{I}/^{129}\text{Xe}$  pair (discussed by Marti). As Fehn *et al.* found that measurements of 16-Ma  $^{129}\text{I}$  are becoming available with high precision, this suggestion seems to be reasonable as it would result in an exposure age scale that would somewhat fill the gap between  $^{53}\text{Mn}$  (3.7 Ma) and  $^{40}\text{K}$  (1.26 Ga) exposure age scales. However, target elements for iodine in meteorites are rare (see Table

1) and most are probably enriched in sulfidic meteorite inclusions. The presence of  $^{129}\text{Xe}$  from the decay of primordial  $^{129}\text{I}$  interferes with the dating using live  $^{129}\text{I}$ .

SNC meteorites, which are supposed by some to have a martian origin, were analyzed for their cosmogenic radioactive isotopes by Pal *et al.* and Sarafin. Different scenarios were developed on the basis of noble gas measurements and other data that describe the sequence of events that could have brought these meteorites from Mars to Earth. Some scenarios require a complex exposure history (Bogard *et al.*, 1984). However, the radionuclide data obtained suggest a complex irradiation history for none of the SNC candidates analyzed by Pal *et al.* and Sarafin, all the data being consistent with single exposures to cosmic radiation. The activities of 1.6-Ma  $^{10}\text{Be}$  in the eight SNC meteorites were consistent with the three groups of exposure ages determined with noble-gas isotopes (Chassigny and the three nakhlites, ~11 Ma; the Antarctic shergottite EETA 79001, ~1 Ma; and the other three shergottites, ~3 Ma). The radionuclides  $^{26}\text{Al}$ ,  $^{10}\text{Be}$ , and  $^{53}\text{Mn}$  measured in the shergottite EETA 79001 gave an exposure age of ~0.8 Ma and a terrestrial age of ~0.3 Ma. Thus EETA 79001 was ejected from deep inside a parent object much later than the other three shergottites. This later ejection of EETA 79001 presents difficulties for the hypothesis of a martian origin for the SNCs, as either EETA 79001 was ejected from the same region of Mars only ~2 Ma after the other three shergottites, or it was ejected at the same time as the others inside a very large object. Both scenarios seem unlikely. The cosmogenic nuclide data for the SNCs are valuable in helping to unfold the recent histories of these interesting meteorites.

One general problem connected with the development of more and better determination methods is the strong increase in data determined in meteorites. The establishment of a data collection of all measured cosmogenic radionuclides along the guidelines set by Schultz and Kruse (1981) for the light noble gas data compilation is planned (discussed at the workshop by Nishiizumi). In addition, a suggestion was made to characterize the samples in which the radionuclides were determined in greater detail than was done for the noble gases. Other points made in the discussion were the standards used (older results sometimes were based on incorrect standards) and the use of atoms instead of dpm/kg.

The entire session on cosmogenetic nuclides in meteorites demonstrated the importance of continued efforts to solve some of the questions in meteorite research. Improved depth and size dependent production rates may be the result of additional studies similar to those presented at the workshop for Knyahinya and Jilin. These improved cosmogenic-nuclide production rates will provide a sharper tool for historical studies of meteorites and the GCR.

## References

- Arnold J. R. (1956) Beryllium-10 produced by cosmic rays. *Science*, **124**, 584-585.
- Arnold J. R. (1975) Monte Carlo simulations of turnover processes in the lunar regolith. *Proc. Lunar Sci. Conf. 6th*, pp. 2375-2395.
- Arnold J. R., M. Honda, and D. Lal (1961) Record of cosmic-ray intensity in the meteorites. *J. Geophys. Res.*, **66**, 3519-3531.
- Batzel R. E., D. R. Miller, and G. T. Seaborg (1951) The high energy spallation products of copper. *Phys. Rev.*, **84**, 671-683.
- Bauer C. A. (1947) Production of helium in meteorites by cosmic radiation. *Phys. Rev.*, **72**, 354-355.
- Beer J., M. Andree, H. Oeschger, B. Stauffer, R. Balzer, G. Bonani, C. Stoller, M. Suter, W. Wölfli, and R. C. Finkel (1983a) Temporal Be variations in ice. *Radiocarbon*, **25**, 269-278.
- Beer J., U. Siegenthaler, H. Oeschger, M. Andree, G. Bonani, M. Suter, W. Wölfli, R. C. Finkel, and C. C. Langway (1983b) Temporal  $^{10}\text{Be}$  variations. *Proc. 18th Int. Cosmic Ray Conf.*, Paper OG7-2.
- Begemann F., J. Geiss, and D. C. Hess (1957) Radiation age of a meteorite from cosmic-ray-produced He-3 and H-3. *Phys. Rev.*, **107**, 540-542.
- Berner W., H. Oeschger, and B. Stauffer (1980) Information on the  $\text{CO}_2$  cycle from ice core studies. *Radiocarbon*, **22**, 227-235.
- Bibron R., R. Chesselet, G. Crozaz, G. Leger, J. P. Mennessier, and E. Picciotto (1973) Extraterrestrial  $^{53}\text{Mn}$  in Antarctic ice. *Earth Planet. Sci. Lett.*, **21**, 109-116.
- Bogard D. D., L. E. Nyquist, and P. Johnson (1984) Noble gas contents of shergottites and implications for the martian origin of SNC meteorites. *Geochim. Cosmochim. Acta*, **48**, 1723-1739.
- Brückner J., R. C. Reedy, and H. Wänke (1984) Neutron-induced gamma rays from thin targets (abstract). *Lunar and Planetary Science XV*, pp. 613-614.
- Chacket K. F., J. Golden, E. R. Mercer, F. A. Paneth, and P. Reasbeck (1950) The Beddgelert meteorite. *Geochim. Cosmochim. Acta*, **1**, 3-14.
- Chew S. H., T. J. L. Greenway, and K. W. Allan (1984) Accelerator mass spectrometry for heavy isotopes at Oxford (OSIRIS). *Nucl. Instrum. & Methods*, **B5**, 179-184.
- Cressy P. J. (1975)  $^{26}\text{Al}$  in cores of the Keyes chondrite. *J. Geophys. Res.*, **80**, 1551-1554.
- Davis R. and O. A. Schaeffer (1955) Chlorine-36 in nature. *Ann. N.Y. Acad. Sci.*, **62-5**, 107-121.
- Eberhardt P. and J. Geiss (1961) Radioactive and stable isotopes in meteorites. *Proceedings of the Varenna Conference on Nuclear Geology*, pp. 38-80, Varenna, Italy (September).
- Eberhardt P. and D. C. Hess (1960) Helium in stone meteorites. *Astrophys. J.*, **131**, 38-46.
- Eberhardt P., O. Eugster, J. Geiss, and K. Marti (1966) Rare gas measurements in 30 stone meteorites. *Z. Naturforsch.*, **21a**, 414-426.
- Edwards R. R. and P. Rey (1968) Terrestrial occurrence and distribution of iodine-129. *US AEC Report NYO 3624-3*.
- Ehmann W. D. (1957) *Cosmic-ray-induced Radioisotopes in Meteorites and Tektites*. Doctoral Dissertation, Carnegie Institute of Technology, Pittsburgh, PA.
- Ehmann W. D. and T. P. Kohman (1958a) Cosmic-ray-induced radioactivities in meteorites—I. Chemical and radiometric procedures for aluminum, beryllium, and cobalt. *Geochim. Cosmochim. Acta*, **14**, 340-363.
- Ehmann W. D. and T. P. Kohman (1958b) Cosmic-ray-induced radioactivities in meteorites—II.  $^{26}\text{Al}$ ,  $^{10}\text{Be}$ ,  $^{60}\text{Co}$  in aerolites, siderites, and tektites. *Geochim. Cosmochim. Acta*, **14**, 364-379.
- Elmore D., B. R. Fulton, M. R. Clover, J. R. Marsden, H. E. Gove, H. Naylor, K. H. Purser, L. R. Kilius, R. P. Beukens, and A. E. Litherland (1979) Analysis of  $^{36}\text{Cl}$  in environmental water samples using an electrostatic accelerator. *Nature*, **277**, 22-25.
- Englert P. (1979) Determination of Exposure and So-called Terrestrial Ages of Stone Meteorites on the Basis of the Cosmogenic Radionuclides Mn-53 and Al-26. Dissertation, University of Köln, West Germany.
- Englert P. and W. Herr (1978) A study of exposure ages of chondrites based on spallogenic  $^{53}\text{Mn}$ . *Geochim. Cosmochim. Acta*, **42**, 1635-1642.
- Englert P. and W. Herr (1980) On the depth dependent production of long-lived spallogenic  $^{53}\text{Mn}$  in the St. Severin chondrite. *Earth Planet. Sci. Lett.*, **47**, 361-369.
- Englert P., D. K. Pal, C. Tuniz, R. K. Moniot, W. Savin, T. H. Kruse, and G. F. Herzog (1984) Manganese-53 and beryllium-10 contents in tektites (abstract). *Lunar and Planetary Science XV*, 250-251.
- Englert P., S. Theis, R. C. Reedy, and J. R. Arnold (1983) On the production of cosmogenic nuclides with high energy secondary particles: Simulation experiments with beam stop neutrons (abstract). *Lunar and Planetary Science XIV*, pp. 175-176.

- Englert P., S. Theis, R. Michel, C. Tuniz, R. K. Moniot, S. Vajda, T. H. Kruse, D. K. Pal, and G. F. Herzog (1984) Production of  $^7\text{Be}$ ,  $^{22}\text{Na}$ ,  $^{24}\text{Na}$ , and  $^{10}\text{Be}$  from Al in a  $4\pi$ -irradiated meteorite model. *Nucl. Instrum. & Methods*, B5, 415-419.
- Fireman E. L. (1955) Tritium production by 2.2-BeV protons on iron and its relation to cosmic radiation. *Phys. Rev.*, 97, 1303-1304.
- Fireman E. L. and R. Goebel (1970) Argon 37 and argon 39 in recently fallen meteorites and cosmic-ray variations. *J. Geophys. Res.*, 75, 2115-2124.
- Fireman E. L. and F. S. Rowland (1955) Tritium and neutron production by 2.2-BeV protons on nitrogen and oxygen. *Phys. Rev.*, 97, 780-782.
- Fireman E. L. and D. Schwarzer (1957) Measurement of Li-6, He-3, and H-3 in meteorites and its relation to cosmic radiation. *Geochim. Cosmochim. Acta*, 11, 252-262.
- Fleischer R. L., P. B. Price, R. M. Walker, and M. Maurette (1967) Origins of fossil charged-particle tracks in meteorites. *J. Geophys. Res.*, 72, 331-353.
- Fruchter G. S., L. A. Rancitelli, J. C. Evans, and R. W. Perkins (1978) Lunar surface processes and cosmic ray histories over the past several million years. *Proc. Lunar Planet. Sci. Conf. 9th*, pp. 2019-2032.
- Gentner W. and J. Zähringer (1955) Argon- und Heliumbestimmungen in Eisenmeteoriten. *Z. Naturforsch.*, 10A, 498-499.
- Gentner W. and J. Zähringer (1957) Argon und Helium als Kernreaktionsprodukte in Meteoriten. *Geochim. Cosmochim. Acta*, 11, 60-71.
- Gerling E. K. and L. K. Levsky (1956) On the origin of rare gases in stony meteorites. *Doklady Akad. Nauk. SSSR*, 110, 750-753.
- Goswami J. N., D. Lal, and L. Wilkening (1984) Gas-rich meteorites: Probes for particle environment and dynamical processes in the inner solar system. *Space Sci. Rev.*, 37, 111-159.
- Hampel W., J. Takagi, K. Sakamoto, and S. Tanaka (1975) Measurement of muon-induced Al-26 in terrestrial silicate rock. *J. Geophys. Res.*, 80, 3757-3760.
- Herpers U., W. Herr, and R. Wölfle (1967) Determination of cosmic-ray produced nuclides  $^{53}\text{Mn}$ ,  $^{45}\text{Sc}$ , and  $^{26}\text{Al}$  in meteorites by neutron activation and gamma coincidence spectroscopy. In *Radioactive Dating and Methods of Low Level Counting*, IAEA, Vienna, pp. 199-205.
- Herpers U., W. Herr, and R. Wölfle (1969) Evaluation of  $^{53}\text{Mn}$  by (n, $\gamma$ ) activation,  $^{26}\text{Al}$  and special trace elements in meteorites by  $\gamma$ -coincidence techniques. In *Meteorite Research* (P. M. Millman, ed.) D. Reidel, Dordrecht, pp. 387-396.
- Herzog G. F. and P. J. Cressy (1974) Variability of the  $^{26}\text{Al}$  production rate in ordinary chondrites. *Geochim. Cosmochim. Acta*, 38, 1827-1841.
- Heusser G., Z. Ouyang, T. Kirsten, U. Herpers, and P. Englert (1985) Conditions of cosmic ray exposure of the Jilin chondrite. *Earth Planet. Sci. Lett.*, 72, 263-272.
- Hintenberger H., H. König, L. Schultz, and H. Wänke (1964) Radiogene, Spallogene und Primordiale Edelgase in Steinmeteoriten. *Z. Naturforsch.*, 19a, 327-341.
- Honda M. and J. R. Arnold (1961) Radioactive species produced by cosmic rays in the Aroos iron meteorite. *Geochim. Cosmochim. Acta*, 23, 219-232.
- Honda M. and J. R. Arnold (1964) Effects of cosmic rays on meteorites. *Science*, 143, 203-212.
- Honda M. and J. R. Arnold (1967) Effects of cosmic rays on meteorites. In *Handbuch der Physik*, XLVI/2, Springer Verlag, pp. 613-632.
- Honda M., J. P. Shedlovsky, and J. R. Arnold (1961a) Radioactive species produced by cosmic rays in iron meteorites. *Geochim. Cosmochim. Acta*, 22, 133-154.
- Honda M., K. Nishiizumi, M. Imamura, M. Takaoka, O. Nitoh, K. Horie, and K. Komura (1982) Cosmogenic nuclides in the Jilin chondrite. *Earth Planet. Sci. Lett.*, 57, 101-109.
- Honda M., S. Umemoto, and J. R. Arnold (1961b) Radioactive species produced by cosmic rays in Bruderheim and other meteorites. *J. Geophys. Res.*, 66, 3541-3546.
- Imamura M., H. Matsuda, K. Horie, and M. Honda (1969) Applications of neutron activation method for  $^{53}\text{Mn}$  in meteoritic iron. *Earth Planet. Sci. Lett.*, 6, 165-172.
- Imamura M., T. Inoue, K. Nishiizumi, and S. Tanaka (1979)  $^{53}\text{Mn}$  in deep-sea sediment cores—An indicator of past solar activity. *Proc. 16th Int. Cosmic Ray Conf.*, Vol. 2, pp. 304-307.
- Kaye J. H. and P. J. Cressy (1965) Half-life of Manganese-53 from meteorite observations. *J. Inorg. Nucl. Chem.*, 27, 1889-1892.
- Kirsten T. and W. Hampel (1975) Weak radioactivities induced by cosmic ray muons in terrestrial minerals. *Proc. Int. Conf. on Radioactivity Measurements and Applications*, High Tatras, CSSR, pp. 428-435.
- Kirsten T., D. Krankowsky, and J. Zähringer (1963) Edelgas- und Kalium-Bestimmungen an Einer Groesseren Zahl von Steinmeteoriten. *Geochim. Cosmochim. Acta*, 27, 13-42.

- Kohman T. P. and M. L. Bender (1967) Nuclide production by cosmic rays in meteorites and on the Moon. In *High Energy Nuclear Reactions in Astrophysics* (B. S. P. Shen, ed.), W. A. Benjamin, New York, pp. 169-245.
- Kutschera W. (1984) Rare particles. *Nucl. Instrum. & Methods*, B5, 420-425.
- Lal D. and B. Peters (1962) Cosmic ray produced isotopes and their application to problems in geophysics. In *Progress in Elementary Particle and Cosmic Ray Physics* (J. G. Wilson and S. A. Wonthysen, eds.) John Wiley, New York, pp. 1-74.
- Lal D., J. R. Arnold, and M. Honda (1960) Cosmic-ray production rate of Be-7 in oxygen, P-32, P-33, S-35 in argon at mountain altitude. *Phys. Rev.*, 118, 1626-1632.
- Langevin Y., J. R. Arnold, and K. Nishiizumi (1982) Transport processes on the lunar surface: Comparison of model calculations with radionuclide data. *J. Geophys. Res.*, 87, 6681-6691.
- Libby W. F. (1955) *Radiocarbon Dating*, 2nd edition, Univ. of Chicago Press.
- Litherland A. E. and J. C. Rucklidge (1981) Radioisotope detection and dating with accelerators. *EOS*, 62, 105-106.
- Michel R. and G. Brinkmann (1980) On the depth-dependent production of radionuclides ( $44 \leq A \leq 59$ ) by solar protons in extraterrestrial matter. *J. Radioanal. Chem.*, 59, 467-510.
- Michel R. and R. Stück (1983) On the production of cosmogenic nuclides in meteorites by primary galactic particles: Cross sections and model calculations. *Proc. Lunar Planet. Sci. Conf. 14th*, in *J. Geophys. Res.*, 89, B673-B684.
- Michel R., H. Weigel, K. Kulus, and W. Herr (1974) Simulation of the interaction of cosmic rays with the lunar surface by proton bombardment of a 'Thick Target.' Part I: Reactions of low energy neutrons. *Radiochim. Acta*, 21, 169-178.
- Michel R., P. Dragovitsch, R. Stück, D. Filges, and P. Kloth (1984) 600 MeV irradiation experiment to simulate the  $4\pi$  bombardment of meteorites by galactic cosmic protons (abstract). *Lunar and Planetary Science XV*, pp. 542-543.
- Millard H. T. Jr., (1965) Thermal neutron activation: Measurement of cross section for Manganese-53. *Science*, 147, 503-504.
- Miller C. M., N. S. Nogar, A. J. Gancarz, and W. R. Shields, Selective laser photoionization for mass spectrometry. *Anal. Chem.*, 54, 2377-2378.
- Müller O. W. Hampel, T. Kirsten, and G. F. Herzog (1982) Cosmic-ray consistency and cosmogenic production rates in short-lived chondrites. *Geochim. Cosmochim. Acta*, 45, 447-460.
- Nishiizumi K. (1978) Cosmic-ray produced  $^{53}\text{Mn}$  in 31 meteorites. *Earth Planet. Sci. Lett.*, 41, 91-100.
- Nishiizumi K., S. Regnier, and K. Marti (1980) Cosmic ray exposure ages of chondrites, preirradiation and constancy of the cosmic ray flux in the past. *Earth Planet. Sci. Lett.*, 50, 156-170.
- Nyquist L. E. (1984) Semi-empirical model for spallogenic He and Ne in chondrites: Implications for irradiation history of SNCs (abstract). In *Lunar and Planetary Science XV*, pp. 613-614.
- Osadnik G., U. Herpers, W. Herr, and P. Englert (1981) Spallogenic  $^{53}\text{Mn}$  in the Jilin chondrite. *Meteoritics*, 16, 371-372.
- Ouyang Z. and Zhou Xiaoxia (1979) A study of cosmogenic radionuclides in meteorites fallen recently in China. *Proc. 16th Int. Cosmic Ray Conf.*, pp. 315-318.
- Paneth F. A., P. Reasbeck, and K. I. Mayne (1952) Helium 3 content and age of meteorites. *Geochim. Cosmochim. Acta*, 2, 300-303.
- Paneth F. A., P. Reasbeck, and K. I. Mayne (1953) Production by cosmic rays of helium-3 in meteorites, *Nature*, 172, 200-201.
- Reedy R. C. (1978) Planetary gamma-ray spectrometry. *Proc. Lunar Planet. Sci. Conf. 9th*, 2961-2984.
- Reedy R. C. (1980) Lunar radionuclide records of average solar-cosmic-ray fluxes over the last ten million years. *Proc. Conf. Ancient Sun*, pp. 365-386.
- Reedy R. C. and J. R. Arnold (1972) Interaction of solar and galactic cosmic-ray particles with the Moon. *J. Geophys. Res.*, 77, 537-555.
- Reedy R. C., G. F. Herzog, and E. K. Jessberger (1979) The reaction  $\text{Mg}(n,\alpha)\text{Ne}$  at 14.1 and 14.7 MeV: Cross sections and implications for meteorites. *Earth Planet. Sci. Lett.*, 44, 341-348.
- Reedy R. C., J. R. Arnold, and D. Lal (1983) Cosmic-ray record in solar system matter. *Annu. Rev. Nucl. Part. Sci.*, 33, 505-537.
- Reyss J. L., Y. Yokoyama, and S. Tanaka (1976) Aluminum-26 in deep-sea sediment. *Science*, 193, 1119-1121.
- Schultz L. and H. Kruse (1981) Light noble gases in stony meteorites—A compilation. *Nuclear Track Detection*, 2, 65-103.
- Schultz L. and P. Signer (1976) Depth dependence of spallogenic helium, neon, and argon in the St. Severin chondrite. *Earth Planet. Sci. Lett.*, 30, 191-199.

- Shedlovsky J. P., M. Honda, R. C. Reedy, J. C. Evans, D. Lal, R. M. Lindstrom, A. C. Delany, J. R. Arnold, H. H. Loosli, J. S. Fruchter, and R. C. Finkel (1970) Pattern of bombardment-produced radionuclides in Rock 10017 and in lunar soil. *Proc. Apollo 11 Lunar Sci. Conf.*, pp. 1503-1532.
- Signer P. and A. O. Nier (1960) The distribution of cosmic-ray-produced rare gases in iron meteorites. *J. Geophys. Res.*, 65, 2947-2964.
- Takagi J., W. Hampel, and T. Kirsten (1974) Cosmic-ray muon-induced I-129 in tellurium ores. *Earth Planet. Sci. Lett.* 24, 141-150.
- Theis S., P. Englert, R. Michel, R. C. Reedy, and J. R. Arnold (1984) Simulation of the interaction of the galactic cosmic radiation with matter: Long lived cosmogenic nuclides produced in different irradiation experiments (abstract). *Lunar Planet. Sci. XV*, 854-855.
- Tuniz C., C. M. Smith, R. K. Moniot, T. H. Kruse, W. Savin, D. K. Pal, G. F. Herzog, and R. C. Reedy (1984) Beryllium-10 contents of core samples from the St. Severin chondrite. *Geochim. Cosmochim. Acta*, 48, 1867-1872.
- Van Dilla M. A., J. R. Arnold, and E. C. Anderson (1960) Spectrometric measurement of natural and cosmic-ray induced radioactivity in meteorites. *Geochim. Cosmochim. Acta*, 20, 115-121.
- Voshage H. (1962) Eisenmeteorite als Raumsonden fuer die Untersuchung des Intensitaetsverlaufes der Kosmischen Strahlung waehrend der Letzten Milliarden Jahre. *Z. Naturforsch.*, 17a, 422-432.
- Wolfsberg K., G. A. Cowan, E. A. Bryant, K. S. Daniels, S. W. Downey, Haxton W. C., V. G. Niesen, N. S. Nogar, C. M. Miller, and D. J. Rokop (1985) The molybdenum solar neutrino experiment. In *Solar Neutrinos and Neutrino Astronomy (Homestack, 1984)*, AIP Conf. Proc. No. 120, pp. 196-202.
- Yokoyama Y., J. L. Reyss, and F. Guichard (1977) Production of radionuclides by cosmic rays at mountain altitudes. *Earth Planet. Sci. Lett.*, 36, 44-50.

# ABSTRACTS

PRECEDING PAGE BLANK NOT FILMED

NUCLIDE PRODUCTION IN (VERY) SMALL METEORITES; James R. Arnold and Kunihiro Nishiizumi, Dept. of Chemistry, Univ. of Calif., San Diego, La Jolla, CA 92093.

One of the most interesting open questions in the study of cosmic-ray effects in meteorites is the expected behavior of objects which are very small compared to the mean interaction length of primary GCR particles. A reasonable limit might be a pre-atmospheric radius of  $5 \text{ gram/cm}^2$ , or 1.5 cm for chondrites. These are interesting for at least three reasons: (1) this is a limiting case for larger objects, and can help us make better models, (2) this size is intermediate between usual meteorites and irradiated grams (spherules), and (3) these are the most likely objects to show SCR effects. We are now engaged in a search for suitable objects for experimental study.

Reedy (1984) has recently proposed a model for production by GCR of radioactive and stable nuclides in spherical meteorites. We expect the very small objects to deviate from this model in the direction of fewer secondary particles (larger spectral shape parameter  $\alpha$ ), at all depths. The net effect will be significantly lower production of such low-energy products as  $^{53}\text{Mn}$  and  $^{26}\text{Al}$ . The SCR production of these and other nuclides will be lower, too, because meteorite orbits extend typically out into the asteroid belt, and the mean SCR flux must fall off approximately as  $r^{-2}$  with distance from the sun. Kepler's laws insure that for such orbits most of the exposure time is spent near aphelion.

None the less the "equivalent mean exposure distance"  $R_{\text{exp}}$ , is slightly less than the semimajor axis  $A$ , in fact  $A(1 - e^2)^{1/4}$ , because of the weighting by  $R^{-2}$ . For the three meteorite orbits we have,  $R_{\text{exp}}$  has a narrow range, from about 1.6 to 2.1 a.u. This is probably true for the great majority of meteorites. If we take 1.8 a.u. as representative, the SCR flux is lowered by a factor of 3.24.

For a very small meteorite, we can estimate that  $^{26}\text{Al}$  produced by GCR is perhaps 30 dpm/kg, while the SCR production will add another 30-40 dpm/kg, with no ablation. Obviously such objects are unlikely to be identified by non-destructive counting. The rarity of high  $^{26}\text{Al}$  values is to be expected.

Reference:

Reedy, R. C., Proc. 15th, LPSC (in press).

**SIMULATION EXPERIMENTS FOR GAMMA-RAY MAPPING OF PLANETARY SURFACES: SCATTERING OF HIGH-ENERGY NEUTRONS.** J. Brückner<sup>1</sup>, P. Englert<sup>2</sup>, R. C. Reedy<sup>3</sup>, and H. Wänke<sup>1</sup>. (<sup>1</sup>Max-Planck-Institut für Chemie, Mainz, FRG; <sup>2</sup>Institut für Kernchemie, Köln, FRG; <sup>3</sup>Los Alamos National Laboratory, Los Alamos, NM, USA)

The concentration and distribution of certain elements in surface layers of planetary objects specify constraints on models of their origin and evolution. This information can be obtained by means of remote sensing gamma-ray spectroscopy (1), as planned for a number of future space missions, i.e. Mars, Moon, asteroids, and comets.

The surface of a planetary body is bombarded by energetic particles of cosmic-rays, which produce a cascade of secondary particles, such as neutrons. Nonelastic scattering and capture reactions of these neutrons play an important role in the production of discrete-energy gamma-ray lines which can be measured by a gamma-ray detector on board of an orbiter. This allows to determine the abundances of many elements, as O, Al, Si, K, Ca, Fe, Th, and U, in the upper 50 centimeters of a planet's surface layer.

To investigate the gamma-rays made by interactions of neutrons with matter, thin targets of different composition were placed between a neutron-source and a high-resolution germanium spectrometer. Gamma-rays in the range of 0.1 to 8 MeV were accumulated.

In one set of experiments (2) a 14-MeV neutron generator using the T(d,n) reaction as neutron-source was placed in a small room. Scattering in surrounding walls produced a spectrum of neutron energies from 14 MeV down to thermal. This complex neutron-source induced mainly neutron-capture lines and only a few scattering lines. As a result of the set-up, there was a considerable background of discrete lines from surrounding material. A similar situation exists under planetary exploration conditions: gamma-rays are induced in the planetary surface as well as in the spacecraft.

To investigate the contribution of neutrons with higher energies, an experiment for the measurement of prompt gamma radiation was set up at the end of a beam-line of the isochronous cyclotron of the KFA Jülich, FRG (cf. fig. 1). Energetic neutrons were produced by bombardement of a 1 cm thick

### In-Beam Gamma Ray Spectroscopy with High Energy Neutrons

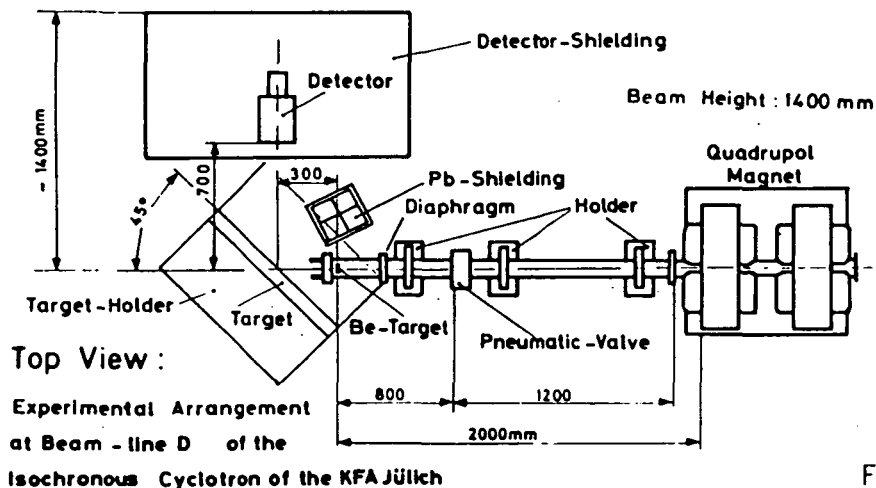


Fig. 1

## SIMULATION EXPERIMENTS FOR GAMMA-RAY MAPPING

Brückner, J. et al.

Be-target with deuterons of energies of 45, 60, and 78 MeV, resulting in maximal neutron energies of 22.5, 30, and 39 MeV respectively. Typical deuteron-beam currents varied between 200 and 600 pA depending on the target material exposed to them. The majority of the neutrons produced by the Be(d,n) reaction is emitted in forward direction and hits the extended targets positioned at an angle of 45° to the beam axis.

Gamma-rays were measured with a 92-cm<sup>3</sup> high purity germanium-detector located at an angle of 90° to the beam axis and 70 cm away from the geometric center of the target-plates. The front side of the detector was shielded by a 2 cm plate made of borated polyethylene. The other sides were consecutively surrounded by lead, boron, and paraffin in order to shield it from background gamma radiation and scattered neutrons. Gamma radiation from the Be-target and its direct environment was suppressed by an additional 20-cm lead shield.

During in-beam operation, the germanium-detector had a resolution of about 6 keV at 7 MeV. The detector signals were processed by conventional amplifiers and ADCs, and stored in 8000 channels of two combined multichannel analyzers.

The gamma-ray spectra were unfolded by an interactive computer program using a modified Gauss-Newton algorithm. A large gamma-ray library provided data for the identification of the source-reactions.

Several correction factors had to be applied to the measured line intensities: i) the total neutron-flux factor was determined by using peaks of suitable reactions in the spectrum itself; ii) the background correction was determined by comparing the gamma-ray emission of targets of different composition; iii) the absolute efficiency was determined by using radioactive standards for the low energy range and by an iron-target for the high-energy range; iv) the mass attenuation coefficient of the detector shielding-material was determined experimentally and the energy dependent absorption factor of the gamma-rays was calculated; v) the gamma selfabsorption factor of the three-dimensional target was calculated by using the appropriate mass attenuation coefficients.

Several targets were irradiated with neutrons of different energies. In contrast to the 14-MeV experiments, the capture lines are very weak and result mainly from the surrounding material. The scattering and (n,2n) reaction gamma-rays dominate the spectra (cf. Fe-spectrum in fig. 2).

The gamma-ray lines of e.g. iron and their measured intensities, considering all necessary corrections, are listed in table 1. It can be seen, that the intensities for 30 and 39-MeV neutrons are very similar in most cases. For 22.5-MeV neutrons increased intensities are found for almost all energies. This is a result of the general decrease of the cross sections with increasing energy in the energy interval under question. Compared to 14-MeV, four more lines were observed in the 22.5 and 30-MeV experiments: 1038, 2113, 2523, and 3601 keV. 39-MeV neutrons revealed an additional scattering line at 2601 keV.

Combining the results of the 14-MeV and the 'high-energy' experiments we get a rather realistic simulation of the expected gamma-flux from planetary surfaces. The complexity of the accumulated gamma-ray spectra illustrates what a gamma-ray experiment may encounter during a mission.

- Ref.: (1) R. C. Reedy (1978) Proc. Lunar Planet. Sci. Conf. 9th, p. 2961  
(2) J. Brückner, R. C. Reedy, and H. Wänke (1984) Lunar Plan. Sci. XV, p.98

## SIMULATION EXPERIMENTS FOR GAMMA-RAY MAPPING

Brückner, J. et al.

GAMMA-ENERGY [keV]	SOURCE-REACTION	NEUTRON ENERGY		
		22.5 MeV	30 MeV	39 MeV
846.7	Fe(n,ng)	$1.51 \cdot 10^8$	$9.65 \cdot 10^7$	$9.81 \cdot 10^7$
931.2	Fe(n,2ng)	$9.17 \cdot 10^6$	$9.43 \cdot 10^6$	$1.01 \cdot 10^7$
1038.0	Fe(n,ng)	$8.17 \cdot 10^6$	$6.78 \cdot 10^6$	$6.82 \cdot 10^6$
1238.3	Fe(n,ng)	$3.36 \cdot 10^7$	$2.42 \cdot 10^7$	$2.33 \cdot 10^7$
1316.4	Fe(n,2ng)	$7.05 \cdot 10^6$	$8.56 \cdot 10^6$	$9.11 \cdot 10^6$
1407.7	Fe(n,ng)	$7.77 \cdot 10^6$	$8.33 \cdot 10^6$	$1.16 \cdot 10^7$
1810.9	Fe(n,ng)	$1.83 \cdot 10^7$	$9.23 \cdot 10^6$	$1.01 \cdot 10^7$
2112.9	Fe(n,ng)	$9.60 \cdot 10^6$	$4.02 \cdot 10^6$	$4.41 \cdot 10^6$
2523.1	Fe(n,ng)	$4.39 \cdot 10^6$	$2.62 \cdot 10^6$	$2.80 \cdot 10^6$
2601.0	Fe(n,ng)	n.d.	n.d.	$7.28 \cdot 10^5$
3601.9	Fe(n,ng)	$9.69 \cdot 10^5$	$2.20 \cdot 10^6$	$1.45 \cdot 10^6$

Table 1. Measured and corrected intensities [dpm] of iron gamma-rays for different neutron energies (n.d. = not determined).

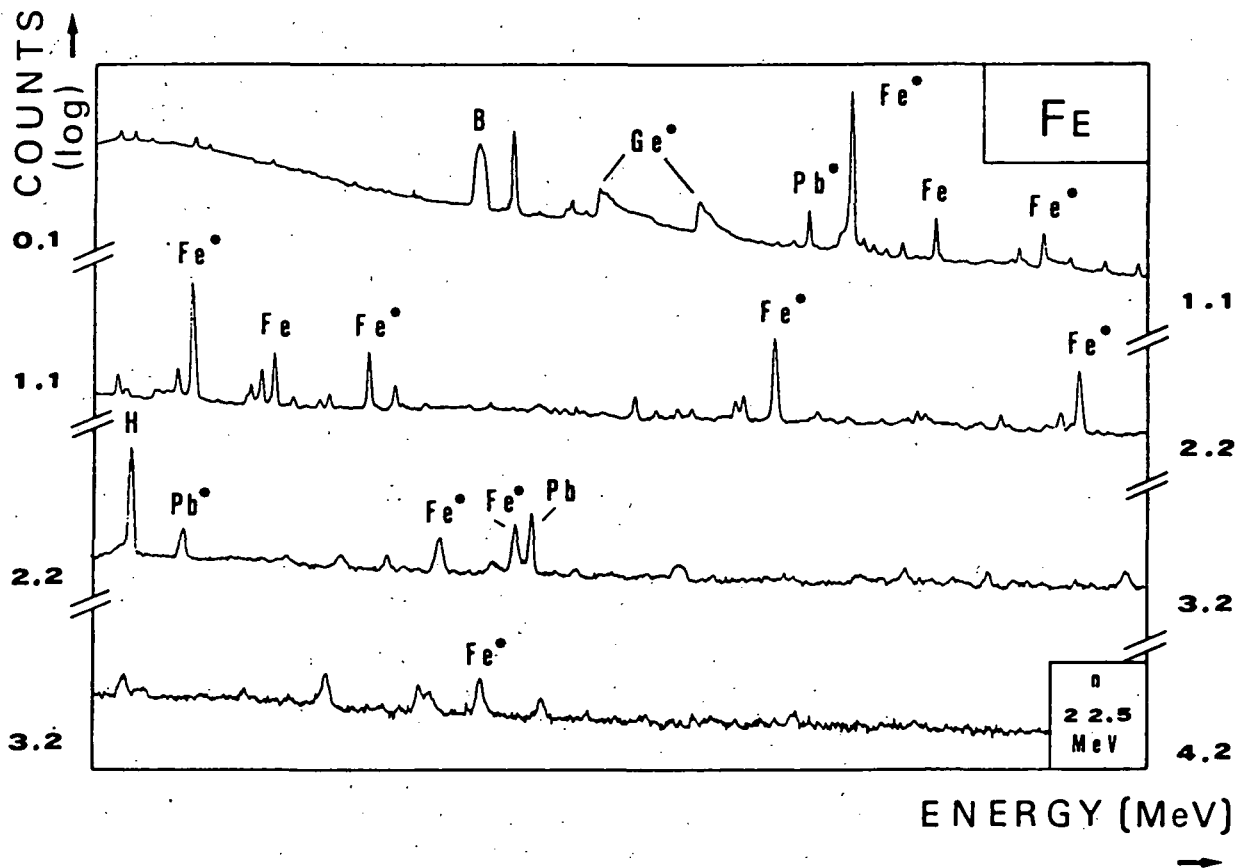


Fig. 2 Low energy part of in-beam gamma-ray spectrum of iron and surrounding material, induced by 22.5 MeV neutrons (\* = (n,n $\gamma$ )).

PRECOMPACTION IRRADIATION EFFECTS: PARTICLES FROM AN EARLY ACTIVE SUN? M. W. Caffee<sup>1</sup>, J. N. Goswami<sup>2</sup>, C. M. Hohenberg<sup>1</sup>, and T. D. Swindle<sup>1</sup>.  
<sup>1</sup>McDonnell Center for the Space Sciences, Washington University, St. Louis, MO 63130. <sup>2</sup>Physical Research Laboratory, Ahmedabad, India.

Two recent studies have shown that solar flare irradiated grains from Murchison and Kapoeta have excess spallogenic <sup>21</sup>Ne compared to unirradiated grains, indicating large precompaction particle irradiation effects. The quantity of cosmogenic neon in these grains presents serious difficulties for either galactic cosmic ray or normal solar flare sources. In the first study it was suggested that the effect might be the result of exposure to an early active sun [1]. The more recent experiment both confirms the earlier results and provides constraints on the characteristic energy spectrum of the irradiation [2].

The first results were obtained from Murchison olivines and Kapoeta pyroxenes by mass spectrometric analysis of sets of grains selected on the basis of the presence or absence of solar flare particle tracks. In the second work plagioclase feldspar grains from Kapoeta were studied, in addition to more olivine grains from Murchison. The feldspars were chosen because the cosmogenic <sup>21</sup>Ne/<sup>22</sup>Ne ratio expected from lower energy (present day) solar flare irradiation is about .5, compared to about .8 for the cosmogenic neon produced by the more energetic particles found in galactic cosmic rays [3, 4].

As in the earlier experiment, large precompaction exposure effects were observed. The feldspars show a substantial abundance of cosmogenic neon from high energy particle irradiations, with measured isotopic compositions populating a mixing line between a trapped (solar-type) endmember and a cosmogenic endmember similar in composition to GCR-produced neon (see figure). For both Kapoeta and Murchison the irradiated grains contain at least an order of magnitude more cosmogenic neon than their unirradiated counterparts. This enrichment is somewhat smaller than that observed in the previous study and may reflect statistical variations in precompaction irradiation effects among individual grains.

The size of the effect in the first study precludes easy explanation in terms of precompaction exposure to galactic cosmic rays, since grains from both meteorites have two orders of magnitude more cosmogenic neon than predicted by most models for the formation of gas-rich meteorites. Little solar wind neon was detected. If the effects are due to galactic cosmic ray exposure, then either the flux of galactic cosmic rays was anomalously high (by at least two orders of magnitude), or models for the formation of gas-rich meteorites have seriously underestimated the duration of exposure of individual grains to cosmic rays.

Solar cosmic rays have even more difficulty. An SCR origin requires a similarly long pre-compaction exposure time (in excess of 100 m.y. at 3 A.U. under present conditions [1]). In addition, the observed isotopic composition of the cosmogenic neon suggests production by more energetic particles and solar wind effects are small. These observations led to the suggestion that pre-compaction irradiation effects may have been due to an early active sun. The most recent results better constrain the energy spectrum of the nuclear-active particles. If the effects are indeed due to an energetic primitive sun, it must have had both a higher flux and a harder energy spectrum than is currently observed.

[1] Caffee, M.W., et al. (1983) Cosmogenic neon from precompaction irradiation of Kapoeta and Murchison. Proc. Lunar Planet. Sci. Conf. 14th, in J. Geo-

PRECOMPACTION IRRADIATION  
 CAFFEE M. C. et al.

- phys. Res., **88**, B267-B273.
- [2] Caffee, M.W., et al. (1984) Confirmation of cosmogenic neon from precompaction irradiation of Kapoeta and Murchison (abstract). In Papers Presented to the 47th Meteoritical Society Meeting, Albuquerque.
  - [3] Hohenberg, C.M., et al., (1978) Comparisons between observed and predicted cosmogenic noble gases in lunar samples. Proc. Lunar Planet. Sci. Conf. 9th, 2311-2344.
  - [4] Walton, J.R., et al. (1974) Evidence for solar cosmic ray proton produced neon in fines 67701 from the rim of North Ray Crater. Proc. Lunar Sci. Conf. 5th, 2045-2060.

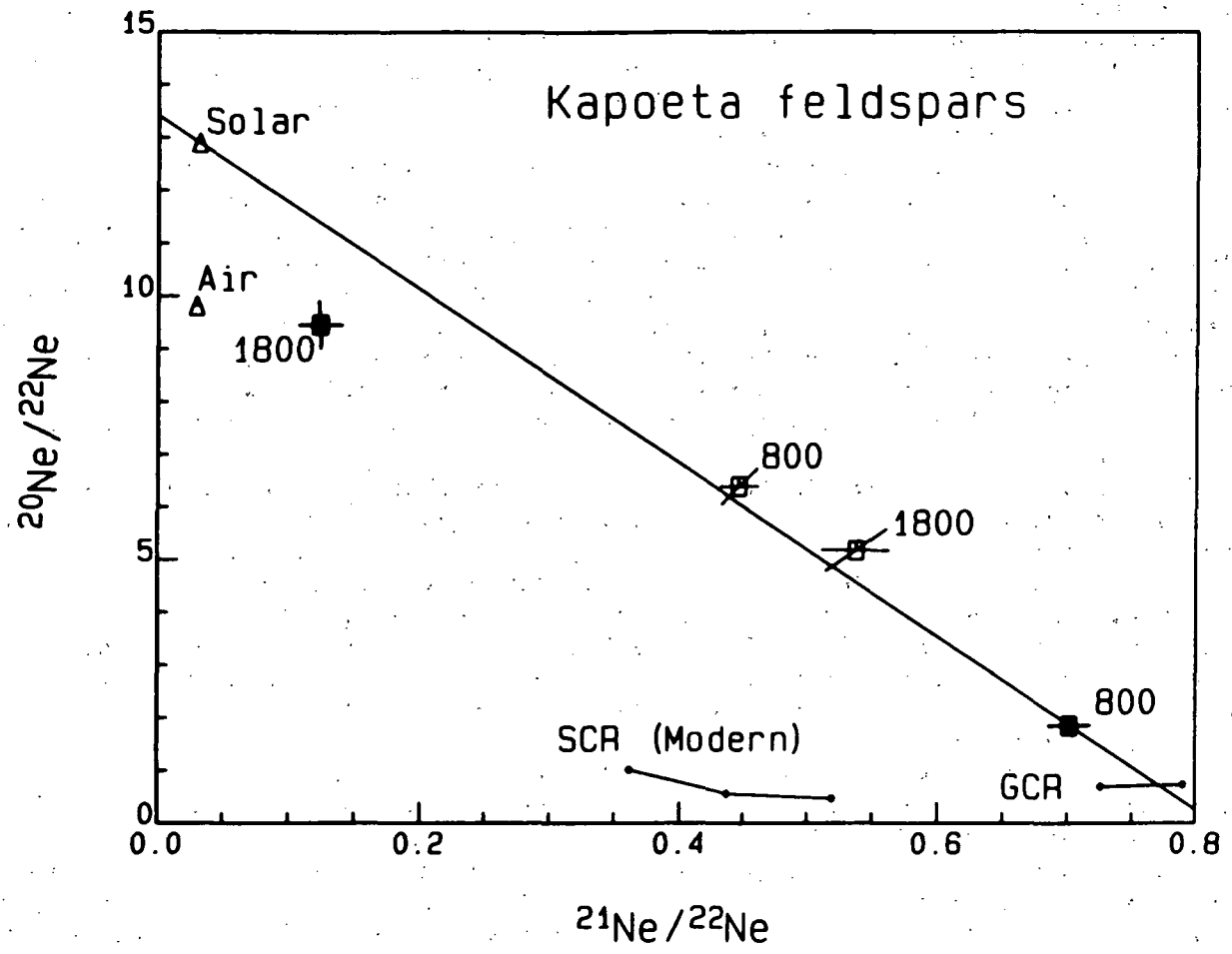


Figure caption: Neon from selected Kapoeta feldspar grains. Closed symbols are solar-flare irradiated grains (identified by the presence of heavy ion tracks), open symbols are grains which do not show solar flare irradiation effects. Numbers represent extraction temperatures in degrees Celsius. Line marked 'GCR' gives range of compositions expected for galactic cosmic ray spallation on targets with the chemistry of the Kapoeta feldspars with shielding of 0 to 40 g/cm<sup>2</sup>. Curve marked 'SCR (Modern)' gives expected compositions from solar cosmic ray irradiation under present solar conditions for shielding depths of 0 to 10 g/cm<sup>2</sup>. Predicted spectra computed from [3].

DETERMINATION OF CA-41, I-129 AND OS-187 IN THE ROCHESTER TANDEM ACCELERATOR AND SOME APPLICATIONS OF THESE ISOTOPES; U.Fehn, D.Elmore, H.E.Gove, P.Kubik, R.Teng, L.Tubbs, G.R.Holdren Nuclear Structure Research Lab., University of Rochester, Rochester, NY 14627

The TAMS program at the University of Rochester was started about seven years ago at the MP Van de Graaff accelerator (nominal voltage 12 MV). At present we measure several hundred samples per year using roughly a third of the accelerator's up-time. Most of the work is concerned with the determination of long-lived, cosmogenic radioisotopes such as Be-10, C-14 and Cl-36. Examples of investigations recently completed or still in progress are the determination of Be-10 in lake sediments in New York [1], the measurement of C-14 in prehistoric vegetables in North America [2] and the investigation of Cl-36 in meteorites [3]. Two more isotopes were added to this list recently, Ca-41 and I-129, the measurement of which will be the focus of this paper. In addition, we will report on our plans to use the  $^{187}\text{Os}/^{186}\text{Os}$  ratio for the differentiation of extraterrestrial material in a meteor crater in Germany.

Calcium-41 has a half-life of 100,000 yrs and is produced in the top few meters of the earth's crust by the interaction of secondary cosmic ray neutrons with Ca-40. After it is released because of weathering it enters the hydrologic cycle and the biosphere. It is thus of potential use for the dating of groundwater as well as of bones in the age range between 50,000 and 1 million years. The expected equilibrium concentrations  $^{41}\text{Ca}/\text{Ca}$  are about  $10^{-14}$  [4], which make detection limits of  $10^{-15}$  necessary for these applications.

A major problem for the measurement of Ca-41 with TAMS is the fact that calcium does not readily form negative atomic ions. It does, however, form negative molecular ions such as  $\text{CaO}^-$  and  $\text{CaH}_2^-$ . Another problem is the separation of Ca-41 from its isobar K-41, which is quite common in samples as well as in the cesium of the ion source.

One way to eliminate both of these problems would be to use  $\text{CaH}_2^-$  because  $\text{KH}_2$  apparently does not form negative ions [5]. The probability for formation of  $\text{CaH}_2^-$  is, however, very low unless calcium metal samples are used. Since the reduction of calcium from small natural samples is quite inefficient and difficult we investigated a different approach, namely the production of negative ions from oxygen bearing Ca molecules. Natural samples (such as bones where Ca occurs as Calcium phosphate) can easily be transformed into  $\text{CaO}$  or  $\text{CaCO}_3$  compounds. We studied the production of  $\text{CaO}^-$  ions from compounds such as  $\text{CaO}$  and  $\text{CaCO}_3$ , and from oxygen free Ca molecules which were sprayed with oxygen gas. The best results were obtained from  $\text{CaO}^-$  and from  $\text{CaCO}_3$  samples.  $\text{KO}^-$  ions are, however, present in contrast to  $\text{KH}_2^-$  ions. The interference of K-41 ions sets a detection limit of approx.  $5 \times 10^{-13}$  for the  $^{41}\text{Ca}/\text{Ca}$  ratio under the present conditions.

This detection limit is not sufficient for the measurement of terrestrial samples. Improved chemical procedures during the preparation of the sample and a reduction of the potassium content in the cesium of the ion source will help to lower this detection limit. In addition, we plan to install a new high intensity ion source [6] which should result in a significantly higher ionization rate for the Ca-41 in the samples.

## DETERMINATION OF CA-41, I-129 AND OS-187

FEHN, U; ELMORE, D; GOVE, H; KUBIK, P; TENG, R; HOLDREN, G.

Iodine-129 has several characteristics which are outstanding among the cosmogenic radioisotopes, among them its relatively long half-life of 16 m.y. In nature it has two sources: It is produced in the atmosphere by the interaction of cosmic rays with xenon, and in the crust as daughter product of the spontaneous fission of long-lived radioisotopes, mainly U-238. In addition, a significant amount comes from nuclear bomb tests in the atmosphere.

Because of its low natural concentration relatively few data are available concerning production rates and equilibrium values in the various natural reservoirs. The steady-state ratio of  $^{129}\text{I}/\text{I}$  in the hydrosphere is estimated to be between  $3 \times 10^{-13}$  and  $3 \times 10^{-12}$  [7,8]. I-129 in this reservoir is derived probably in equal parts from the production in the lithosphere and in the atmosphere [7,9].

These ratios are approx. one order of magnitude higher than the detection limit presently reached with TAMS [10]. A recent measurement of  $^{129}\text{I}/\text{I}$  in the Great Artesian Basin in Australia gave values of  $5.7 \times 10^{-13}$  [11] which is in good agreement with the predicted prebomb equilibrium values in the atmosphere. The recent installation of a new injector system will lower the detection limit for I-129 by about one order of magnitude.

A major project we are about to start is the application of I-129 as tracer for hydrothermal convection in sediment-covered oceanic crust. For quite a while now it has been postulated that during the cooling of newly formed oceanic crust seawater penetrates the crust. The reactions occurring between basalt and seawater during this convection change drastically the composition of the circulating fluids and thus may be of great consequence for the element budget of the oceans. Although the most vigorous form of this process occurs right at the active spreading centers, heat flow investigations show that this process is widespread also in older oceanic crust. Because the movement in sediments and older crust is very slow a highly sensitive tracer is needed for the detection of this movement. We plan to use I-129 profiles in conjunction with heat flow measurements in order to determine rate, continuity and extent of this convection in older crust. As a preliminary step of this investigation we are in the process of determining the I-129 content in deep sea sediments from piston cores taken off Cape Hatteras.

Osmium and rhenium are both significantly but not to the same extent depleted in crustal material as compared to extraterrestrial material. This observation combined with the fact that Re-187 is radioactive and decays into Os-187 has led to the suggestion to use the isotopic distribution of osmium as tracer for extraterrestrial material. The Cretaceous-Tertiary boundary is a well publicized example of such an application [12].

We plan to use this approach for the Ries crater in Germany. Although the meteoric origin of this crater has been widely accepted by now it has not been possible so far to identify material of definite extraterrestrial origin. One major obstacle is the dilution of the meteoric material which is significantly higher in the Ries crater than the dilution estimated for the C-T boundary. Calculations of the expected differences in the isotopic composition of Os in the various rock units show, however, that they should be of sufficient magnitude in order to be detectable with TAMS. At present we are in the process of establishing the sensitivity of the accelerator for this isotope system by measuring the Os ratios in artificial samples and in meteorites.

## REFERENCES

- [1] Wahlen M., Kothari B., Mitchell J., Schwenker C., Elmore D., Tubbs L., Ma X., Gove H.E. (1983) UR-NSRL-267.
- [2] Conard N., Asch D.L., Asch N.B., Elmore D., Gove H.E., Rubin M., Brown J.A., Wiant M.D., Farnsworth K.B., Cook T.G. (1984) Nature 308, 443-446.
- [3] Nishiizumi K., Arnold J.R., Elmore D., Ma X., Newman D., Gove H.E. (1983) Earth Planet.Sci.Lett. 62, 407
- [4] Raisbeck G.M. and Yiou F. (1979) Nature 277, 42
- [5] Raisbeck G.M., Yiou F., Peghaire A., Guillot J., Uzureau J. (1981) Proc. Symp. Accel. Mass Spectr., Argonne Nat. Lab.
- [6] Middleton R. (1982) Nucl.Instr.Meth. 214, 139-150.
- [7] Fabryka-Martin J. (1984) Ms.Thesis, University of Arizona.
- [8] Kohman T.P. and Edwards R.R. (1966) U.S. A.E.C. NYO-3624-1, 41p.
- [9] Edwards R.R. and Rey P. (1968) U.S. A.E.C. NYO-3624-3, 30p.
- [10] Fabryka-Martin J., Bentley H., Elmore D., Airey P.L. (1984) Geochim. Cosmochim. Acta, submitted.
- [11] Elmore D., Gove H.E., Ferraro R., Kilius L.R., Lee H.W., Chang K.H., Beukens R.P., Litherland A.E., Russo C.J., Purser K.H., Murrell M.T., Finkel R.C. (1980) Nature 286 138-140.
- [12] Luck J.M. and Turekian K.K. (1983) Science 222, 847.

SOLAR MODULATION OF GALACTIC COSMIC RAYS: CONTEMPORARY OBSERVATIONS AND THEORIES: M. A. Forman, Dept. of Earth and Space Sciences, State University of New York at Stony Brook, NY 11794

The flux of galactic cosmic rays inside the solar system is modulated by the action of the complex magnetic fields carried from the sun by the solar wind. This is apparent from the recurrent decrease of about 20% in the intensity of relativistic cosmic rays during sunspot maximum compared to sunspot minimum, from transient decreases due to solar flares and many other subtler effects observed by ground stations for the last 50 years. Spacecraft observations of the spatial and temporal variations of cosmic ray flux during the last ten years have shown that the solar wind and cosmic-ray modulation extend to at least 30 astronomical units in the ecliptic plane. Present best guesses are that it goes out to 100 or 200 AU, perhaps less over the poles.

Understanding the mechanism and detailed effect of modulation on the intensity, energy and composition of galactic cosmic rays is important for three reasons:

For interpreting cosmogenic nuclide fluctuations, we need to know what solar parameters control their production rates in order to know what aspect of solar variability they measure; and we need to predict production rate fluctuations from known solar parameters, to find the geophysical component of variations in cosmogenic nuclide concentration.

For galactic astrophysics, to understand the origin of cosmic rays in the galaxy, we need to know how to remove the modulation effect from the data. We need to find the spectrum of each element and isotope, including exotic species such as helium-3 and anti-protons far outside the solar system from the measurements we can make inside it.

For high energy plasma astrophysics, cosmic-ray behavior in the solar wind is a locally observable phenomenon which suggests and tests theories later applied to solar flares, x-ray stars, pulsars, quasars and other objects where energetic particles and supersonic turbulent plasma flows have been inferred.

The mechanism of solar modulation is understood in part, but how the parts act together to make the whole effect is still controversial. Parker's (1958) original concept of modulation by diffusion and convection in the solar wind remains the basis for all current descriptions. Until a few years ago, the "force-field" approximation seemed to be adequate, at least for relativistic particles. It included all the important physics of modulation and described the observations reasonably well. "Force-field" will be described in the talk, but the conditions of its validity and meaningfulness will be made clear.

Observations in the outer heliosphere show that there is a positive radial gradient of 3% per astronomical unit in the ecliptic plane. In addition, abrupt decreases occur behind certain flare-initiated shock structures. These structures, and the modulation behind them propagate outward with the solar wind. One view is that the steady gradient is always present, due to local diffusion, but that the variation during the solar cycle is due simply to the increase in the number of these regions of abrupt decrease in the heliosphere at solar maximum.

66228-26N

SOLAR MODULATION  
Forman, M.A.

At the same time, observations of the heliospheric magnetic field near solar minimum a little off the ecliptic plane showed a very large-scale coherent structure. Field is directed outward in the northern solar hemisphere, and inward in the south, with a warped and wavy neutral sheet between these huge volumes.

Theoretically, this magnetic geometry forces galactic cosmic rays to "drift" down from the poles and out through the neutral sheet. The flow of energetic particles is reversed in the next solar minimum. The wavy character of the neutral sheet and the changing source region makes successive solar minima different-as they seem to be in the cosmic ray flux. The drift mechanism accounts for the amount of modulation at solar minimum only by the strength of the magnetic field. The amount of turbulence and the speed of the solar wind are irrelevant.

Drifts must occur at solar minimum when the fields are smooth, but are not necessarily important at solar maximum when the field is choppy and changing. On the other hand, drifts provide the least level of solar modulation. These must have disappeared during the Maunder and earlier minima in the radiocarbon record. This would imply that the solar magnetic field was very weak, but not that the solar wind was weak or absent. Drift effects are strongly three-dimensional poleward of the wavy neutral sheet. It is hoped that the single spacecraft mission over the solar poles in the late 1980's will resolve the question of the role of drifts in the solar modulation of galactic cosmic rays.

EVOLUTION OF GAS-RICH METEORITES : CLUES FROM COSMOGENIC NUCLIDES, J.N. Goswami, Physical Research Laboratory, Ahmedabad 380 009, India.

The evolution of gas-rich meteorites in general, and the setting in which the observed solar-wind, solar-flare irradiation records were imprinted in individual components of these meteorites are understood only in qualitative terms, although contrary viewpoints do exist (Goswami et al. 1984 and references therein). The regolith irradiation hypothesis, bolstered by the observations of irradiation features in lunar regolith materials, similar to those observed in gas-rich meteorites, is accepted by many workers in this field. However, a close analysis of the problem suggests that the regolith irradiation may not be the dominant mode in producing the observed precompaction irradiation features in the gas-rich meteorites.

It is generally assumed that the irradiated and non-irradiated components in the gas-rich meteorites, and particularly in the so-called 'dark-phase' material evolved together. Starting with this assumption, one can use the data on cosmogenic nuclides in gas-rich meteorites to impose strong constraints on the maximum residence time for the individual components of these meteorites within the nuclear active zone (approximately the upper meter) of the asteroidal regolith. This turns out to be  $\leq 10^5$  years in the case of CI and CM chondrites and  $\leq 10^6$  years for H-chondrites and achondrites (Goswami and Lal 1979; Goswami and Nishiizumi 1982; Goswami et al 1984; Goswami and Nishiizumi 1984). These values were obtained by considering the difference between the cosmogenic noble gas ( $^{21}\text{Ne}$ ;  $^{38}\text{Ar}$ ) and radionuclide ( $^{26}\text{Al}$ ;  $^{53}\text{Mn}$ ) exposure ages of these meteorites. Such an approach is valid as the precompaction irradiation of gas-rich meteorites must have taken place during their early evolutionary history. Although the short precompaction exposure durations for gas-rich meteorites was noted earlier by Anders (1975), this constraint was never considered explicitly in treating the problem of evolution of these meteorites. The implications of a very short ( $\leq 10^5$  years) precompaction exposure duration in the case of carbonaceous chondrites have been discussed in detail by Goswami and Lal (1979), Goswami and Macdougall (1983) and Goswami et al. (1984), which clearly show the incompatibility of the regolith irradiation scenario for these meteorites given our present understanding of asteroidal regolith dynamics (Housen et al. 1979; Langevin and Maurette 1980; Housen and Wilkening 1982a). The 'small body' irradiation model was proposed instead (Goswami and Lal 1979; Goswami et al. 1984) in which the irradiation preceds formation of the parent bodies of the carbonaceous chondrites and occur when the individual components of these meteorites were part of cm to meter-sized objects. In the case of gas-rich H-chondrites and achondrites, the time constraint imposed by cosmogenic nuclide data is barely within the limit of the regolith model (Housen and Wilkening

Goswami, J.N.

1982b). However consideration of certain specific aspects, e.g. finer details of solar flare irradiation records and petrographic constraint (presence of significant fraction of gas-rich H-chondrites among all petrographic types) suggest that the regolith model may not adequately explain all these observations. Unfortunately only one achondrite (Kapoeta) and a couple of H-chondrites with high solar-wind content have been analysed in detail for their cosmogenic records (Goswami and Nishiizumi 1982; 1984). This is primarily due to the fact that saturation effect in  $^{26}\text{Al}$  and  $^{53}\text{Mn}$  concentrations constrain the analysis to gas-rich meteorites with exposure age  $<10$  m.y. In this context it will be extremely useful to use the newly developed accelerator mass-spectrometry method of determining cosmogenic  $^{129}\text{I}$  (Nishiizumi et al. 1983) to analyse a suite of gas-rich H-chondrites with noble gas exposure age exceeding 10 m.y., and having high level of solar-wind and solar-flare irradiation. Fayetteville and Elm Creek will be two ideal candidates for such a study.

A new dimension to the problem of evolution of gas-rich meteorites was added by the recent findings of Caffee et al. (1983) that the solar flare irradiated grains in the gas-rich meteorites Kapoeta and Murchison have more than an order of magnitude higher cosmogenic  $^{21}\text{Ne}$  in them compared to the concentrations measured in non-irradiated grains from these same meteorites. Whether this can be taken to imply an early active Sun, characterized by a harder solar flare proton spectrum, or is indicative of a very different evolutionary pathway for the irradiated components in gas-rich meteorites could be ascertained only through further work in this direction. In summary, a reappraisal of our understanding of the evolution of gas-rich meteorites is necessary considering the new inputs provided by the records of cosmogenic nuclides in these meteorites.

References: Anders E. (1975) Icarus 24, 363-371; Caffee M.W. et al (1983) J. Geophys. Res. 88, B 267-B 273; Goswami J.N. and Lal D. (1979) Icarus 40, 510-521; Goswami J.N. and Nishiizumi K. (1982), LPI Tech. Rep. 82-02, 44-48; Goswami J.N. and Macdougall J.D. (1983) J. Geophys. Res. 88, A 755-A 764; Goswami J.N. and Nishiizumi K. (1984) In Preparation; Goswami J.N., Lal D. and Wilkening L.L. (1984) Sp. Sci. Rev. 37, 111-159; Housen K. et al. (1979) Icarus 39, 317-351; Housen K. and Wilkening L.L. (1982a) Ann. Rev. Earth Planet. Sci. 10, 355-376; Housen K. and Wilkening L.L. (1982b) Lunar and Planetary Sci. XIII, 339-340; Langevin Y. and Maurette M. (1980) Lunar and Planetary Sci. XI, 602-604; Nishiizumi K. et al (1983) Nature 305, 611-612.

THE EXPOSURE HISTORY OF JILIN AND PRODUCTION RATES OF COSMOGENIC NUCLIDES; G. Heusser, Max-Planck-Institut f. Kernphysik, POB 103980, D-6900 Heidelberg, Germany

Jilin the largest known stone meteorite is a very suitable object for studying the systematics of cosmic ray-produced nuclides in stony meteorites. Its well established two stage exposure history (1,2,3) even permits to gain information about two different irradiation geometries (2π and 4π).

All stable and long-lived cosmogenic nuclides measured in Jilin so far correlate well with each other (3,4,5). An example is shown in Fig. 1 where the <sup>26</sup>Al activities are plotted vs. the spallogenic <sup>21</sup>Ne concentration (6,7).

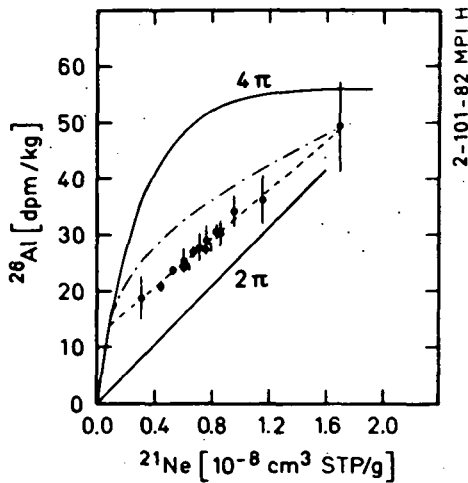


Figure 1: <sup>21</sup>Ne-<sup>26</sup>Al correlation in Jilin and its evolution from a 2π irradiation geometry followed by a 4π irradiation geometry. <sup>21</sup>Ne from (6,7).

These records of cosmic-ray interaction in Jilin can be used both to determine the history of the target and to study the nature of production rate profiles. This is unavoidably a bootstrap process, involving studying one with assumption about the other.

The good correlation (dotted line in Fig. 1) with a positive ordinate intercept is interpreted in terms of a 2π irradiation followed by a 4π irradiation.

The production of stable (S) and radioactive (R) nuclides by cosmic rays in a large body (2π geometry) can be described by:

$$S(d) = P_S(d) t \quad (1)$$

$$R(d) = P_R(d) (1 - e^{-\lambda t}) \quad (2)$$

where  $P_S(d)$  and  $P_R(d)$  are the depth-dependent production rates of the stable and radioactive species, respectively and  $t$  is the exposure time. Both expressions can be combined:

$$R(d) = \frac{P_R(d)}{P_S(d)} \frac{1 - e^{-\lambda t}}{t} S(d) \quad (3)$$

For a given  $t$  and a constant production rate ratio  $P_R(d)/P_S(d)$  this is the equation of a straight line  $R = m \cdot S$  through the origin (solid line labelled 2π in Fig. 1). Its slope is determined by the production rate ratio and the duration of exposure.

For a 4π irradiation with negligible depth effects for the production of spallogenic nuclides as indicated by the measured <sup>22</sup>Na activities in Jilin (3) the production equations

$$R = P_R(1 - e^{-\lambda t}) \text{ and } S = P_S t$$

represent the curve of growth in the R vs. S diagram (Fig. 1, labelled 4π)

G. Heusser

$$R = P_R \left(1 - e^{-\lambda \frac{S}{P_S}}\right) \quad (4)$$

If a  $2\pi$  irradiation is followed by a  $4\pi$  irradiation, the relevant production rates are expressed by:

$$S(d) = P_{S1}(d)t_1 + P_{S2}t_2 \quad (5)$$

$$R(d) = P_{R1}(d)(1 - e^{-\lambda t_1}) e^{-\lambda t_2} + P_{R2}(1 - e^{-\lambda t_2}) \quad (6)$$

where  $P_1$  and  $P_2$  are the production rates of the first ( $2\pi$ ) stage and the second ( $4\pi$ ) stage, respectively and  $t_1$  and  $t_2$  are the respective exposure ages. Again with the assumption of a constant production ratio we get:

$$R(d) = \frac{P_R(d)}{P_S(d)} \frac{1 - e^{-\lambda t_1}}{t_1} e^{-\lambda t_2} S(d) + P_{R2} \left\{1 + \frac{t_2}{t_1} e^{-\lambda t} - \frac{t}{t_1} e^{-\lambda t_2}\right\} \quad \text{with } t = t_1 + t_2 \quad (7)$$

For  $t_1$  and  $t_2$  fixed equation 7 is the equation of a straight line of the form  $R = mS + b$  with slope

$$m = \frac{P_R(d)}{P_S(d)} \frac{1 - e^{-\lambda t_1}}{t_1} e^{-\lambda t_2} \quad (8)$$

As  $t_2$  increases for  $t$  fixed, the intercept of the original  $2\pi$  straight line is shifted upwards along the curve of growth while its slope is decreasing. The fit line through the data points obtained for Jilin (dotted line in Fig.1) illustrates this behaviour. The straight line and the curve of growth intersect at

$$R_{\text{inters.}} = P_{R2}(1 - e^{-\lambda t_2}) \quad (9)$$

Hence  $t_2$  can be calculated if  $P_{R2}$  is known. We can then enter the value of  $t_2$  into equation (8) and obtain  $t_1$  by iteration, provided that we know the production rate ratio. With well founded assumptions about the individual production rates eq. (9) yields  $t_2 = 0.4$  Myr and eq. (8)  $t_1 = 9$  Myr (3). If the stable isotope is replaced by a long-lived radionuclide, the general equation of the correlation line has the form:

$$R_A(d) = \frac{R_A}{R_B} \frac{e^{-\lambda_A t_2} - e^{-\lambda_A t}}{e^{-\lambda_B t_2} - e^{-\lambda_B t}} (R_B(d) - P_{A2} + P_{A2} e^{-\lambda_B t_2}) + (1 - e^{-\lambda_A t_2}) P_{A2} \quad \text{with } t = t_1 + t_2$$

A is the radionuclide with the shorter half life.

## THE EXPOSURE HISTORY OF JILIN...

G. Heusser

Accepting the nature of Jilin's exposure history, we can now turn to the information provided by these correlations in view of production rate ratios and individual production profiles. The perfect straight line fit of the data points (Fig.1) confirms our assumption of a constant production ratio (eq. 3, 7, and 8), i.e. the production rate of  $^{26}\text{Al}$  must have a depth dependence very similar to  $^{21}\text{Ne}$ . The sensibility of this behaviour is illustrated as an example for the case that the mean half thickness of  $^{21}\text{Ne}$  is twice that of  $^{26}\text{Al}$ . The calculation was normalized for the highest data point. The resulting correlation (point-dotted curve in Fig.1) corresponds to a bend curve which is very distinct from the straight line formed by the experimental points. In this way, the depth dependence of production rates of other long-lived and stable cosmogenic nuclides could be investigated in Jilin as well.

References

- (1) Honda M., Nishiizumi K., Imamura M., Takaoka M., Nitoh O., Horie K and Komura K. (1982) *Earth Planet.Sci.Lett.* 57, p. 101
- (2) Heusser G., Ouyang Z. (1981) *Meteoritics* 16, p. 326-327.
- (3) Heusser G., Ouyang Z, Kirsten T., Herpers U. and Englert P. (1984) to be published in *Earth Planet.Sci.Lett.*
- (4) Pal D.K., Moniot R.K., Kruse T.H., Tuniz C. and Herzog G.F. (1982) *Proc. 5th Int.Conf. Geochronology, Cosmochronology, Isotope Geology, Nikko/ Japan*, p. 300 -301.
- (5) Osadnik G., Herpers U. and Herr W. (1981) *Meteoritics* 16, p. 371-372.
- (6) Begemann F., Li Z., Schmitt-Strecker S., Weber H.W. and Xu Z. (1984) to be published in *Earth Planet.Sci.Lett.*
- (7) Weber H.W., private communication.

RADIONUCLIDE MEASUREMENTS BY ACCELERATOR MASS SPECTROMETRY AT ARIZONA. A. J. T. Jull, D. J. Donahue, and T. H. Zabel\*. NSF Accelerator Facility for Radioisotope Analysis, University of Arizona, Tucson, Arizona 85721. \*current address: IBM Thomas J. Watson Research Center, Yorktown Heights, New York 10598.

Over the past few years, Tandem Accelerator Mass Spectrometry (TAMS) has become established as an important method for radionuclide analysis. Measurements of  $^{10}\text{Be}$  and  $^{14}\text{C}$  are now routine in several laboratories (1). The basic principles of accelerator mass spectrometry have been reviewed by Litherland (2). All systems are basically similar in principle.

In the Arizona system (see fig. 1) we operate the accelerator at a terminal voltage of 1.8MV for  $^{14}\text{C}$  analysis, and 1.6 to 2MV for  $^{10}\text{Be}$  (3). Samples are inserted into a cesium sputter ion source in solid form. Negative ions sputtered from the target are accelerated to about 25kV, and the injection magnet selects ions of a particular mass. In the case of  $^{14}\text{C}$ , N does not produce negative ions and an important source of background is eliminated. The ions are accelerated to the terminal potential of up to 2MV. They then pass through a stripper canal, losing electrons. The resultant positive ions are then accelerated back to ground. Ions of the 3+ charge state, having an energy of about 8MeV are selected by an electrostatic deflector, surviving ions pass through two magnets, where only ions of the desired mass-energy product are selected. The final detector is a combination ionization chamber to measure energy loss (and hence, Z), and a silicon surface-barrier detector which measures residual energy. After counting the trace isotope for a fixed time, the injected ions are switched to the major isotope ( $^{13}\text{C}$  or  $^9\text{Be}$ ) used for normalisation. These ions are deflected into a Faraday cup after the first high-energy magnet (M1). Repeated measurements of the isotope ratio of both sample and standards results in a measurement of the concentration of the radionuclide.

An important part of TAMS dating is the ability to produce accelerator targets on a consistent and routine basis. For  $^{14}\text{C}$ , graphite is the best target because of its high negative ion yield and stability for extended periods of time. Recent improvements in sample preparation for  $^{14}\text{C}$  (4) make preparation of high-beam current graphite targets directly from  $\text{CO}_2$  feasible. Routine measurements up to now at Arizona have been made on iron-carbon targets, made by dissolution of about 1 mg carbon in 15 mg iron (5). The  $^{14}\text{C}$  background using this method is equivalent to approximately 2% modern carbon. This level is almost entirely due to  $^{14}\text{C}$  introduced during sample preparation. Lower backgrounds of as low as 0.4% modern carbon ( $^{14}\text{C}/^{12}\text{C} = 4 \times 10^{-15}$ ) have been measured from carbon produced directly from  $\text{CO}_2/\text{H}_2$  gas mixtures. If the background level is constant, it can be subtracted, and the detection limit is the error in the background (2 sigma).

Extraction of spallogenic  $^{14}\text{C}$  from rocks and meteorites (6) requires temperatures at or near the melting point and oxidising conditions to ensure complete extraction of  $^{14}\text{C}$ . By contrast, the chemistry for extraction of  $^{10}\text{Be}$  is relatively standardised, the only criterion is to limit contamination by the isobar  $^{10}\text{Be}$ .

## RADIONUCLIDE MEASUREMENTS

Jull, A. J. T. et al.

Except for some measurements of standards and backgrounds for  $^{10}\text{Be}$ , our measurements to date have been on  $^{14}\text{C}$ . We expect to have more  $^{10}\text{Be}$  measurements in the near future. The facility at Arizona has produced a large amount of data on  $^{14}\text{C}$ . Although most results have been in archaeology and quaternary geology (3,7), we have expanded our studies to include cosmogenic  $^{14}\text{C}$  in meteorites, in collaboration with Fireman (8). The data obtained so far tend to confirm the antiquity of Antarctic meteorites from the Allan Hills site. Data on three samples of Yamato meteorites gave terrestrial ages of between about 3 and 22 thousand years. More samples need to be studied, and comparisons made with other cosmogenic nuclides on the same material, before conclusions as to the terrestrial age distribution of the Yamato collection. The study of samples exposed to simulated cosmic-ray irradiation should also aid in the intercomparison of data on different radionuclides.

## References.

- 1.) Wölfli, W., ed. (1984), Third International Symposium on Accelerator Mass Spectrometry, Zurich. Nuclear Inst. Methods, in press.
- 2.) Litherland, A. E. (1980), Ann. Rev. Nucl. Part. Phys. 30, 437-473.
- 3.) Donahue, D. J. et al. (1983), Nucl. Inst. Methods 218, 425-429.
- 4.) Vogel, J. et al. (1984), Nucl. Inst. Methods, in press.
- 5.) Jull, A. J. T. et al. (1984), Nucl. Inst. Methods 218, 509-514.
- 6.) Fireman, E. L. (1979), Proc. Lunar Planet. Sci. Conf. 10th, p. 1053-1060.
- 7.) Donahue, D. J. et al. (1984), Nucl. Inst. Methods, in press.
- 8.) Jull, A. J. T. et al. (1984), Proc. Lunar Planet. Sci. Conf. 15th, in press.

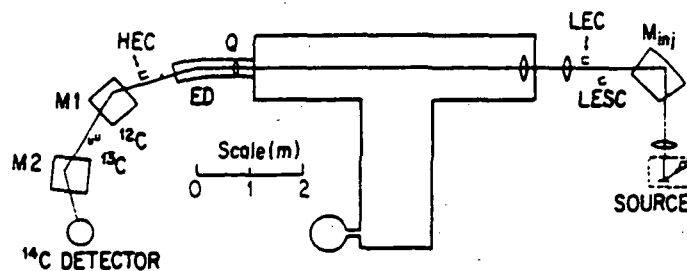


Figure 1. Schematic diagram of system. Abbreviations in the figure are:  $M_{inj}$ , injection magnet; LEC, low-energy Faraday cup (this cup can be moved in and out of the beam); LES, low-energy side cup; Q, electrostatic quadrupole focus; ED, electrostatic deflector; M1 and M2, high-energy magnets,  $^{13}\text{C}$  and  $^{12}\text{C}$ , high-energy Faraday cups.

COSMIC RAY INTERACTIONS IN THE GROUND: TEMPORAL VARIATIONS IN COSMIC RAY INTENSITIES AND GEOPHYSICAL STUDIES; D. Lal, Scripps Institution of Oceanography, Geological Research Division, A-020, La Jolla, CA 92093 (USA).

Temporal variations in cosmic ray intensity have been deduced from observations of products of interactions of cosmic ray particles in the moon, meteorites, and the earth (1). Of particular interest is a comparison between the information based on earth and that based on other samples. Differences are expected at least due to (i) differences in the extent of cosmic ray modulation, and (ii) changes in the geomagnetic dipole field. Any information on the global changes in the terrestrial cosmic ray intensity is therefore of importance. As an illustration, it is generally believed that the slow variation in  $^{14}\text{C}/^{12}\text{C}$  ratios as observed in tree rings is indicative of an appreciable change in the earth's dipole field during the past 10,000 yrs (2). However, I have recently shown (3), on the basis of theoretical considerations and oceanic paleodata covering the past glaciation, that climate-induced changes in the carbon cycle are large and may be responsible for a greater part of the observed variation. To check on this, one would have to study the temporal variations in the production rate of another terrestrial cosmic ray-produced isotope. One of the obvious ways to achieve this goal is to study the temporal variations in the fallout of an isotope. The potential usefulness of  $^{10}\text{Be}$  for this purpose was explored earlier (4) and also recently (5). However, this method presents some difficulties since the fallout of  $^{10}\text{Be}$  depends also on meteorological factors (6).

In this paper we present another possibility of detecting changes in cosmic ray intensity. The method involves human intervention and is applicable for the past 10,000 yrs. Studies of changes over longer periods of time are possible if supplementary data on "age" and history of the sample are available using other methods. We also discuss the possibilities of studying certain geophysical processes, e.g. erosion, weathering, tectonic events based on studies of certain cosmic ray-produced isotopes for the past several million years.

(a) Cosmic ray intensity studies. A direct method of measuring cosmic ray intensity on the earth will be to measure the activation products in a sample exposed to the secondary cosmic ray beam for a known period of time, in a known geometry at atmospheric depth,  $x$  ( $\text{gm}\cdot\text{cm}^{-2}$ ) and geomagnetic latitude,  $\lambda$ . At great depths in the atmosphere, the nucleonic component attenuates with a mean free path of  $165 \text{ gm}\cdot\text{cm}^{-2}$ . Consequently, samples which are buried underground at depths exceeding 10 m.f.p. (5-6 meters of typical surface materials) will be appreciably shielding so that the unshielded production over periods of the order of ( $10^3$ - $10^4$ ) yrs will considerably exceed the earlier production. The in-situ production of  $^{10}\text{Be}$ ,  $^{26}\text{Al}$ ,  $^{36}\text{Cl}$ ,  $^3\text{H}$  and other isotopes can be conveniently measured in rocks exposed for periods of the order of  $10^3$  yrs, in samples of the order of 100 grams. This is based on production rates given earlier (6).

We therefore propose that changes in the cosmic ray intensity can be directly measured from a study of in-situ production of radionuclides in documented samples. A number of possibilities arise; one of the obvious possibilities is to study the pyramidal stones. The pyramids at Dahsur and Giza seem ideal for providing samples exposed for (4500-4600) yrs. The low latitude of the pyramids is favorable for studying decreases in geomagnetic

COSMIC RAY INTERACTIONS IN THE GROUND:  
Lal, D.

dipole field. Tree rings may also serve as ideal in-situ materials for isotope  $^{10}\text{Be}$  in particular. Of course, it would have to be ascertained that no appreciable contributions arise from  $^{10}\text{Be}$  in ground waters. Geological specimens, e.g. volcanics may well provide ideal samples exposed in fixed geometry for longer periods of time, ( $10^4$ - $10^5$ ) yrs.

The in-situ method proposed above was considered earlier (7) for the study of long term variations in the flux of high energy primary cosmic rays ( $E > 130$  GeV). The present proposal for studying variations in the low energy flux of cosmic rays, in the GeV region which is sensitive to changes in the earth's dipole field, is being made for the first time. This would supplement any information based on the fall-out of nuclides, such as that based on  $^{10}\text{Be}$  in polar ice (5).

(b) Geophysical studies. Considering the present detection limits for several isotopes, in the range of  $10^5$ - $10^6$  atoms (8), one can investigate production rates of  $\sim 10^{-11}$  atoms/g·sec in a sample of 1 Kg exposed for a period of  $10^6$  yrs.

At sea level, the nuclear reactions are produced primarily by neutrons and negative mu-mesons (6). At depths exceeding 2-3 meter rock equivalent, fast mu-mesons and slow negative mu-mesons (captures by nuclei) produce most of the nuclear reactions; neutrons are not important at these depths. Fast mu-mesons produce nuclear disintegrations with larger kinetic energy dissipation in the spallation products than in the case of capture of negative mu-mesons. The nuclear disintegration rate at a depth of say 25 meters rock equivalent is about  $2 \times 10^{-9}$ /gm·sec (6, 7). Compared to sea level, this is lower by a factor of  $10^4$ , but nevertheless such disintegration rates can be monitored using present day atom detection methods.

The main aim of the study (9, 10, 11) would be to measure departures from equilibrium concentrations and then determine the rates of geophysical processes responsible using certain models. If, for example, a sample of rock exposed to elements is continually undergoing weathering, the in-situ cosmic ray production rate of isotopes at a test point will change in view of the reduction in the overlying amount of rock. Let  $Q(t)$  be the rate of production. The concentration of a radionuclide in the rock,  $C(T)$ , after an elapse of time  $T$  will then be given by the convolution integral

$$C(T) = C(0) e^{-\lambda T} + \int_0^T Q(t) e^{-\lambda(T-t)} dt \quad (1)$$

where  $\lambda$  is the disintegration constant of the nuclide and  $C(0)$  is the concentration of the nuclide at  $t = 0$ . If one isotope is measured, equation (1) can put some constraints in the temporal changes in the rock geometry due to physical processes. It is clearly advantageous to study as many isotopes as possible and also call on supplementary geophysical evidence to model the isotope production with changing geometry of irradiation, due to geophysical processes.

The crux of application of in-situ production of cosmic ray nuclides to geophysical studies lies in equation (1) and the capabilities to model  $Q(t)$  in a realistic manner. If this can be achieved, a number of applications should become possible:

COSMIC RAY INTERACTIONS IN THE GROUND:

Lal, D.

- i) Rates of erosion of exposed rocks and problems of similar nature involving changes in rock geometry (fragmentation of rocks, sediment burial/denudation, etc.).
- ii) Tectonic uplift or subduction.
- iii) Residence time of materials in particular settings, e.g. ages of glaciers, and turn-over time of sand dunes.

We will present worked out examples to support the above suggestions, and indicate the type of information which is possible with the isotopes which can currently be detected with high sensitivity. Reference is made to the first application of the method by Hampel et al. (10) to study rock erosion rates, and to a paper by Jha and Lal (11) who have specifically considered the application of  $^{10}\text{Be}$  and  $^{26}\text{Al}$  to the study of tectonic movements. These isotopes should allow convenient study of vertical movements in the range  $(10^{-4}-10^{-5}) \text{ cm}\cdot\text{yr}^{-1}$ .

REFERENCES

1. Reedy et al., 1983. Ann. Rev. Nucl. Part. Sci. 33, 505-37.
2. Bucha, V., 1970. In 'Radiocarbon Variations and Absolute Chronology,' ed. I. U. Olsson, John Wiley & Sons, 501-11.
3. Lal, D., 1984. To appear in Proc. AGU Chapman Conf. on 'Carbon Cycle Variations During the past 50,000 Yrs,' Tarpon Springs; USA; Lal, D. and R. Revelle, 1984. Nature 308, 344-46.
4. Harrison, C. G. A. and B. L. K. Somayajulu, 1966. Nature 212, 1193-95.
5. Beer et al., 1984. In Proc. 3rd Int. Symp. on AMS, Zurich, 1984, Nucl. Instr. & Methods (in press).
6. Lal, D. and B. Peters, 1967. Handbuch der Physik (Springer-Verlag, Berlin), XLVI/2, 551-612.
7. Lal, D., 1963. Proc. Int. Cosmic Ray Conf. 6th, 190.
8. Rucklidge et al., 1981. Nucl. Inst. & Methods 191, 1-9.
9. Davis, Jr., R. and O. A. Schaeffer, 1955. Ann. N. Y. Acad. Sci. 62, 105.
10. Hampel et al., 1975. Jour. Geophys. Res. 80, 3757-60.
11. Jha, R. and D. Lal, 1982. In 'Proc. 2nd Symp. on Natural Radiation Environment,' eds. K. G. Vohra, et al. Wiley Eastern, New Delhi, 629-35.

PRODUCTION RATES OF NEON AND XENON ISOTOPES BY ENERGETIC NEUTRONS  
 D. A. Leich, R. J. Borg, and V. B. Lanier, Lawrence Livermore National  
 Laboratory, Livermore, CA 94550

As a first step in a new experimental program to study the behavior of noble gases produced in situ in minerals, we have irradiated a suite of minerals and pure chemicals with 14.5 MeV neutrons at LLNL's Rotating Target Neutron Source (RTNS-II) and determined production rates for noble gases. While neutron effects in meteorites and lunar samples are dominated by low-energy (<1 keV) neutron capture, more energetic cosmic-ray secondary neutrons can provide significant depth-dependent contributions to production of cosmogenic nuclides through endothermic reactions such as (n,2n), (n,np), (n,d) and (n,alpha). Production rates for nuclides produced by cosmic-ray secondary neutrons are therefore useful in interpreting shielding histories from the relative abundances of cosmogenic nuclides.

Samples were vacuum encapsulated in quartz ampoules and irradiated as add-ons to the principle RTNS-II experiments for two to four weeks, during which time they accumulated fluences up to  $10^{17}$  neutrons/cm<sup>2</sup> as determined by activation of iron dosimetry foils. Irradiated samples were stored for at least three months before breaking open the quartz ampoules and weighing portions for analysis. Noble gas isotope dilution analyses were performed by adding an aliquot of our mixed noble gas spike (principally <sup>3</sup>He, <sup>21</sup>Ne, <sup>38</sup>Ar, <sup>80</sup>Kr, and <sup>124</sup>Xe) or of an air standard during a single 1650 C vacuum extraction. Duplicate samples were analyzed without the spike in two-step extractions: a 400 C heating to reveal any tendency for low-temperature gas loss, and a 1650 C extraction. Only insignificant quantities of noble gas reaction products were released in the 400 C steps, leading us to conclude that gas retention was probably quantitative, although we cannot rule out the possibility of some recoil loss during the irradiations or diffusive loss at ambient temperatures during and after the irradiations.

Neon analyses were performed on samples of sodium and magnesium minerals and reagents. The neon extracted from sodalite, albite, and NaCl samples are isotopically similar, determining the composition of Na-derived neon as <sup>20</sup>Ne:<sup>21</sup>Ne:<sup>22</sup>Ne = 0.45:0.017:1, not including the <sup>22</sup>Ne that will grow in from decay of 2.6-year <sup>22</sup>Na from <sup>23</sup>Na(n,2n)<sup>22</sup>Na. The neon extracted from the magnesium minerals enstatite and forsterite are also isotopically similar, with a composition given by <sup>20</sup>Ne:<sup>21</sup>Ne:<sup>22</sup>Ne = 0.61:1:0.090 attributed to

PRODUCTION RATES  
Leich, D. A. et al.

production from natural magnesium. The neon extracted from Mg metal was isotopically different from the neon extracted from the magnesium minerals, probably due partly to differences in the neutron energy spectrum seen by the different samples and partly to atmospheric neon contamination in the Mg metal. Unlike the other reagent samples, it had not been degassed by vacuum melting before encapsulation. At present, we can only give the measured isotopic composition in the unspiked 1650 C extraction from this sample as limits for the Mg-derived neon:  $^{20}\text{Ne}/^{21}\text{Ne} < 0.75$ ,  $^{22}\text{Ne}/^{21}\text{Ne} < 0.095$ . The atmospheric neon contamination does not compromise the isotope dilution analysis of  $^{21}\text{Ne}$  production in Mg-metal, and our value of  $136 \pm 7$  mb for this production cross section is in fair agreement with previous measurements of  $160 \pm 8$  mb at 14.1 MeV and  $152 \pm 12$  mb at 14.7 MeV (1).

Xenon analyses were performed on samples of CsCl and  $\text{Ba}(\text{NO}_3)_2$ . The Cs-derived xenon was dominated by  $^{132}\text{Xe}$  primarily from  $^{133}\text{Cs}(n,2n)^{132}\text{Cs}$ , but  $^{130}\text{Xe}$  from  $^{133}\text{Cs}(n,\alpha)^{130}\text{I}$  was also measured, with  $^{130}\text{Xe}/^{132}\text{Xe} = 0.0014$ . The major isotopes in the Ba-derived xenon were  $^{131}\text{Xe}$  from  $^{132}\text{Ba}(n,2n)^{131}\text{Ba}$  and  $^{129}\text{Xe}$  from  $^{130}\text{Ba}(n,2n)^{129}\text{Ba}$ . Lesser amounts of other xenon isotopes were also produced, with relative abundances given by  $^{129}\text{Xe}:^{130}\text{Xe}:^{131}\text{Xe}:^{132}\text{Xe}:^{134}\text{Xe} = 1:0.019:1.084:0.221:0.194$ .

Absolute production cross sections were calculated from the isotope dilution analyses of the NaCl, Mg, CsCl, and  $\text{Ba}(\text{NO}_3)_2$  samples, assuming purity, stoichiometry, and quantitative noble gas retention and extraction. Relative production cross sections determined from neon isotopic ratios in the mineral samples were also considered in evaluating the neon production cross sections. Results are given in the accompanying table.

Reference: (1) Reedy R. C., Herzog G. F. and Jessberger E. K. (1979) Earth and Planetary Science Letters, 44, p. 341-348.

This work was performed under the auspices of the U. S. Department of Energy by Lawrence Livermore National Laboratory under contract No. W-7405-Eng-48.

PRODUCTION RATES  
Leich, D. A. et al.

Table: Production cross sections for Ne and Xe isotopes by 14.5 MeV neutrons.

Target	Product	Cross Section (mb)	
$^{23}\text{Na}$	$^{20}\text{Ne}$	137	$\pm 7$
$^{23}\text{Na}$	$^{21}\text{Ne}$	5.2	$\pm 0.4$
$^{23}\text{Na}$	$^{22}\text{Ne}$	304*	$\pm 15$
$\text{nat}_{\text{Mg}}$	$^{20}\text{Ne}$	83	$\pm 5$
$\text{nat}_{\text{Mg}}$	$^{21}\text{Ne}$	136	$\pm 7$
$\text{nat}_{\text{Mg}}$	$^{22}\text{Ne}$	12.2	$\pm 0.7$
$^{133}\text{Cs}$	$^{130}\text{Xe}$	2.4	$\pm 0.3$
$^{133}\text{Cs}$	$^{132}\text{Xe}$	1730	$\pm 90$
$\text{nat}_{\text{Ba}}$	$^{129}\text{Xe}$	1.65	$\pm 0.08$
$\text{nat}_{\text{Ba}}$	$^{130}\text{Xe}$	0.031	$\pm 0.002$
$\text{nat}_{\text{Ba}}$	$^{131}\text{Xe}$	1.79	$\pm 0.09$
$\text{nat}_{\text{Ba}}$	$^{132}\text{Xe}$	0.37	$\pm 0.02$
$\text{nat}_{\text{Ba}}$	$^{134}\text{Xe}$	0.32	$\pm 0.02$

\* Not including  $^{22}\text{Ne}$  from  $^{22}\text{Na}$  decay

LIVE  $^{129}\text{I}$  -  $^{129}\text{Xe}$  DATING. Kurt Marti, Chem. Dept. B-017, Univ. of California, San Diego, La Jolla, California 92093.

Introduction: We discuss a new technique of cosmic ray exposure age dating using cosmic ray produced  $^{129}\text{I}$  and  $^{129}\text{Xe}$  components. We will use the term "live  $^{129}\text{I}$ " to set apart from the well established "extinct  $^{129}\text{I}$ " used for early solar system chronology, as introduced by Reynolds (1960) and successfully applied to meteorites and other planetary objects. The chronometer pair in both cases is the radioisotope  $^{129}\text{I}$  ( $T_{1/2} = 1.57 \times 10^7\text{y}$ ) and radiogenic  $^{129}\text{Xe}$  as the stable daughter. Obviously the most useful information can be expected from materials which did not contain extinct  $^{129}\text{I}$ , but which contain target elements for cosmic ray reactions producing  $^{129}\text{I}$ . Before we consider the reactions of interest, it is useful to discuss the need for a new method.

Galactic Cosmic Ray Flux: Nishiizumi *et al.* (1980) carried out a systematic study of cosmic ray exposure ages of chondrites as a test for possible variation of the cosmic ray flux during the past few million years. Four calibrations were carried out using radioisotopes of varying half-lives:  $^{22}\text{Na}$ (2.6y),  $^{81}\text{Kr}$ ( $2.1 \times 10^5\text{y}$ ),  $^{26}\text{Al}$ ( $7.2 \times 10^5\text{y}$ ) and  $^{53}\text{Mn}$ ( $3.7 \times 10^6\text{y}$ ). Three of these calibrations were in very good agreement, indicating constancy of the galactic cosmic ray intensity. Calibrations based on  $^{26}\text{Al}$  disagreed in a systematic way. Moniot *et al.* (1983) used the nuclide  $^{10}\text{Be}$ ( $1.6 \times 10^6\text{y}$ ) in an additional calibration, and the result was in excellent agreement with those of Nishiizumi *et al.* Chondritic meteorites cannot be used to study flux variations on  $10^8\text{y}$  to  $10^9\text{y}$  time scales, but many iron meteorites are well suited for this purpose. There exists an excellent K isotopic data base, due to the work of Voshage and co-workers (e.g. Voshage, 1962), who pointed out a discrepancy between production rates based on  $^{40}\text{K}$ ( $1.28 \times 10^9\text{y}$ ) and those of the much shorter isotopes  $^{39}\text{Ar}$ (269y),  $^{36}\text{Cl}$ ( $3.0 \times 10^5\text{y}$ ),  $^{26}\text{Al}$  and others discussed above. Space erosion was considered as a possible cause, but a "recent" increase of the galactic cosmic ray intensity was the preferred explanation. A different method for calculating ages of iron meteorites was recently developed by Marti *et al.* (1984), which uses shielding corrected  $^{38}\text{Ar}$  production rates and eliminates meteorite samples with multistage irradiations. The results first confirm the suggestions of a "recent" increase of the cosmic ray flux and constrain the timing of the flux change to  $< 2 \times 10^8\text{y}$ . Furthermore, unexplained differences appear if exposure ages less than 200My are compared to those based on the  $^{40}\text{K}$ - $^{41}\text{K}$  method. Monitors for the  $10^7$ - $10^8\text{y}$  interval are required to further constrain the past cosmic ray flux. The  $^{129}\text{I}$  half-life is quite appropriate and makes this nuclide very attractive, since appropriate shielding corrections can be obtained as shown below.

Reactions on Te: Te is an ideal target element for reactions yielding  $^{129}\text{I}$ , and it will be especially suitable if low-energy secondary particles are predominant. The reactions  $^{128}\text{Te}(n,\gamma) ^{129}\text{Te} \xrightarrow{\beta^-} ^{129}\text{I}$  and  $^{130}\text{Te}(n,2n) ^{129}\text{Te} \xrightarrow{\beta^-} ^{129}\text{I}$  are both important. Browne and Berman (1973) estimate the resonance integral  $R = \int_{E_1}^{E_2} \frac{\sigma_\gamma(E)}{E} dE \approx 1.098\text{b}$

( $E_1 = 0.5\text{eV}$ ;  $E_2 = 7\text{KeV}$ ) and the thermal cross-section is  $\sigma_\gamma = 0.215\text{b}$ . The (n,2n) cross-sections are estimated to be  $\sim 1.5\text{b}$  for  $E_n \sim 15\text{MeV}$ , as observed for similar targets (e.g. Leich *et al.*, 1984, this volume). Kohman (1967) estimated the  $^{129}\text{I}$  production rate by (n,2n) reactions on  $^{130}\text{Te}$  to be about  $0.4 \text{ atoms/min}^{-1} \text{ g}^{-1}(\text{Te})$ , using the analogous reaction  $^{56}\text{Fe}(n,2n) ^{55}\text{Fe}$  and measured  $^{55}\text{Fe}$  activity in iron meteorites. Nishiizumi *et al.* (1983) measured  $^{129}\text{I}$  contents in 3 meteorites which are in reasonable agreement with this

92 208 - 0 6 V

Live  $^{129}\text{I} - ^{129}\text{Xe}$  Dating.

Kurt Marti

estimate, but they also notice that (n, $\gamma$ ) reactions are substantial for shielded sample locations. Proton reactions on  $^{130}\text{Te}$  via the reaction channels (p,2n), (p,pn); and (p, $\gamma$ ) on  $^{128}\text{Te}$  all make additional, but small, contribution to  $^{129}\text{I}$ . In all these reactions,  $^{129}\text{Xe}$  is produced via its precursor  $^{129}\text{I}$ , and this presents an ideal parent-daughter relationship. Cosmic ray reactions on Te provide a dating system which is independent of (self-correcting for) shielding, as long as the exposure geometry remains constant, because the fractional isobaric production ratio  $P(^{129}\text{I})/P_{129} \approx 1$ . For the case of a complex exposure history, these assumptions obviously are not valid and, for this reason, this method may also prove useful in identifying complex exposure histories.

The reactions  $^{130}\text{Te}(n,\gamma) ^{131}\text{Te} \xrightarrow{\beta^-} ^{131}\text{I} \xrightarrow{\beta^-} ^{131}\text{Xe}$ , and  $^{130}\text{Te}(p,\gamma) ^{131}\text{I} \xrightarrow{\beta^-} ^{131}\text{Xe}$ , produce  $^{131}\text{Xe}$

which can serve as a convenient monitor for cosmic ray reactions on Te targets. In general, it may be necessary to correct for competing reactions which co-produce  $^{129}\text{Xe}$  by different pathways such as extinct  $^{129}\text{I}$ , discussed earlier, or spallation Xe from Ba or heavier elements. Such reactions may be monitored using other Xe isotopes, and corrections may be small in favorable cases such as in Te-enriched and Ba-depleted minerals (e.g. troilite) which did not incorporate extinct  $^{129}\text{I}$  at the time of formation.

Live  $^{129}\text{I} - ^{129}\text{Xe}$  Ages: The content of  $^{129}\text{Xe} = ^{129}\text{Xe}_T + ^{129}\text{Xe}_R + ^{129}\text{Xe}_S + ^{129}\text{Xe}_{Te}$  can be corrected for trapped (T), radiogenic (R, from extinct  $^{129}\text{I}$ ) and spallation (S) components. The term of interest here ( $^{129}\text{Xe}_{Te}$ ), produced from Te targets, can then be compared to the  $^{129}\text{I}$  presently observed in the sample. The feasibility of  $^{129}\text{I}$  measurements in meteorite samples by accelerator mass spectrometry has been demonstrated by Nishiizumi *et al.* (1983). The sensitivity of the technique can still be improved, and it may become possible to measure  $^{129}\text{I}$  in sample sizes less than one gram. The ratio  $^{129}\text{Xe}_{Te}/^{129}\text{I}$  is related to the exposure age (T) by the relation:

$$F(T) \equiv \frac{\lambda_{129}T - 1 + e^{-\lambda_{129}T}}{1 - e^{-\lambda_{129}T}} = \left( \frac{^{129}\text{Xe}_{Te}}{^{129}\text{I}} \right)$$

It appears that exposure ages of about  $10^7\text{y}$  to several  $10^8\text{y}$  could be obtained, and that this range should overlap existing exposure age data at both ends. Murty and Marti (1984) recently tested the Xe systematics in the Cape York meteorite and observed a suitable mineral for I - Xe dating: Troilite which is free of silicate inclusions has Te concentrations of about 0.6 - 1.2ppm. They found that possible interferences from extinct  $^{129}\text{I}$  may be monitored using  $^{128}\text{Xe}$  from the  $^{127}\text{I}(n,\gamma)$  reaction, and that the products  $^{131}\text{Xe}$  from  $\text{Te}(n,\gamma)$  and  $^{83}\text{Kr}$  from  $^{82}\text{Se}(n,\gamma)$  serve as monitors for the target elements and provide information regarding the neutron energy spectrum.

Conclusion: The live  $^{129}\text{I} - ^{129}\text{Xe}$  method provides an ideal monitor for cosmic ray flux variations on the  $10^7\text{y} - 10^8\text{y}$  time-scale. It is based on low-energy neutron reactions on Te, and these data, when coupled to those from other methods, may facilitate the detection of complex exposure histories.

Acknowledgments: I thank K. Nishiizumi, J. R. Arnold and the late S. Regnier for several stimulating discussions. This work was supported by NASA grant NAG 9-41.

Live  $^{129}\text{I}$  -  $^{129}\text{Xe}$  Dating.

Kurt Marti

#### REFERENCES

- Browne J. C. and Berman B. L. (1973) Phys. Rev. C **8**, #6, 2405-2411.
- Kohman T. P. (1967) Carnegie Institute of Technology Progress Report, NYO-884-71, 50-62.
- Leich D. A., Borg R. J. and Lanier V. B. (1984) "Production Rates of Neon and Xenon Isotopes by Energetic Neutrons". This Volume.
- Marti K., Lavielle B. and Regnier S. (1984) (Abstract). Lunar and Planet. Science XV, p. 511-512, Lunar and Planet. Inst., Houston.
- Moniot R. K., Kruse T. H., Tuniz C., Savin W., Hall G. S., Milazzo T., Pal D. and Herzog G. F. (1983) Geochim. Cosmochim. Acta **4**, 1887-1895.
- Murty S. V. S. and Marti K. (1984) (Abstract). Lunar and Planet. Science XV, p. 581-582, manuscript in preparation.
- Nishiizumi K., Regnier S. and Marti K. (1980) Earth Planet. Sci. Lett. **50**, 156-170.
- Nishiizumi K., Elmore D., Honda M., Arnold J. R. and Gove H. E. (1983) Nature **305**, #5935, 611-612, Oct. 13.
- Reynolds J. H. (1960) Phys. Rev. Lett. **4**, 8.
- Voshage H. (1962) Z. für Naturf. **17a**, 422-432.

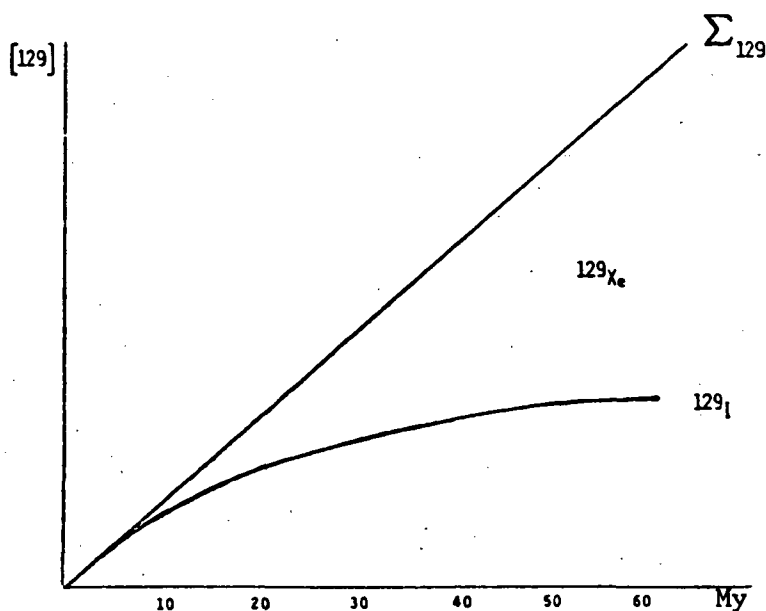


Figure 1: Relative abundances of  $^{129}\text{I}$  and  $^{129}\text{Xe}$  vs. time for a constant cosmic ray flux.

PRODUCTION OF RADIONUCLIDES IN ARTIFICIAL METEORITES IRRADIATED ISOTROPICALLY WITH 600 MeV PROTONS

R.Michel, P.Dragovitsch, P.Englert and U.Herpers, Institut für Kernchemie der Universität zu Köln, Zülpicher Str. 47, D-5000 Köln-1, FRG.

The understanding of the production of cosmogenic nuclides in small meteorites ( $R < 40$  cm) still is not satisfactory. The existing models for the calculation of depth dependent production rates, e.g. /1-6/, do not distinguish between the different types of nucleons reacting in a meteorite. They rather use general depth dependent particle fluxes to which cross sections have to be adjusted to fit the measured radionuclide concentrations. Some of these models not even can be extended to zero meteorite sizes without logical contradictions. Therefore, a series of three thick target irradiations was started at the 600 MeV proton beam of the CERN isochronous cyclotron in order to study the interactions of small stony meteorites with galactic protons. In contrast to earlier thick target experiments /7/, and references therein, and to recent experiments for the simulation of the GCR irradiation of large meteorites /8/, in these new experiments a homogeneous  $4\pi$ -irradiation of the thick targets is performed. The irradiation technique used provides a realistic meteorite model which allows a direct comparison of the measured depth profiles with those in real meteorites. Moreover, by the simultaneous measurement of thin target production cross sections one can differentiate between the contributions of primary and secondary nucleons over the entire volume of the artificial meteorite.

In most earlier thick target experiments only limited aspects of the production of cosmogenic nuclides were studied, i.e. some special radioisotopes or a particular rare gas was measured. In contrast, the new experiments shall provide an universal simulation for a wide variety of cosmogenic nuclides. For this purpose an international collaboration of 10 laboratories was initiated /9/ providing all necessary scientific and technical means. So radionuclide production is measured by  $\gamma$ -spectrometry instrumentally and by low-level counting and accelerator mass spectrometry after chemical separation, while the rare gases from He to Xe are studied by static mass spectrometry. The measurements are supported by Monte Carlo calculations of the nuclear cascades in the thick targets. Model calculations using the thus derived nucleon fluxes and experimental thin target excitation functions in combination with all the measured thick target production depth profiles then will provide a unification of the classical thin target and thick target approaches for the description of the production of cosmogenic nuclides in small meteorites.

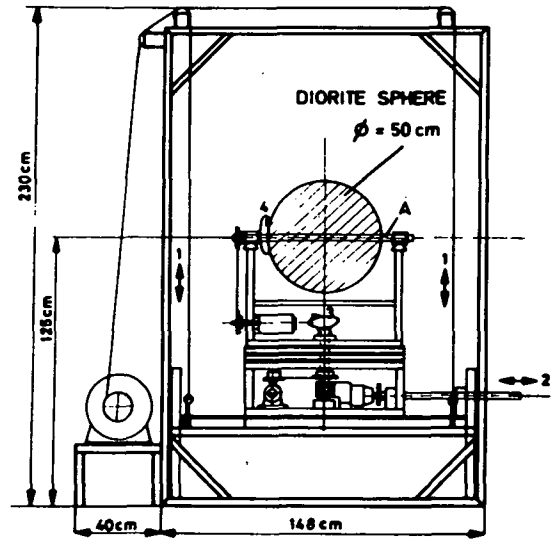


Fig. 1: Experimental set up used for the irradiation of an artificial meteorite with 50 cm diameter. The length of the arrangement was 126 cm.

## RADIONUCLIDES IN ARTIFICIAL METEORITES

Michel, R. et al.

In the first experiment in Feb. 1983 an artificial meteorite with 10 cm diameter was irradiated and a GCR irradiation age of about 76 My was simulated. A description of this experiment and first results are given elsewhere /10-12/. But the measurements and evaluations are still going on.

In the second experiment an artificial meteorite of 50 cm diameter was irradiated for 12 h with a proton flux of 2.5  $\mu\text{A}$  in Dec. 1983. The homogeneous  $4\pi$ -irradiation of the target was achieved by a machine (fig. 1) performing 4 independent movements of the artificial meteorite in the beam. Two translational movements (1) and (2) moved the sphere in the indicated directions by 50 cm, each, with velocities of 3.3 cm/min (vertical) and 11. cm/min (horizontal). They simulated a parallel homogeneous proton rain over a  $50 \times 50 \text{ cm}^2$  plane. Further the stony sphere made two rotations (3) and (4) with 2 and 5 rpm respectively, thus resulting in a perfect  $4\pi$ -irradiation. The primary proton flux through the sphere was measured by a 50 cm x 50 cm Al-foil which also made the translational movements and which shadowed the artificial meteorite during irradiation. By the investigation of this Al-foil the homogeneity of the parallel proton rain was proved.

The sphere itself was made out of diorite slabs ( $\rho=3.0 \text{ g/cm}^3$ ,  $\text{H}_2\text{O} \leq 10^{-3} \text{ g/g}$ ). It contained a Fe tube (A) with an inner diameter of 1.9 cm. This tube contained 9 Al boxes which were filled with pure element target foils, some chemical compounds and carefully degassed samples of the meteorite JILIN. These targets covered the elements O, Mg, Al, Si, S, Ca, Ti, V, Mn, Fe, Co, Ni, Cu, Zr, Rh, La, Lu, Ba, Te, Au, and Pb. First results are shown in fig. 2. The artificial meteorite received a 600 MeV proton dose of  $2.49 \times 10^{14} \text{ cm}^{-2}$  which is equivalent to a cosmic irradiation age of 4 My. The homogeneity of the irradiation can be seen from the results for Be-7 which - at least from Fe - is exclusively produced by primary particles. The Be-7 profiles from Al and Fe are constant over the entire artificial meteorite within 8.0 % and 3.5 %, respectively. For the other radionuclides the depth profiles show strong increases from the surface to the interior exhibiting important contributions of secondary particles. For Na-22 and Na-24 from Al the increase is by factors of 1.6 and 1.7, respectively. The profiles are fairly symmetric. The production of Mn-54 and Co-56 from Fe increases by factors of 1.6 and 1.5.

Co-56 from Fe is of particular interest, since it is exclusively produced by proton induced reactions. Thus the depth profiles of Co-56 from Fe exhibits the action of secondary protons while for Mn-54 and other low energy products reaction of both, secondary protons and neutrons, have to be taken into account.

Generally, the production of Co-56 and Mn-54 from Fe in this meteorite model (fig. 2) are higher than in the sphere with 10 cm diameter (fig. 3). The depth profiles measured for the small sphere show a smaller but still significant increase from the surface to the interior by 20 to 30 %. The generally higher production rates of these nuclides in the big sphere surely are due to the larger amount of secondaries produced in the total targets. For Co-56, however, the maximum production rates are higher by 20 % in the big sphere than in the small one, while for Mn-54 the center production rates even are higher by a factor of 1.6 in the large meteorite model. These first results already demonstrate that in small meteorites the contributions of secondary protons and neutrons are changing with the meteorite sizes and that these

## RADIONUCLIDES IN ARTIFICIAL METEORITES

Michel, R. et al.

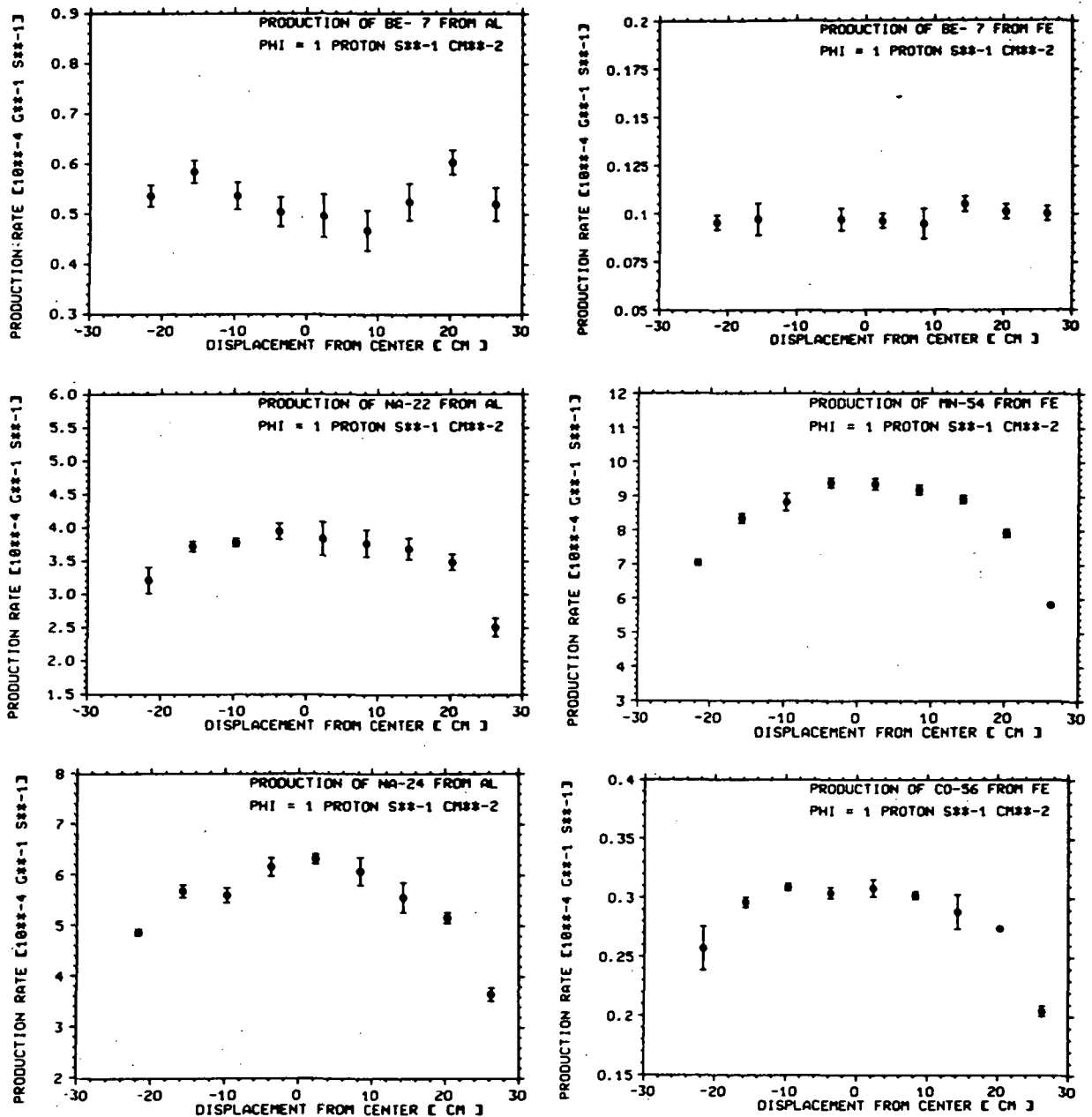


Fig. 2: Depth profiles for the production of radionuclides from Al and Fe in an artificial meteorite ( $\rho=3 \text{ g/cm}^3$ ) with a diameter of 50 cm. The production rates are normalized to a  $4\pi$ -integrated flux of primary protons of  $1 \text{ cm}^{-2} \text{ s}^{-1}$ .

changes are depending on the types of the secondary nucleons.

Consequently, a model describing the production of cosmogenic nuclides in small meteorites has carefully to distinguish between the different types of reacting particles and their depth dependent fluxes. Such a model has to consider the contributions of primary and secondary galactic as well as of solar particles. The interaction of primary solar and galactic cosmic rays with

## RADIONUCLIDES IN ARTIFICIAL METEORITES

Michel, R. et al.

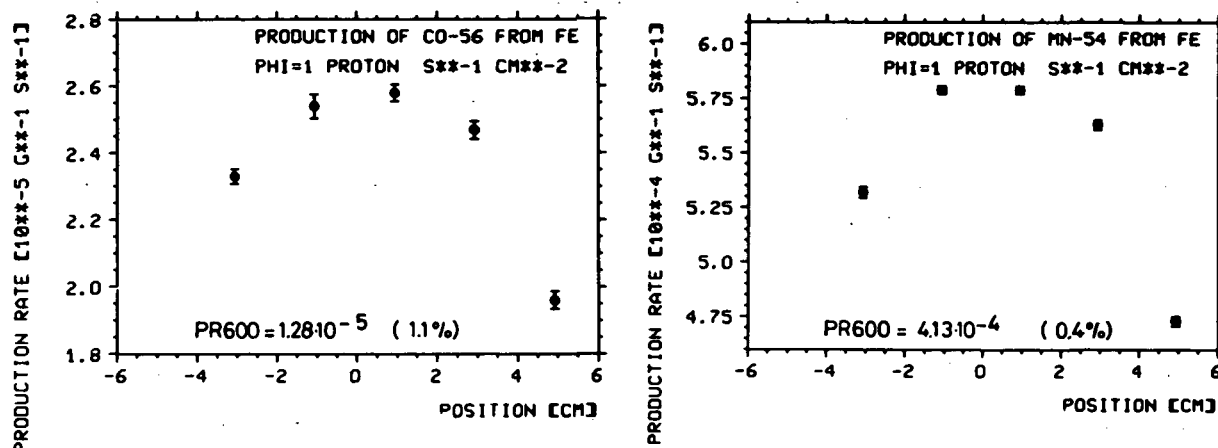


Fig. 3: Depth profiles for the production of Mn-54 and Co-56 from Fe in an artificial meteorite ( $\rho=3 \text{ g/cm}^3$ ) with a diameter of 10 cm. The production rates are normalized to a  $4\pi$ -integrated flux of primary protons of  $1 \text{ cm}^{-2} \text{ s}^{-1}$ . The PR 600 values are the production rates due to primary 600 MeV protons only. The errors of these production rates are given in parentheses.

meteorites can be calculated with good a priori accuracy /13,14/. A description of the depth dependent contributions of secondary protons and neutrons will be possible on the basis of the experimental thick target production rates measured in the present simulation experiments.

#### References

- 1) J.R.Arnold et al., J.Geophys.Res. 66 (1961) 3519
- 2) A.K.Lavrukina and G.K.Ustinova, EPSC 15 (1972) 137
- 3) R.C.Reedy et al., EPSC 44 (1979) 341
- 4) S.K.Bhattacharya et al., EPSC 51 (1980) 45
- 5) M.Bhandari and M.B.Potdar, EPSC 58 (1982) 116
- 6) R.C.Reedy, LPS XV (1984) 675, and Proc. 15th Lun.Plan.Sci. (1984) in press
- 7) H.Weigel et al., Radiochimica Acta 21 (1974) 179
- 8) P.Englert et al., LPS XIV (1983) 175
- 9) R.Michel for Cologne Collaboration in: "Experiments at CERN in 1983", Geneve Sept. 1983, p 278
- 10) R.Michel et al., LPS XV (1984) 542
- 11) S.Theis et al., LPS XV (1984) 854
- 12) P.Englert et al., Nucl.Inst.Methods (1984) in press
- 13) R.Michel et al., EPSL 59 (1982) 33, *ibid* 64 (1983) 174
- 14) R.Michel and R.Stüch, J.Geophys.Res. 89, Suppl. (1984) B673

Acknowledgement: This work was supported by the Deutsche Forschungsgemeinschaft

RESONANCE IONIZATION MASS SPECTROMETRY FOR ISOTOPIC ABUNDANCE  
MEASUREMENTS; C. M. Miller, Los Alamos National Laboratory

Resonance ionization mass spectrometry (RIMS) is a relatively new laser-based technique for the determination of isotopic abundances. The resonance ionization process depends upon the stepwise absorption of photons from the laser, promoting atoms of the element of interest through progressively higher electronic states until an ion is formed. Sensitivity arises from the efficiency of the resonant absorption process when coupled with the power available from commercial laser sources. Selectivity derives naturally from the distinct electronic structure of different elements. This isobaric discrimination has provided the major impetus for development of the technique.

Resonance ionization mass spectrometry in our laboratory has been explored for analysis of the isotopic abundances of the rare earth lutetium. Isobaric interferences from ytterbium severely affect the ability to measure small amounts of the neutron-deficient Lu isotopes (mass 170-174) by conventional mass spectrometric techniques. Separation chemistry is of limited utility to date in eliminating the ytterbium interferences.

Resonance ionization for lutetium is performed using a continuous-wave laser operating at 452 nm, through a sequential two-photon process, with one photon exciting the intermediate resonance and the second photon causing ionization. Ion yields for microgram-sized quantities of lutetium lie between  $10^6$  and  $10^7$  ions per second, at overall ionization efficiencies approaching  $10^{-4}$ . Discrimination factors against ytterbium greater than  $10^6$  have been measured. Table 1 shows the results of a recent analysis of a 60 nanogram Lu sample, where the RIMS ratios are compared to thermal ionization ratios. The effect of isobaric Yb in the latter is readily apparent. Also, it should be noted that the  $^{173}\text{Lu}$  content of the sample was only  $10^8$  atoms.

Resonance ionization for technetium is also being explored, again in response to an isobaric interference, molybdenum. Because of the relatively high ionization potential for Tc, three-photon, two-color RIMS processes are being developed. A variety of these schemes have been cataloged, virtually assuring a selective excitation process can be found. To date, however,

Resonance Ionization Mass Spectrometry  
 Miller C. M.

sensitivity has been limited, with ionization efficiencies of only  $10^{-8}$  demonstrated. Evidence exists for a molecular Tc species that is not responsive to resonant excitation. Development work for Tc RIMS is continuing.

Table 1 - Isotope Ratio Measurements

<u>Ratio</u>	<u>RIMS (Lu alone)</u>	<u>Thermal (Lu and Yb)</u>
173/175	$4.4 \times 10^{-7}$	$3.36 \times 10^{-3}$
174/175	$3.62 \times 10^{-6}$	$9.29 \times 10^{-4}$
176/175	$2.64 \times 10^{-2}$	$2.63 \times 10^{-2}$

## COMPILATION OF COSMOGENIC RADIONUCLIDES IN METEORITES.

K. Nishiizumi, Dept. of Chemistry, B-017, Univ. of Calif., San Diego,  
La Jolla, CA 92093

Since 1958, when long half-life cosmogenic nuclides in meteorites were first reported, a large amount of data has been published in different journals. The rapid growth in the accumulation of data in the last decade was caused by two new techniques. The neutron activation method was developed for  $^{53}\text{Mn}$  determination. Accelerator mass spectrometry was now widely used for other nuclides. The cosmogenic nuclide data provide much information about the meteorites, especially concerning the last few million years time scale. Some examples are cosmic-ray exposure age, terrestrial age, complex irradiation history, size and depth of the sample in the meteoroid, cosmic-ray intensity and so on. If one combines the cosmogenic radionuclide data and noble gas and cosmic-ray track data, more detailed discussion will be possible. Schultz and Kruse have previously compiled light noble gas data in meteorites [1]. Bhandari et al compiled nuclear track data [2].

I have compiled all available data for the concentration of cosmogenic nuclides  $^{53}\text{Mn}$  ( $t_{1/2} = 3.7 \times 10^6$  years),  $^{26}\text{Al}$  ( $7.05 \times 10^5$  years),  $^{10}\text{Be}$  ( $1.6 \times 10^6$  years),  $^{36}\text{Cl}$  ( $3.0 \times 10^5$  years) and  $^{21}\text{Ne}$ , and  $^{22}\text{Ne}/^{21}\text{Ne}$  ratios in stony, iron, and stony-iron meteorites. For iron meteorites, the  $^4\text{He}/^{21}\text{Ne}$  ratio was adopted instead of  $^{22}\text{Ne}/^{21}\text{Ne}$  ratio, because the  $^4\text{He}/^{21}\text{Ne}$  ratio in iron meteorites indicates the shielding condition of the sample. The compilation contains over 2000 different analyses for four cosmogenic radionuclides (see Table 1). The list also contains about 200 unpublished data by the author. A preliminary version of the table will be presented at the meeting. Final compilation will be published elsewhere soon. I would be most grateful to receive additional data, published or unpublished.

## REFERENCES:

- [1] Schultz L. and Kruse H. (1978) Nucl. Track Detection 2, p. 65-103.  
[2] Bhandari N., Lal D., Rajan R. S., Arnold J. R., Marti K. and Moore C. B. (1980) Nucl. Track 4, p. 213-262.

TABLE 1

	No. of meteorites	$^{53}\text{Mn}$	$^{26}\text{Al}$	$^{10}\text{Be}$	$^{36}\text{Cl}$
Stony	674	431	839	128	110
Stony-iron	20	27	6	7	31
Iron	89	125	87	55	146
Total	783	583	982	190	287

REDETERMINATION OF PARAMETERS FOR SEMI-EMPIRICAL MODEL FOR SPALLOGENIC He AND Ne IN CHONDRITES. L.E. Nyquist, SN4/NASA Johnson Space Center, Houston, TX 77058 and A.F. McDowell, Lunar and Planetary Institute, 3303 NASA Rd 1, Houston, TX 77058

The semi-empirical model described previously (1,2) satisfactorily reproduced a number of shielding-dependent variations in the relative production rates of spallogenic He and Ne in chondrites. However, data for cores of the Keyes and St. Severin meteorites (3,4) showed a subsurface build-up in <sup>3</sup>He which was not predicted with the original model parameters and the model was not pursued. Renewed interest in the preatmospheric size of meteorites, spurred in part by the desirability of understanding the exposure history of the SNC meteorites, justifies redetermination of model parameters.

In the semi-empirical model (5) the production rate of nuclide i is

$$P_i = A_i [e^{-\mu_a d} - B_i e^{-\mu_s d}]$$

where  $\mu_j = N\rho\sigma_j/A$ , j = a,s. N is Avogadro's number and A and  $\rho$  are the average atomic weight and the density, respectively, of the meteoritic material.  $\sigma_a$  and  $\sigma_s$  are the interaction cross sections for primary and secondary cosmic rays, respectively. Values of  $\mu_a$  and  $\mu_s$  were obtained by scaling the values determined by (5) for the Grant iron meteorite assuming that  $\sigma_a$  and  $\sigma_s$  are proportional to  $A^{2/3}$ (1). In principle, these parameters can also be independently determined from the Keyes and St. Severin data. However, this was not attempted since it was found to be possible to fit those data by varying only the  $A_i$  and  $B_i$ .

Values of  $A_i$  and  $B_i$  obtained from various applications of the model are summarized in Table 1. It is possible to obtain good fits to the concentration gradients of <sup>3</sup>He, <sup>21</sup>Ne, and <sup>22</sup>Ne with depth and to reproduce the <sup>3</sup>He/<sup>21</sup>Ne vs. <sup>22</sup>Ne/<sup>21</sup>Ne trends in the Keyes and St. Severin meteorites with the same model parameters. It is also possible to reproduce the "Bern line" (6) by varying the size of the model meteoroids. However, in this latter case, different model parameters are required than those which yield fits to the Keyes and St. Severin data. This result is a consequence of the fact that the <sup>3</sup>He/<sup>21</sup>Ne-<sup>22</sup>Ne/<sup>21</sup>Ne trends for the individual meteorites do not parallel the "Bern line". It is possible to mimic the general trend of the "Bern correlation" by juxtaposition of a family of lines calculated with the same  $B_i$  as used for Keyes and St. Severin by assuming that all meteoroids are similar in size and by varying the values of  $A_3/A_{21}$  and  $A_{22}/A_{21}$  within the limits given in Table 1 for the "Bern family". One possible physical interpretation of this result is that the effective cosmic ray flux varies for different meteorites, perhaps due to a spatial concentration gradient which affects primarily the lower energy particles.

TABLE 1. MODEL PARAMETERS

	A <sub>3</sub>	A <sub>21</sub>	A <sub>22</sub>	A <sub>3</sub> /A <sub>21</sub>	A <sub>22</sub> /A <sub>21</sub>	B <sub>3</sub>	B <sub>21</sub>	B <sub>22</sub>
St. Severin	17.6	4.78	4.63	3.68	0.968	0.91	0.97	0.947
Keyes	31.6	8.21	8.29	3.85	1.01	0.91	0.97	0.953
Bern line				3.3	1.04	0.85	0.97	0.954
Bern family				2.4-5.5	0.965-1.11	0.91	0.97	0.953

REFERENCES: (1) Nyquist L.E. (1969) Ph. D. Thesis, Univ. of Minn. (2) Nyquist L.E. (1984) LPS XV, 613. (3) Wright R.J. et al. (1973) JGR 78, 1308. (4) Schultz L. and Signer P. (1976) EPSL 30, 191. (5) Signer P. and Nier A.O. (1960) JGR 65, 2945. (6) Eberhardt P. et al. (1966) Z. Naturforsch. 21A, 414.

CALCULATIONS OF COSMOGENIC NUCLIDE PRODUCTION RATES IN THE EARTH'S ATMOSPHERE AND THEIR INVENTORIES; Keran O'Brien, Environmental Measurements Laboratory, New York, N.Y. 10014

The production rates of cosmogenic isotopes in the Earth's atmosphere and their resulting terrestrial abundances have been calculated, taking into account both geomagnetic and solar-modulatory effects.

The local interstellar flux was assumed to be that of Garcia-Munoz, et al. (1) Solar modulation was accounted for using the heliocentric potential model (2) and expressed in terms of the Deep River neutron monitor count rates. (3) The geomagnetic field was represented by vertical cutoffs calculated by Shea and Smart (4) and the non-vertical cutoffs calculated using ANGRI. (5)

Variations in geomagnetic field strength were modelled by changing the magnitude of the vertical cutoffs in proportion to the change in the magnitude of the geomagnetic field strength.

The local interstellar particle flux was first modulated using the heliocentric potential field. The modulated cosmic-ray fluxes reaching the earth's orbit then interacted with the geomagnetic field as though it were a high-pass filter.

The interaction of the cosmic radiation with the earth's atmosphere was calculated utilizing the Boltzmann transport equation. (6) Spallation cross sections for isotope production were calculated using the formalism of Silberberg and Tsao (7,8) and other cross sections were taken from standard sources.

Inventories were calculated by accounting for the variation in solar modulation and geomagnetic field strength with time. Results for many isotopes, including C-14, Be-7 and Be-10 are in generally good agreement with existing data. The C-14 inventory, for instance, amounts to  $1.75 \text{ cm}^2 \text{ s}^{-1}$ , in excellent agreement with direct estimates. (9,10)

#### REFERENCES

1. Garcia-Munoz, M., Mason, G. M. and Simpson, J. A. (1975) Ap. J., 202, pp. 265-275.
2. Gleeson, L. J. and Axford, W. I. (1967) Ap. J., 147, pp. L116-L118.
3. O'Brien, K. and Burke, G. de P. (1973) J. Geophys. Res., 78, pp. 3013-3019.
4. Shea, M. A. and Smart, D. (1967) J. Geophys. Res., 72, pp. 2021-2027.

## CALCULATIONS OF COSMOGENIC NUCLIDES

O'Brien, K.

5. Bland, C. J. and Cioni, G. (1968) Earth Planet. Sci. Lett. 4, pp. 339-405.
6. O'Brien, K. (1975) Natural Radiation Environment II, USERDA rep. CONF-72085, pp. 15-54.
7. Silberberg, R. and Tsao, C. H. (1973) Ap. J. Supplement Series 25, pp. 315-333.
8. Silberberg, R. and Tsao, C. H. (1973) Ap. J. Supplement Series 25, pp. 335-367.
9. Grey, D. (1974) PhD Thesis, Univ. of Ariz., Univ. Microfilms, Ann Arbor, Michigan.
10. Damon, P. E., Lerman, J. C. and Long, A. (1978), Ann. Rev. Earth Planet. Sci., 6, pp. 457-494.

$^{10}\text{Be}$  CONTENTS OF SNC METEORITES; D.K. Pal, C. Tuniz<sup>1</sup>, R.K. Moniot<sup>2</sup>, W. Savin<sup>3</sup>, S. Vajda, T. Kruse, and G.F. Herzog, Depts. Chemistry and Physics, Rutgers Univ., New Brunswick NJ 08903. <sup>1</sup>Istituto di Fisica, Univ. degli Studi, Trieste, Italy and Istituto Nazionale Fisica Nucleare, Sez. di Trieste, Italy, <sup>2</sup>Div. Sci. Math., Fordham Univ., New York, NY 10023, <sup>3</sup>Dept. Physics, NJ Inst. Tech., Newark, NJ 07100

Several authors have explored the possibility that the Shergottites, Nakhlites, and Chassigny came from Mars (e.g., 1-3). The spallogenic gas contents of the SNC meteorites have been used to constrain the sizes of the SNC's during the last few million years, to establish groupings independent of the geochemical ones and to estimate the likelihood of certain entries in the catalog of all conceivable passages from Mars to Earth (3-5).

Measurements of the radioactive, cosmogenic nuclides supplement the stable isotope data. The  $^{26}\text{Al}$  contents of six of the SNC meteorites are known but their interpretation is complicated by the sensitivity of the  $^{26}\text{Al}$  production rate to the bulk Al content, a property that varies more than tenfold among the SNC meteorites. In contrast, differences in chemical composition are expected to induce variations of less than 10% in the  $^{10}\text{Be}$  contents (6). Furthermore, the  $^{10}\text{Be}$  production rate,  $P_{10}$ , varies relatively little over the typical range of meteoroid sizes, i.e., in bodies with preatmospheric radii between 20 and 150 g/cm<sup>2</sup> although it does fall rapidly in larger bodies and rises in the interior of St-Severin-sized objects (7-11). The particular shielding dependence of  $^{10}\text{Be}$  makes the isotope a good probe of the irradiation conditions experienced by the SNC meteorites. We have measured the  $^{10}\text{Be}$  contents of all the members of the group by using the technique of accelerator mass spectrometry (9). The results appear in Table 1.

Samples. With the possible exception of Chassigny, the samples analyzed for  $^{10}\text{Be}$  come from the same meteorite fragments as those analyzed for the noble gases. The  $^{26}\text{Al}$  measurements for EETA 79001, ALHA 77005 and Nakhla also refer to the same fragments. The samples of EETA 79001 had been prepared by E. Jarosewich for other purposes. We used about 50 mg of meteorite for each  $^{10}\text{Be}$  determination.

Adjustments for Chemical Composition. To remove the effects of chemical composition from the  $^{10}\text{Be}$  and  $^{21}\text{Ne}$  data we multiplied each one by a chemical normalization factor, C, calculated according to the relation  $C = P_{\text{Shergotty}}/P_X$ . The production rates were obtained from equations and composition data in the literature.

$^{10}\text{Be}$  Contents and Shielding. The  $^{10}\text{Be}$  contents of Nakhla, Governador Valadares, Chassigny, and probably Lafayette, about 20 dpm/kg, exceed the values expected from irradiation of the surface of a large body. The  $^{10}\text{Be}$  data therefore do not support scenario III of Bogard et al. (5), one in which most of the  $^{10}\text{Be}$  in the SNC meteorites would have formed on the Martian surface; they resemble rather the  $^{10}\text{Be}$  contents found in many ordinary chondrites subjected to  $4\pi$  exposures. Judging from the calculations of Reedy (10), the meteorites named above orbited for several million years as bodies with radii less than 2 m or so.

$^{10}\text{Be}$  Exposure Ages. The uncertainties of the  $^{10}\text{Be}$  contents lead to appreciable errors in the  $^{10}\text{Be}$  ages,  $t_{10} = -1/\lambda \ln(1 - ^{10}\text{Be}/^{10}\text{Be}_0)$ , given in Table 1. Nonetheless, the  $^{10}\text{Be}$  ages are consistent with the  $^{21}\text{Ne}$  ages calculated assuming conventional, small-body production rates and short terrestrial ages for the finds. We believe that this concordance strengthens the case for at least 3 different irradiation ages for the SNC meteorites (5). Given the similar half-thicknesses of the  $^{10}\text{Be}$  and  $^{21}\text{Ne}$  production rates, the ratios of

the  $^{10}\text{Be}$  and  $^{21}\text{Ne}$  contents do not appear consistent with common ages for any of the groups. In view of the general agreement between the  $^{10}\text{Be}$  and  $^{21}\text{Ne}$  ages it does not seem useful at this time to construct multiple-stage irradiation histories for the SNC meteorites.

REFERENCES 1) Wood, C.A. and Ashwal, L.D. (1981), Proc. 12 Lunar Planet. Sci. Conf., 1359-1375. 2) McSween, H.Y. and Stolper, E.M. (1980), Scientific American 242, 54-63. 3) Wasson, J.T. and Wetherill, G.W. (1979), in Asteroids (Ed. T. Gehrels) Univ. Arizona Press, Tucson, pp. 926-974; Wetherill, G.W. (1984), Meteoritics 19, 1-13. 4) Pepin, R.O. and Becker, R.H. (1984), Lunar Planet. Sci. 15, 637-8. 5) Bogard, D.D., Nyquist L.E. and Johnson, P. (1984), preprint. 6) Pal, D.K., Tuniz, C., Moniot, R.K., Savin, W., Kruse, T.H. and Herzog, G.F. (1984), in preparation. 7) Pal, D.K., Moniot, R.K., Kruse, T.H., Tuniz, C. and Herzog, G.F. (1982), Proc. 5th Int. Conf. Geochron. Cosmochron. Isotope Geol., Nikko Natl. Park, Japan. pp. 300-1. 8) Nishiizumi, K., Arnold, J.R., Elmore, D., Tubbs, L.E., Cole, G. and Newman, D. (1982), Lunar Planet. Sci. 13, 596-7. 9) Moniot, R.K., Kruse, T.H., Savin, W., Hall, G., Milazzo, T. and Herzog, G.F. (1982), Nucl. Inst. Meth. 203, 495-502. 10) Reedy, R.C. (1984), Lunar Planet. Sci. 15, 675-6. 11) Tuniz, C., Smith, C.M., Moniot, R.K., Savin, W., Kruse, T.H., Pal, D.K., Herzog, G.F. and Reedy, R.C. (1984), Geochim. Cosmochim. Acta, in press; Tuniz, C., Moniot, R.K., Savin, W., Kruse, T.H., Smith, C.M., Pal, D.K. and Herzog, G.F. (1984), 3rd Int. Symp. Accelerator Mass Spectrom. Zurich, Switzerland. Abstract. 12) Bogard, D.D., Cressy, Jr., P.J. (1973), Geochim. Cosmochim. Acta 37, 527-546. 13) Hohenberg, C.M., Marti, K., Podosek, F.A., Reedy, R.C. and Shirck, J.R. (1978), Proc. Lunar Sci. Conf., 9th, 2311-2344. 14) Hampel, W., Wanke, H., Hofmeister, H., Spettel, B. and Herzog, G.F. (1980), Geochim. Cosmochim. Acta 44, 539-547. 15) Heymann, D., Mazor, E., and Anders, E. (1968), Geochim. Cosmochim. Acta 32, 1241-1268. 16) Ganapathy, R. and Anders, E. (1969), Geochim. Cosmochim. Acta 33, 775-787. 17) Lancet, M.S. and Lancet, K. (1971), Meteoritics 6, 81-86. 18) Schultz, L. and Kruse, H. (1978), Nucl. Track Detection 2, 65-103.

Table 1.  $^{10}\text{Be}$  Contents of SNC Meteorites.

Meteorite	IDA <sup>a</sup>	$^{21}\text{Ne}$ ( $10^{-8}\text{cm}^3\text{STP/g}$ )	Ref.	C <sub>21</sub>	t <sub>21</sub> <sup>b</sup> (Ma)	$^{10}\text{Be}$ (dpm/kg)	C <sub>10</sub>	t <sub>10</sub> <sup>b</sup> (Ma)
Shergotty	U817	0.58	15	1.0	3.2	13±1.5	1	2.2
Zagami	O1966,54	0.69	15	0.95	3.6	18.6±2.6	0.99	4.6
ALHA 77005	U/EJ	0.75	5	0.56	2.3	15±3	0.95	2.6
EETA 79001A	U/EJ	0.14	4,5	0.78	0.6	7.8±1.1	0.96	1.0
EETA 79001B	U/EJ	0.12d	5	1.06	0.7	8.5±1.1	0.99	1.2
Nakhla	Me804	3.10	16	0.95	16.3	19.7±3.3	1.02	>5c
Lafayette	Me2116	2.70	16	0.95	14.2	18.1±2.5	1.02	>5c
Governador Valadares	LN	2.10	5	1.0	11.7	25.6±3.6	1.03	>5c
Chassigny	P2523	4.14	17,18	0.53	12.2	20.5±3.1	0.97	>5c

- a) We thank the sample donors: LN=L. Nyquist (JSC); Me=E. Olsen (Field Museum); O=R. Hutchinson (Brit. Museum); U=E. Jarosewich (Smithsonian).
- b) Assumes  $P_{10}=21.3$  dpm/kg and  $P_{21}=0.18 \times 10^{-8}\text{cm}^3\text{STP/g-Ma}$  in Shergotty. Uncertainties in t<sub>10</sub> range from 25 to 50%.
- c) High gas and  $^{10}\text{Be}$  contents indicate unreliable  $^{10}\text{Be}$  age.
- d) Considered doubtful by Bogard et al. (Ref. 5).

STUDIES ON COSMOGENIC NUCLIDES IN METEORITES WITH REGARD TO AN  
APPLICATION AS POTENTIAL DEPTH INDICATORS

R.Sarafin, U.Herpers and P.Englert

Institut für Kernchemie der Universität zu Köln,  
D-5000 Köln 1

R.Wieler and P.Signer

Institut für Kristallographie und Petrographie der ETH Zürich,  
CH-8092 Zürich

G.Bonani, H.J.Hofmann, E.Morenzoni, M.Nessi, M.Suter and W.Wölfli

Laboratorium für Mittelenergiephysik der ETH Zürich,  
CH-8093 Zürich

Measurements of stable and radioactive spallation products in meteorites allow to investigate their histories, especially with respect to the exposure to galactic cosmic ray particles and the pre-atmospheric size of the object. While the concentrations of spallation products lead to the determination of exposure and terrestrial ages, production rate ratios are characteristic for the location of the sample in the meteorite. So, one of the aims of our investigations on meteorites is to obtain depth indicators from suitable pairs of cosmogenic nuclides.

Because of the different depth profiles for nuclide productions it is necessary to determine the concentrations of a larger number of spallation products in aliquots of a single small sample. Such "same sample" measurements of  $^{10}\text{Be}$  and light noble gases were performed on 15 ordinary chondrites (7 H- and 8 L-chondrites) which had previously been studied for  $^{26}\text{Al}$  and  $^{53}\text{Mn}$  at Cologne [1,2].  $^{10}\text{Be}$  was determined by accelerator mass spectrometry using the AMS-facility at the ETH Zürich, the noble gases were measured by static mass spectrometry. The experimental details are given elsewhere [3], some of the results are summarized in table 1. The errors of the  $^{10}\text{Be}$ - and  $^{26}\text{Al}$ -values are 3-5%, based on counting statistics. In the case of the  $^{22}\text{Ne}/^{21}\text{Ne}$ -ratios and the  $^{53}\text{Mn}$ -data the errors are estimated to be 2% and 5-10% respectively, including statistical and systematical uncertainties.

Tab. 1: Compilation of data on cosmogenic nuclides from aliquot samples of 15 ordinary chondrites. The production rates were calculated from the  $^{21}\text{Ne}$ -ages [3] and normalized to chemical composition. ( $^{10}\text{Be}$ - and Ne-data from [3] and recent measurements,  $^{26}\text{Al}$  and  $^{53}\text{Mn}$  unless otherwise cited cf. [1]).

Meteorite	Class	spall. $^{22}\text{Ne}/^{21}\text{Ne}$	Production - Rates		
			$^{10}\text{Be}$ [dpm/kg]	$^{26}\text{Al}$ [dpm/kg Si <sub>equ</sub> ]	$^{53}\text{Mn}$ [dpm/kg Fe]
Armel Yuma	L5	1.155	17.8	354	500
Atwood	L6	1.124	16.9	195	413
Bledsoe	H4	1.087	19.2	251	555
Calliham	L6	1.109	18.2	294	497
Claytonville	L5	1.139	18.6	314	407
Eva	H5	1.113	17.9	241	271
Floyd	H4	1.091	19.9	386	470
Hardtner	L	1.085	17.9	288	181
Kiel	L6	1.251	18.3		317 [2]
Loop	L6	1.118	17.6	309	294
Portales No.3	H4-5	1.077	21.0	311	599
Potter	L6	1.109	17.3	274	440
Seminole	H4	1.096	19.6	329	424
Toulon	H5	1.139	17.7	408	319
Willowdale	H	1.066	18.4	328	492

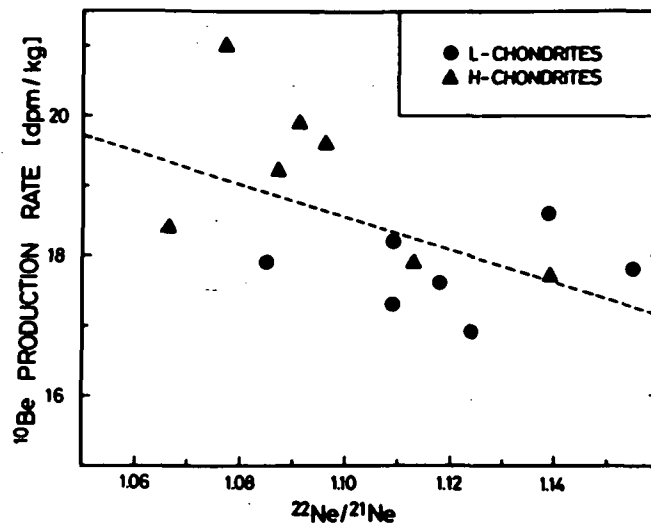
Since long the ratio  $^{22}\text{Ne}/^{21}\text{Ne}$  has been applied as an indicator for irradiation hardness. The results of our measurements allow to investigate the shielding dependence of the radionuclides mentioned above.

As an example the correlation between  $^{10}\text{Be}$  production rates (normalized to H-group chemistry according to Moniot et al. [4]) and the shielding parameter  $^{22}\text{Ne}/^{21}\text{Ne}$  is given in figure 1, showing that the  $^{10}\text{Be}$  production rates slightly depend on sample depth and/or meteorite size. It should be mentioned, that recent results on documented samples of the Knyahinya chondrite exhibit a clear correlation between  $^{10}\text{Be}$  production and irradiation hardness [5]. In the corresponding plot for  $^{26}\text{Al}$  no trend can be detected.  $^{53}\text{Mn}/^{26}\text{Al}$  systematics [1] indicate the possibility of considerable terrestrial ages for some of the meteorites. Even taking corrections for terrestrial residence times into account the data show no distinct relationship. The correlation line  $^{53}\text{Mn}$  vs.  $^{22}\text{Ne}/^{21}\text{Ne}$  falls close to the ones derived from core samples of the St. Severin and Keyes chondrites [6,7]. Plots of  $^{26}\text{Al}$  vs.  $^{10}\text{Be}$  and  $^{53}\text{Mn}$  vs.  $^{10}\text{Be}$  do not

## STUDIES ON COSMOGENIC NUCLIDES

Sarafin R. et al.

Fig. 1: Shielding dependence of the normalized  $^{10}\text{Be}$  production rates [3, updated].



reveal strong dependences between the respective production rates. More analyses, especially on meteorite falls, will be necessary to ensure these results. In addition, it is essential to investigate samples from documented locations to confirm the theoretical production profiles. The absence of correlations discussed might be a hint, that there is an opportunity to distinguish between size and depth effects by measuring various spallation nuclides.

## Acknowledgements

The Cologne part of this work was supported by the Bundesministerium für Forschung und Technologie, the Zürich part by the Swiss National Science Foundation, grants No. 2.263-0.81 and 2.443-0.82.

## References

- [1] U.Herpers and P.Englert (1983) Proc. Lunar Planet. Sci. Conf. 14th, in J. Geophys. Res. 88, B312 - B 318 and references cited therein.
- [2] P.Englert et al. (1981) Proc. Lunar Planet. Sci. 12 B, 1209 - 1215.
- [3] R.Sarafin et al. (1984) Nucl. Instr. and Meth. (in press).
- [4] R.K.Moniot et al. (1983) Geochim. Cosmochim. Acta 47, 1887 - 1895.
- [5] R.Wieler et al. (1984) this volume.
- [6] P.Englert and W.Herr (1980) Earth Planet. Sci. Lett. 47, 361 - 369.
- [7] P.Englert (1984) Lunar Planet. Sci. XV, 248 - 249.

THE PRODUCTION RATE OF COSMOGENIC 21-NE IN CHONDRITES DEDUCED FROM 81-KR MEASUREMENTS: L. Schultz and M. Freundel, Max-Planck-Institut für Chem. D-6500 Mainz, W. Germany.

Cosmogenic 21-Ne is used widely to calculate exposure ages of stone meteorites. In order to do so, the production rate  $P(21)$  must be known. This rate, however, is dependent on the chemical composition of the meteorite as well as the mass of, and position within, the meteoroid during its exposure to the cosmic radiation. Even for a mean shielding the production rates determined from measurements of different radionuclides vary by a factor of two (e.g. [1]).

A method that can be used to determine exposure ages of meteorites that avoids shielding and chemical composition corrections is the 81-Kr-Kr-method [2,3]. However, for chondrites, in many cases, the direct determination of production rates for the Kr isotopes are prevented by the trapped gases and the neutron effects on bromine. Therefore, we have applied this method to four eucrite falls and then compared their 81-Kr-83-Kr-ages to their cosmogenic 21-Ne and 38-Ar concentrations.

The eucrites - Bouvante-le-Haut, Juvinas, Sioux County, and Stannern - were chosen for these measurements because their similar chemical composition regarding the major elements. The mean concentrations (in wt%) are: Mg-(4.1 ± .1); Al-(6.7 ± .5); Si-(22.8 ± .3); Ca-(7.52 ± .12); Fe+Ni (14.3 ± .3).

The Kr-exposure ages of the four eucrites are calculated from the measured isotopic composition of Kr. It is assumed that the trapped component has atmospheric isotopic composition and that the cosmogenic 83-Kr/86-Kr=0.015. Tab. 1 contains the 81-Kr exposure ages together with the cosmogenic 38-Ar concentrations. For all samples the correction for trapped 38-Ar is less than 1%. Fig. 1 shows the correlation between cosmogenic 38-Ar and 81-Kr exposure age of the four eucrites measured.

The production rate of 38-Ar in eucrites -  $P(38)_E$  - is given by the slope of the line in Fig. 1. Considering the errors in both coordinates [4], this slope is calculated to be

$$P(38)_E = (0.139 \pm 0.005)10^{-8} \text{ccSTP/gMa}$$

This production rate is about 2% lower than recently published by us [5] due to the additional measurement of Stannern B. Both numbers agree within the uncertainties.

The given production rate  $P(38)_E$  is a value which pertains to the mean shielding of the five samples. In the following it is assumed that this shielding is equivalent to the mean shielding of ordinary chondrites characterized by 22-Ne/21-Ne = 1.11. Using  $P(38)_E$  and the measured 38-Ar/21-Ne - ratios the production rate  $P(21)_E$  can be calculated. For the four investigated eucrites a mean value 38-Ar/21-Ne = 0.752 ± .041 is received. The resulting production rate is

$$P(21)_E = (0.185 \pm 0.013)10^{-8} \text{ccSTP/gMa.}$$

With the mean chemical concentration of Mg, Al, Si, S, Ca, Fe and Ni of eucrites and the following production rate ratios  $P(21)_{\text{Mg}}/P(21)_{\text{Si}} = 5.15 \pm .3$ ;  $P(21)_{\text{Mg}}/P(21)_{\text{S}} = 7.5 \pm 1.0$ ;  $P(21)_{\text{Al}}/P(21)_{\text{Si}} = 1.9 \pm .6$ ;

$P(21)^{Ca}/P(21)^{Mg} = 0.04 \pm 0.04$ ; and  $P(21)^{Fe,Ni} = (0.021 \pm 0.04)10^{-8} \text{ccSTP/gMa}$  an elemental production rate equation (in  $10^{-8} \text{ccSTP/gMa}$ ) is given by

$$P(21) = 1.63[Mg] + 0.6[Al] + 0.32[Si] + 0.22[S] + 0.07[Ca] + 0.021[Fe,Ni]$$

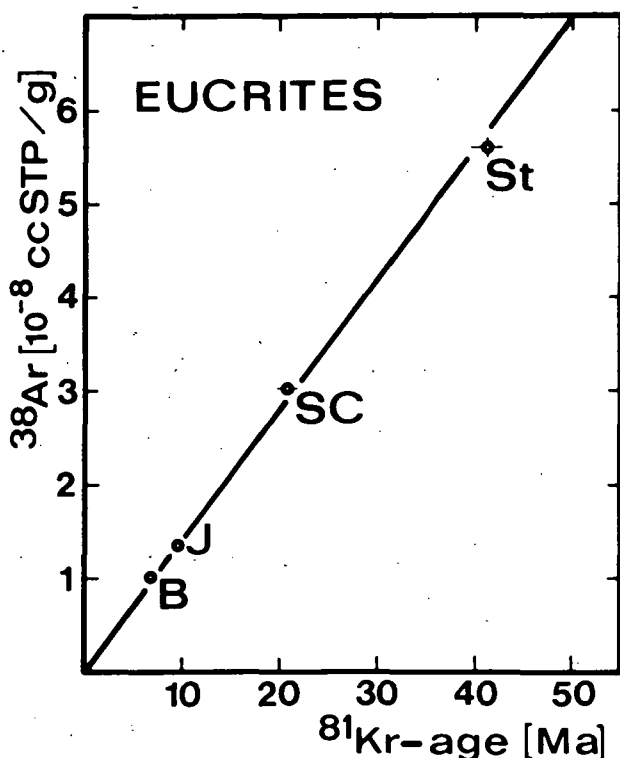
$\pm 0.18 \quad \pm 0.2 \quad \pm 0.04 \quad \pm 0.04 \quad \pm 0.07 \quad \pm 0.004$

([X] = concentration of element X as weight fraction).

From this equation a mean  $P(21)_L$  is calculated for L-group chondrites using the chemical composition of the respective group [6]:

$$P(21)_L = (0.32 \pm 0.04)10^{-8} \text{ccSTP/gMa}$$

For H-group chondrites the production rate is 6% lower.



The major contribution to the production of 21-Ne in ordinary chondrites comes from Mg (about 76%) and Si (about 18%). The large uncertainties connected with the production rate ratios of the other elements are of less importance for  $P(21)_L$ .

The given value for  $P(21)_L$  is within the limits of error in the range of recently determined production rates using other cosmogenic radionuclides [1,7,8] but 26-Al. This isotope tends to yield higher production rates for 21-Ne. This discrepancy may be caused by variations in the cosmic ray flux e.g. [1]. Also inadequate corrections for shielding and chemical composition variations cannot be ruled out [8].

Fig.1: Correlation of cosmogenic 38-Ar and the 81-Kr-exposure age of four eucrites. From the slope of the correlation line the production rate of 38-Ar is calculated.

Meteorite	38-Ar ( $10^{-8} \text{cc/g}$ )	81-Kr-age (Ma)
Bouvante	1.01 $\pm$ 0.05	6.71 $\pm$ 0.37
Juvinas	1.35 $\pm$ 0.05	9.55 $\pm$ 0.63
Sioux County	3.03 $\pm$ 0.10	20.55 $\pm$ 0.88
Stannern A	5.60 $\pm$ 0.19	41.1 $\pm$ 1.3 42.0 $\pm$ 2.1
Stannern B	5.50 $\pm$ 0.15	41.8 $\pm$ 1.9

Tab. 1: Cosmogenic 38-Ar and 81-Kr-83-Kr-exposure ages of 4 eucrite falls.

#### References:

- [1] Nishiizumi K. et al. (1980) Earth Planet. Sci. Lett. 50, 156. [2] Marti K. (1967) Phys. Rev. Lett. 18, 264.  
 [3] Eugster O. et al. (1967) Earth Planet. Sci. Lett. 2, 77. [4] Williamson (1968) Can. J. Phys. 46, 1845.  
 [5] Freundel M. et al. (1983) Meteoritics 18, 300. [6] Mason B. (1979) U.S. Geol. Survey Prof. Paper 440-B-1.  
 [7] Müller et al. (1981) Geochim. Cosmochim. Acta 45, 447. [8] Moniot et al. (1983) GCA 47, 1887.

A direct time series comparison between the La Jolla  
and Belfast radiocarbon records.

C.P. Sonett, Dept. of Planetary Sciences and Lunar and Planetary Laboratory, University of Arizona, Tucson, AZ 85721, and H.E. Suess, Dept. of Chemistry, University of California at San Diego, La Jolla, CA 92093.

For many years it has been widely assumed that the variations in the level of atmospheric carbon-14 were due to statistical fluctuations arising from experimental error. This is understandable since the signal/noise ratio is very low and the time sequences representing the variations are strongly stochastic. Interlaboratory comparisons show that baseline variations in the absolute value of the carbon-14 concentration do exist. However, assuming linearity, the  $\Delta^{14}\text{C}$  values are independent of these. The importance of assessing the quantitative reality of the  $\Delta^{14}\text{C}$  values is based upon their expression of the interplanetary cosmic ray source function, because in the range of 100-1000 year periods, there appears to be no evidence that the Earth's magnetic field is the source modulating function. Therefore the modulation is either due to changes in the solar atmosphere propagated out into the solar wind, or extra-heliospheric pressure effects, but these appear to be unlikely for the periods noted here. Periods in the range of 100-1000 years are so far entirely unexplained by solar physics (cf. Boyer) but are broadly consistent with the sunspot index and the sparse data on long term variations of the solar radius, e.g. Gilliland [1981]. The recent availability of the new high quality Belfast time sequence of  $\Delta^{14}\text{C}$  now permits a simple mutual assessment of the several sequences which are available. Since the La Jolla record has been a standard for many years (and also subject to criticism), we chose these two for a simple comparison. The basic "lumped" statistics are as follows:

TABLE 1.

	La Jolla <sup>†</sup>	Belfast
Time interval	3985BC-1832AD	3982BC-1840AD
No. data pts.	502	282
$\Delta^{14}\text{C}$ minimum	-32	-28
Maximum	88	86
Mean	15.1	13.1
St. dev.	30.0	29.4
3rd moment	0.6	0.7
4th moment	-0.8	-0.6

<sup>†</sup>La Jolla data truncated to approximately match Belfast sequence length. Fourth moment (kurtosis) is referenced to the value of three for a normal distribution. The negative value signifies lesser peakedness than normal. All statistics are based on per mil. It is clear from Table 1 that the two sequences are in close accord, that the internal spread (sigmas) are very similar, that only a small baseline (mean) difference exists, and that both sequences closely follow a symmetrical normal distribution.

Although Table 1. gives a statistical summary, it contains no information linking data points, e.g. autocorrelations. Some of these have recently been reported on [Sonett, 1984], and the reader is referred to these for details.

Here we make the simplest of comparisons, but because of the simplicity, it is especially direct and straightforward. The two sequences are first truncated to the same interval. No corrections for the large scale trend is made, nor is the data splined and interpolated. Thus both sequences are pristine. We have, however filtered them with a low pass Martin filter set to reduce the bandwidth by about a factor of ten at the 3 db point (Fig. 1 insert). The uncertainty arises from the definition of filtering of a series of unequally spaced points for which a Nyquist period cannot be exactly defined.

Although close similarities are apparent in the unfiltered data, the periods in the range of 100-1000 years are of most interest and least corrupted by the unequal spacing. The filter operation removes these higher frequencies and brings out the obvious longer period correlations. Fig 1. shows the two sequences superimposed on a common time scale. Although differences exist, the close agreement between these two sequences, one determined over a period of years beginning about 1955 and carried out on White mountain Bristlecone pines, and the other done later in Belfast using Irish peat bog wood, is striking. Fig. 1 confirms the validity of the two dendrochronologically established annual tree ring sequences and shows that, as expected on geochemical grounds, a close global relation exists, and that these two laboratories have obtained data in which the similarities outweigh differences. This correlation between the two strongly reinforces the statistical view that the  $\Delta^{14}\text{C}$  record is that of real interplanetary modulation of the cosmic ray source leading to the generation of atmospheric  $^{14}\text{C}$ .

This work was supported by NSF grant ATM 8308378 from the terrestrial and climate programs.

REFERENCES: Gilliland, R.L., *Ap. J.*, **284**, 1144 (1981); Boyer, D., Ph.D. Thesis, University of Arizona (1983); Martin, M.A., *IEEE Trans. on Space Electronics and Telemetry*, **5**, 33 (1959); Pearson, G.W., Doctoral Dissertation, Queen's University of Belfast (1983); Sonett, C.P., *Reviews of Geophys. & Spa. Phys.*, (in press); Suess, H.E., *Radiocarbon* **22(2)**, 200-209, (1980); see also Damon, P.E., Lerman, J.C., Long, A., Bannisher, B., Klein, J., and Linnick, T.W., *ibid* **22(3)** 947-949 (1980).

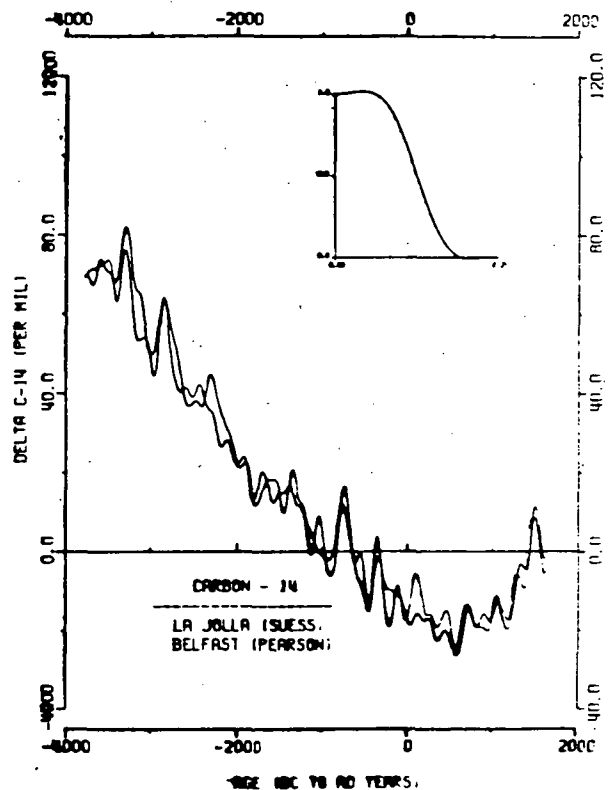


Fig. 1. La Jolla (heavy line) vs. Belfast  $\Delta^{14}\text{C}$  for the interval 3980 BC - 1840 AD. Data is unsplined and long period "sine wave" is not removed.

NEUTRON CAPTURE PRODUCTION RATES OF COSMOGENIC  $^{60}\text{Co}$ ,  $^{59}\text{Ni}$  AND  $^{36}\text{Cl}$  IN STONY METEORITES; M. S. Spergel, York College of CUNY, Jamaica, New York, 11451, USA; R. C. Reedy, Los Alamos National Laboratory, Los Alamos, New Mexico, 87545, USA; O. W. Lazareth and P. W. Levy, Brookhaven National Laboratory, Upton, New York 11973 USA

To unfold the cosmic-ray exposure history of a meteorite, it is best to use a variety of cosmogenic products (tracks and nuclides) with different production profiles. Neutron-capture reactions have production rates which vary considerably with sample depth and meteorite size<sup>1</sup>. Their production profiles differ appreciably from those for tracks or nuclides created by energetic cosmic ray particle spallation reactions. In large meteorites neutron-capture reactions are the main sources of cosmic-ray produced nuclides such as  $^{59}\text{Ni}$  and  $^{60}\text{Co}$ .<sup>1</sup> The cosmogenic radionuclide  $^{60}\text{Co}$ , from the  $^{59}\text{Co}(n,\gamma)^{60}\text{Co}$  reaction, has been a very useful tool for unfolding the cosmic-ray exposure record of the large Jilin (Kirin) chondrite<sup>2,3</sup>.

The neutron-capture reaction rates producing  $^{36}\text{Cl}$ ,  $^{59}\text{Ni}$ , and  $^{60}\text{Co}$  in meteorites were calculated by Eberhardt, et al.<sup>1</sup> using neutron slowing-down theory. Lingenfelter et al.<sup>4</sup> used neutron-transport theory to calculate the low-energy neutron flux and neutron-capture induced isotopic anomalies in the moon. Previously we reported neutron-transport theory calculation of the low-energy neutron, as a function of depth, in spherical meteoroids<sup>5</sup> and preliminary results for  $^{59}\text{Ni}$  and  $^{60}\text{Co}$  production rates.<sup>6-7</sup> Reported here are complete results for neutron flux calculations in stony meteoroids, of various radii and compositions, and production rates for  $^{36}\text{Cl}$ ,  $^{59}\text{Ni}$ , and  $^{60}\text{Co}$ .

New neutron source strengths have been calculated that increase our calculated production rates by about 30% in larger meteorites.<sup>11</sup> The  $^{59}\text{Ni}/^{60}\text{Co}$  production ratio in spherical L-chondrites with radii  $>150\text{ g/cm}^2$  is usually within agreement with measurements on various large meteorites; but higher than the ratio as calculated by Eberhardt, et al.<sup>1</sup> Neutron-capture calculations for a C3-chondrite with 100-ppm hydrogen and for an aubrite ( $\approx 1\%$  Fe) provide neutron-capture systematics that differ considerably from those obtained with L-chondrites. Measured neutron-capture radionuclides in the Allende meteorite agree better with calculation for a dry chondrite than for one with 100-ppm H; indicating that Allende had a low H content. Our lunar calculations agree with the calculation of Lingenfelter et al.<sup>4</sup>, Kornblum et al.<sup>9</sup>, and with the lunar neutron measurements.<sup>8</sup> Both the absolute values and the activity-versus-depth profiles calculated for  $^{60}\text{Co}$  formation in the Moon agree with the measurements of Wahlen et al.<sup>10</sup> For large spheres the calculated results converge to those obtained for the Moon, but there are significant differences between the lunar results and those predicted for a meteorite with a radius of  $1000\text{ g/cm}^2$ . The calculated neutron fluxes and nuclide production rates for small spheres are quite different from those for large meteorites.

The  $^{59}\text{Ni}/^{60}\text{Co}$  ratio is nearly constant with depth in most meteorites: this effect is consistent with the neutron flux and capture cross

NEUTRON CAPTURE PRODUCTION RATES

Spergel, M. S., Reedy, R. C., Lazareth, O. W. and Levy, P. W.

section properties. The shape of the neutron flux energy spectrum, varies little with depth in a meteorite. The size of the parent meteorite can be determined from one of its fragments, using the  $^{59}\text{Ni}/^{60}\text{Co}$  ratios, if the parent meteorite was less than  $75 \text{ g/cm}^2$  in radius. If the parent meteorite was larger, a lower limit on the size of the parent meteorite can be determined from a fragment. In C3 chondrites this is not possible.

In stony meteorites with  $R < 50 \text{ g/cm}^2$  the calculated  $^{60}\text{Co}$  production rates (mass  $< 4 \text{ kg}$ ), are below 1 atom/min g-Co. The highest  $^{60}\text{Co}$  production rates occur in stony meteorites with radius about  $250 \text{ g/cm}^2$  (1.4 m across). In meteorites with radii greater than  $400 \text{ g/cm}^2$  the maximum  $^{60}\text{Co}$  production rate occurs at a depth of about  $175 \text{ g/cm}^2$  in L-chondrite,  $125 \text{ g/cm}^2$  in C3 chondrite, and  $190 \text{ g/cm}^2$  in aubrites. Production results for  $^{60}\text{Co}$  and  $^{59}\text{Ni}$  in meteorites of radius  $300 \text{ g/cm}^2$  ( $\approx 86 \text{ cm}$ ) are shown in Fig. 1 and Fig. 2 respectively. The figures contain results for L Chondrite and C3 type meteorites.

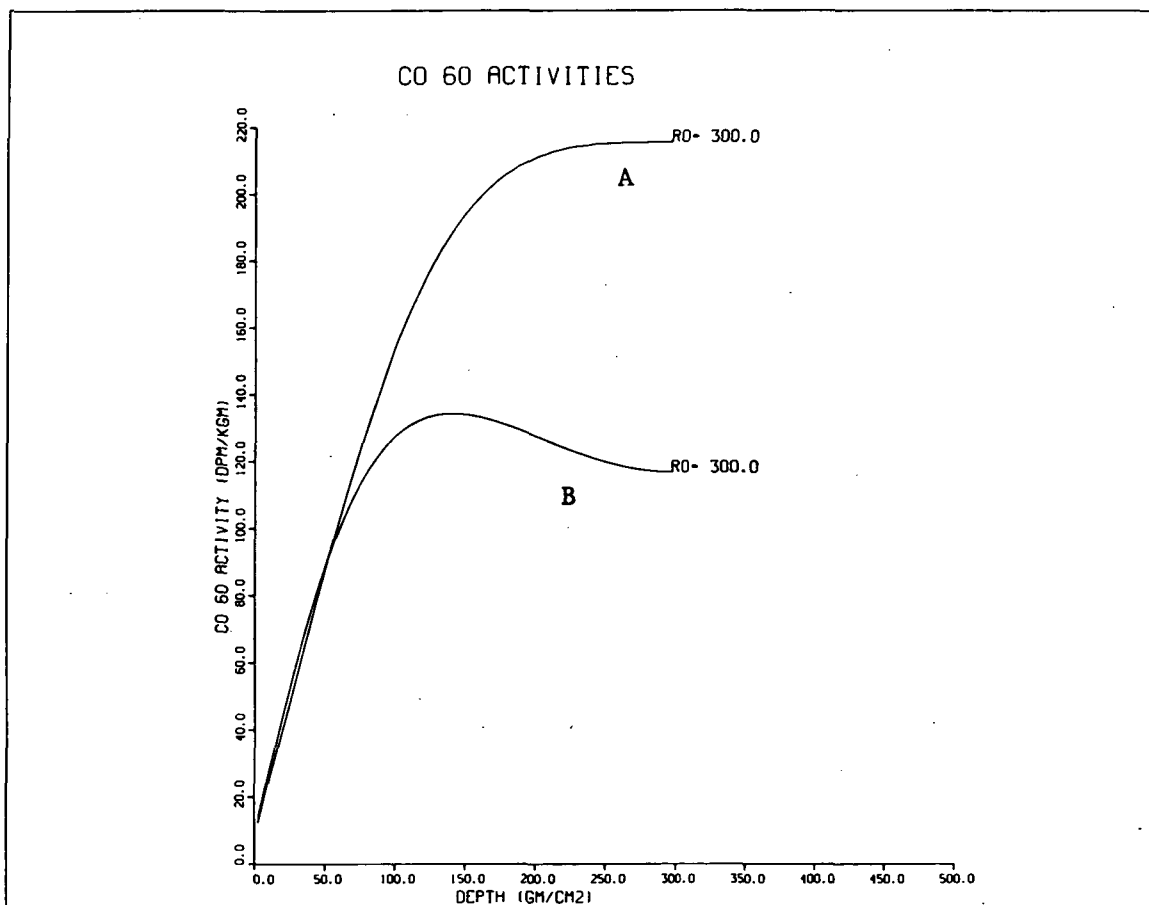


FIG. 1.  $^{60}\text{Co}$  production (DPM/Kg) curves in a L Chondrite (A) and a C3 (B). Peak activity occurs closer to the surface in the C3 Chondrite. Cobalt activity levels are effected by the different hydrogen abundances in the meteorites.

## NEUTRON CAPTURE PRODUCTION RATES

Spergel, M. S., Reedy, R. C., Lazareth, O. W. and Levy, P. W.

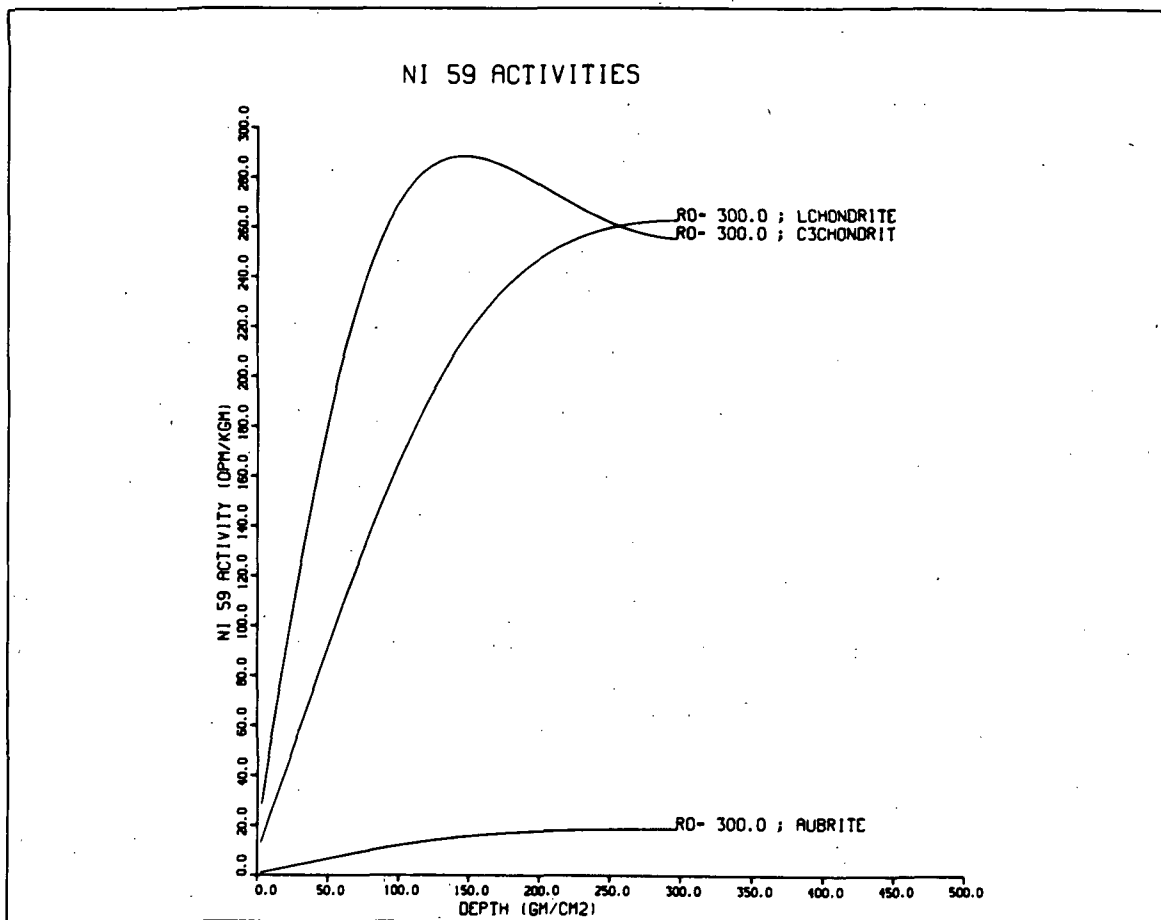


FIG. 2.  $^{59}\text{Ni}$  production (DPM/Kg) curves in L Chondrite, C3 Chondrite and Aubrite type meteorites. Peak activity occurs closest to the surface with the C3 Chondrite.

1. Eberhardt, P., Geiss, T., and Lutz, M. (1963) Neutrons in meteorites, Earth Sci. and Meteoritics, North Holland, Amsterdam, p. 143-168.
2. Honda, M., Nishiizumi, K., Imamura, T., Takaoka, N., Nitoh, O., Horie, K., and Komura, K. (1982) Earth Planet. Sci. Lett. 57, p. 101-109.
3. Heusser, G. and Ouyang, Z. (1981) Meteoritics 16, p. 326-327.
4. Lingenfelter, R. E., Canfield, E. H., and Hempel, V. E. (1972) Earth Planet. Sci. Lett. 16, p. 355-369.
5. Spergel, M. S., Reedy, R. C., Lazareth, O. W., and Levy, P. W. (1980) Meteoritics, 15, p. 370.
6. Spergel, M. S., Reedy, R. C., Lazareth, O. W., and Levy, P. W. (1981) Meteoritics 16, p. 387-388.
7. Spergel, M. S., Reedy, R. C., Lazareth, O. W., and Levy, P. W. (1982) Lunar and Planetary Science XIII, p. 756-757.
8. Woolum, D. S., Burnett, D. S., Furst, M., and Weiss, J. R. (1975) The Moon 12, p. 231-250.
9. Kornblum, J. J., Fireman, E. L., Levin, M., and Aronson, A. (1973) Proc. Lunar Sci. Conf. 4th, p. 2171-2182.
10. Wahlen, M., Finkel, R. C., Imamura, M., Kohl, C. P., and Arnold, J. R. (1973) Earth Planet. Sci. Lett. 19, p. 315-320.

SIMULATION OF COSMIC IRRADIATION CONDITIONS IN THICK TARGET ARRANGEMENTS

S.Theis, P.Englert, Institut für Kernchemie der Universität zu Köln, Zülpicher Str. 47, D-5000 Köln-1, W.-Germany; R.C.Reedy, INC-11, Los Alamos, National Laboratory, Los Alamos, NM 87545, USA; J.R.Arnold, University of California, San Diego, Department of Chemistry, La Jolla, Ca 92093, USA.

Interpreting abundances of cosmogenic nuclides in meteorites, planetary atmospheres and surfaces in terms of exposure history, shielding parameters and cosmic ray flux requires knowledge of the nuclear reactions that produce them in the object or environment considered.

Bombardment experiments with thin and thick targets with energetic charged particles or particle fields have been performed in order to gain a pool of production data (production rates, ratios, cross sections) for cosmogenic nuclides [1,2,3], of which the stable and the long-lived radioactive species are of special interest as they have been measured in many extraterrestrial samples and are used in evaluating the exposure ages and histories of these bodies [4,5]. In order to correlate the simulation experiments with the systematics of spallogenic nuclide production during exposure to the galactic cosmic radiation, it is necessary to determine long-lived radionuclides as well as stable isotopes in targets from such experiments.

An important point in thick target experiments is to transform the available beam geometry to the isotropic irradiation conditions in space. This can be done by mathematical transformations of the data obtained from static thick targets exposed to focussed monoenergetic beams [6], by defocussing the beam and moving the target in the beam line during the irradiation [7] or by using secondary particle fields for the irradiation as they occur in the interior of extraterrestrial objects [8].

nuclide	T <sub>1/2</sub>	decay mode	carrier amount[mg]	chemical yield[%]	detection method
Be-7	53.29 d	ε	1-2	80-90	G, E <sub>γ</sub> = 478 keV
Be-10	1.6x10 <sup>6</sup> a	β <sup>-</sup>	1-2	80-90	AMS
Na-22	2.607 a	β <sup>+</sup>	0.05-0.1	99.99	G, E <sub>γ</sub> = 1275 keV
Al-26	7.16x10 <sup>6</sup> a	β <sup>+</sup>	~2	60-95	GGC, AMS
Ti-44	47.3 a	ε	~4	90-95	G, GGC (via Sc-44)
Mn-54	312.2 d	ε	~3	80-85	G, E <sub>γ</sub> = 835 keV
Co-56	78.76 d	ε, β <sup>+</sup>	instrumental		G, E <sub>γ</sub> = 847, 1238 KeV
Co-57	271.3 d	ε	instrumental		G, E <sub>γ</sub> = 122, 136 keV
Co-58	70,78 d	ε	instrumental		G, E <sub>γ</sub> = 811 keV
Co-60	5.272 a	β <sup>-</sup>	instrumental		G, E <sub>γ</sub> = 1173, 1332 keV

Table 1: Nuclear properties of radionuclides determined in this study. In columns 4 and 5 carrier amounts and chemical yields of the applied separation procedures are listed. The determination methods in column 6 are: G: high resolution (low-level) γ-spectroscopy, GGC: γ-γ-coincidence spectroscopy, AMS: accelerator mass spectroscopy.

## SIMULATION OF COSMIC IRRADIATION

Theis, S. et al.

This study is dedicated to the analysis of long-lived cosmogenic radionuclides produced in pure elemental targets during various simulation experiments by using pure instrumental as well as radiochemical methods (see table 1). The nature of the chemical purification procedures depend on the isotope to be separated, the target material, the interfering isotopes present, and the detection method. Some examples of the applied separation schemes have been published previously [8,9]. In all experiments short-lived isotopes were determined prior to chemistry in most of the target elements by high resolution  $\gamma$ -spectroscopy.

A first set of production data was obtained from a high energy neutron ( $E_n \leq 800$  MeV) irradiation at several positions under the LAMPF beam stop (Los Alamos Meson Physics Facility) and is given in table 2. The beam stop environment produces secondary particle and especially neutron fields, which resemble those in planetary surfaces (depth  $>180$  g/cm<sup>2</sup>) exposed to the GCA [8]. The samples were exposed in three positions with different absolute neutron fluxes and spectral hardness [9].

The nuclide Ti-44 ( $T_{1/2} = 47,3$  a) was measured in Ti-targets where it is produced via (n,xn) reactions from all stable Ti isotopes (Ti-46,47,48,49,50). The main target isotope, however, is Ti-48 (73.8 %), which contributes via a (n,5n) reaction to the Ti-44 activity. Compared to the (n,4n) product Co-56 from the monoisotopic Co-59 the Ti-44 production rates are one order of magnitude lower for the respective irradiation positions.

Ti-44 could be of special interest in lunar surface samples. It is produced by SCR reactions in the upper layers and - because of its half-life - able to monitor the mean solar activity for at least 4-5 eleven-year solar

product	sample location			ref.
	2001	2005	2006	
	[accum. atoms g <sup>-1</sup> ]			
Al-26(Al)	1.3x10 <sup>14</sup>	6.4x10 <sup>13</sup>	4.1x10 <sup>13</sup>	[9]
Na-22(Al)	3.2x10 <sup>13</sup>	1.7x10 <sup>13</sup>	8.8x10 <sup>12</sup>	[9]
Be- 7(Al)	1.2x10 <sup>12</sup>	6.7x10 <sup>11</sup>	3.8x10 <sup>11</sup>	[9]
Co-60(Co)	4.4x10 <sup>15</sup>	1.7x10 <sup>16</sup>	2.1x10 <sup>16</sup>	
Co-58(Co)	3.0x10 <sup>14</sup>	1.8x10 <sup>14</sup>	1.0x10 <sup>14</sup>	
Co-57(Co)	1.0x10 <sup>14</sup>	5.7x10 <sup>13</sup>	3.9x10 <sup>12</sup>	
Co-56(Co)	1.6x10 <sup>13</sup>	8.3x10 <sup>12</sup>	---	
Ti-44(Ti)	1.6x10 <sup>12</sup>	1.2x10 <sup>12</sup>	5.2x10 <sup>11</sup>	
Na-22(Ti)	---	1.2x10 <sup>11</sup>	4.9x10 <sup>10</sup>	
Be- 7(Ti)	---	1.8x10 <sup>11</sup>	5.5x10 <sup>10</sup>	
Be- 7(Fe)	2.0x10 <sup>11</sup>	1.4x10 <sup>11</sup>	---	[9]
Na-22(Ni)	2.6x10 <sup>10</sup>	1.8x10 <sup>10</sup>	6.5x10 <sup>9</sup>	[9]

**Table 2:** Production of low and high energy products in various targets (target elements in brackets) in different irradiation positions under the LAMPF beam stop. For comparison selected results of instrumentally determined Co-isotopes are given.

cycles. As demonstrated, another very important source of Ti-44 in lunar samples are reactions of high energy secondary neutrons with Ti, which has an abundance of several % in the moon [10]. These reactions can occur in greater depths, where the lunar secondary particle cascade is well developed. Here spallation production in iron is of less significance.

Another approach to simulate 2- $\pi$  irradiation conditions of planetary surfaces which has been widely applied in the past are bombardments of so called thick targets [11]. A very large thick target was exposed recently to

## SIMULATION OF COSMIC IRRADIATION

Theis, S. et al.

2.1 GeV protons at the Bevatron-Bevalac in Berkeley [12]. In a 100x100x180 cm steel surrounded granodiorite target radioactive medium and high energy spallation products of the incident primary and of secondary particles were analyzed along the beam axis down to depths of 140 g/cm<sup>2</sup> in targets such as Cu, Ni, Co, Fe, Ti, Si, SiO<sub>2</sub> and Al. Activities of these nuclides were exclusively determined via instrumental  $\gamma$ -ray spectroscopy. Figure 1 shows relative yields of neutron capture and spallation products induced in Co and Cu targets during the thick target bombardment as a function of depth. The majority of the medium energy products such as Co-58 from Co targets exhibit a maximum at shallow depths of 40-60 g/cm<sup>2</sup> and then decrease exponentially.

In a comparable 600 MeV proton bombarded thick target such a slight maximum for medium energy products was not observed [13]. Rather, Co-58 activities in Co decreased steadily with the highest activity at the surface.

The activities of the n-capture product Co-60 increase steadily starting at the surface. This indicates the rapidly growing flux of low energy neutrons ( $E_n \leq 1$  keV) within the target. The maximum of the low energy neutron distribution lies between 130 and 170 g/cm<sup>2</sup> [12], which is significantly deeper than in the 600 MeV proton bombarded artificial lunar regolith [3]. Be-7 activities representing high energy spallation in Co decrease, as expected, exponentially with depth.

The comparison of the two experiments shows that both, experimental arrangement and incident particle energy have a significant influence of the results obtained. To gain more insight in the development of secondary particle fluxes within planetary surfaces which are exposed to an energetically diverse particle field, results of both simulation experiments will be discussed in detail.

References: [1] e.g. R.Michel et al., 1978, *J.Inorg.Nucl.Chem.* **40**, 1845; [2] R.C.Reedy et al., 1979, *Earth Planet. Sci.Lett.* **44**, 341; [3] R.Michel et al., 1974, *Radiochim.Acta* **21**, 169; [4] P.Englert et al., 1978, *Geochim.Cosmochim.Acta* **42**, 1635; [5] S.Regnier et al., 1983, *Meteoritics* **18**, 384; [6] M.Honda, 1962, *J.Geophys.Res.* **67**, 4847; [7] R.Michel et al., 1984, *Lun.Planet.Sci. Conf. XV*, 542; [8] P.Englert et al., 1983, *Lun.Planet.Sci. Conf. XIV*, 175; [9] S.Theis et al., 1984, *Lun.Planet. Sci.Conf. XV*, 855; [10] R.W.Perkins et al., 1970, *Proc.Apollo 11 Lun.Sci.Conf.*, 1455; [11] T.B.Kohmann et al., 1967, In: *High Energy Nuclear Reactions in Astrophysics*, Benjamin, New York, 169; [12] P.Englert et al., 1983, *Meteoritics* **18**, 294; [13] H.Weigel et al., 1974, *Radiochim.Acta* **21**, 179.

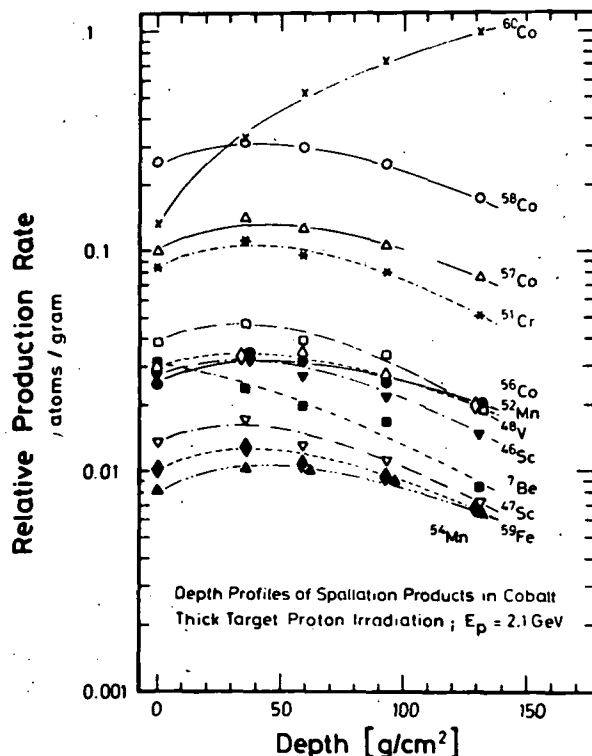


Figure 1

**COSMOGENIC RARE GASES AND 10-BE IN A CROSS SECTION OF KNYAHINYA.** R. Wieler, P. Signer, ETH Zürich, NO C61, 8092 Zürich, Switzerland; U. Herpers, R. Sarafin, Univ. Köln, Zülpicherstr.47, 5000 Köln, FRG; G. Bonani, H. J. Hofmann, E. Morenzoni, M. Nessi, M. Suter, W. Wölfli, ETH Zürich, HPK, 8093 Zürich, Switzerland.

We initiated a study of the concentrations of cosmogenic nuclides as a function of shielding on samples from a cross section of the 293 kg main fragment of the L5 chondrite Knyahinya. The stone broke into two nearly symmetrical parts upon its fall in 1866. The planar cross section has diameters between 40 and 55 cm. We measured He, Ne, and Ar on about 20 samples by mass spectrometry and determined the 10-Be activities on aliquots of 10 selected samples by AMS.

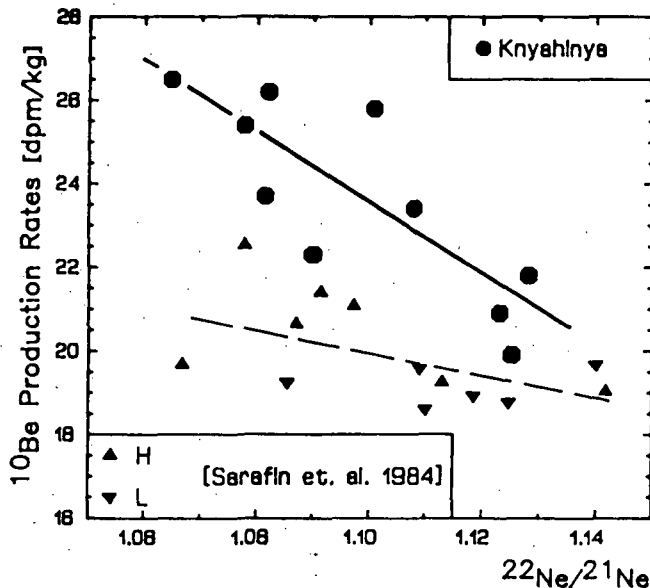
The noble gas data are presented in (1). Here we show the 10-Be data and compare the abundances of spallogenic nuclides with the model calculations reported by Reedy (2) for spherical L chondrites. The figure shows the 10-Be production rates in Knyahinya versus the shielding parameter 22-Ne/21-Ne. Typical errors for 10-Be are  $\pm 5\%$ . In addition, production rates we determined on 13 individual chondrites (3) are also shown. Noble gases and 10-Be were measured on aliquots in all cases. The 10-Be production rates for H chondrites were normalized to L chondrite chemistry by multiplication with 1.075 (4).

The Knyahinya data are in good agreement with 10-Be determinations on the St. Severin core (5). The slopes of the linear best fits through these two sets of data points are equal within error limits. The 21-Ne/10-Be ratios in Knyahinya are constant within error limits over the whole section, indicating a comparable shielding dependence of the 21-Ne and the 10-Be production rates in this meteorite. In the individual chondrites, the 10-Be production rate appears to depend less on shielding than in Knyahinya. This is similar to the observed variations in a 3-He/21-Ne vs. 22-Ne/21-Ne diagram, where data from the meteorites Keyes and St. Severin do not coincide with the "Bern line" obtained on individual chondrite samples (cf. 1).

The observed noble gas profiles are in fair agreement with Reedy's model predictions for a spherical meteoroid of about 150 g/cm<sup>2</sup> (2), if we assume the area of maximum shielding observed in the cross section to correspond to the center of mass of the meteoroid. The postatmospheric surface closest to the meteoroid surface seems to have suffered an ablation of about 20 g/cm<sup>2</sup>. 10-Be activities in Knyahinya are up to about 25% higher than the largest values to be found according to the calculations in L chondrites of 150 g/cm<sup>2</sup> preatmospheric radius.

Refs: 1) Wieler R. et al., 1984, Meteoritics 19, 4; to be publ. 2) Reedy R. C., 1984, Proc. Lun. Planet. Sci. Conf. 15th; to be publ. 3) Sarafin R. et al., 1984, Proc. Symp. AMS' 84, Nucl. Inst. & Methods. 4) Moniot R. K. et al., 1983, Geochim. Cosmochim. Acta 47, 1887. 5) Tuniz, C. et al., 1984, Geochim. Cosmochim. Acta; to be publ.

Work supported by the Swiss National Science Foundation and the Bundesministerium für Forschung und Technologie.



# List of Registered Attendees

- James R. Arnold  
*Department of Chemistry, B-017*  
*University of California, San Diego*  
*La Jolla, CA 92093*
- J. Louis Birck  
*Laboratoire de Geochimie*  
*Institut de Physique du Globe*  
*4 Place Jussieu*  
*F-75230 Paris Cedex 05, France*
- Johannes Brückner  
*Max-Planck-Institut für Chemie*  
*Postfach 3060*  
*D-6500 Mainz, Fed. Rep. Germany*
- Marc Caffee  
*Department of Physics*  
*Box 1105*  
*Washington University*  
*St. Louis, MO 63130*
- Ghislaine Crozaz  
*Department of Earth and Planetary Sciences*  
*Box 1105*  
*Washington University*  
*St. Louis, MO 63130*
- Peter Eberhardt  
*Physikalisches Institut*  
*University of Bern*  
*Sidlerstrasse 5*  
*CH-3012, Bern, Switzerland*
- Peter Englert  
*Institut für Kernchemie*  
*Universität zu Köln*  
*Zùlpicher Str. 47*  
*D-5000 Köln 1, Fed. Rep. Germany*
- Udo Fehn  
*Nuclear Structure Research Laboratory*  
*University of Rochester*  
*Rochester, NY 14627*
- Jitendra N. Goswami  
*Physical Research Laboratory*  
*Navrangpura,*  
*Ahmedabad 380009, India*
- Ulrich Hergers  
*Institut für Kernchemie*  
*Universität zu Köln*  
*Zùlpicher Str.-47*  
*D-5000 Köln 1, Fed. Rep. Germany*
- Gregory F. Herzog  
*Department of Chemistry*  
*Douglass College, Rutgers University*  
*New Brunswick, NJ 08903*
- Gerd Heusser  
*Max-Planck-Institut für Kernphysik*  
*Postfach 103980*  
*D-6900 Heidelberg 1, Fed. Rep. Germany*
- Charles M. Hohenberg  
*Department of Physics*  
*Box 1105*  
*Washington University*  
*St. Louis, MO 63130*
- A. J. Timothy Jull  
*Department of Physics*  
*University of Arizona*  
*Tucson, AZ 85721*
- Brian D. Leavy  
*Mail Stop J978*  
*Los Alamos National Laboratory*  
*Los Alamos, NM 87545*
- Douglas A. Leich  
*L-232*  
*Lawrence Livermore National Laboratory*  
*Livermore, CA 94550*
- Kurt Marti  
*Department of Chemistry, B-017*  
*University of California, San Diego*  
*La Jolla, CA 92093*
- Charles M. Miller  
*Mail Stop J514*  
*Los Alamos National Laboratory*  
*Los Alamos, NM 87545*
- Chandra M. Nautiyal  
*Room 305*  
*Physical Research Laboratory*  
*Ahmedabad 380009, India*
- Kunihiko Nishizumi  
*Department of Chemistry, B-017*  
*University of California, San Diego*  
*La Jolla, CA 92093*
- Laurence E. Nyquist  
*SN4, Experimental Planetology Branch*  
*NASA Johnson Space Center*  
*Houston, TX 77058*
- Keran O'Brien  
*Environmental Measurements Laboratory*  
*U. S. Department of Energy*  
*376 Hudson St.*  
*New York, NY 10014*
- Ulrich Ott  
*Max-Planck-Institut für Chemie*  
*Postfach 3060*  
*D-6500 Mainz, Fed. Rep. Germany*
- Robert O. Pepin  
*School of Physics and Astronomy*  
*University of Minnesota*  
*Minneapolis, MN 55455*
- Fred M. Phillips  
*Department of Geoscience*  
*New Mexico Institute of Mining and Technology*  
*Socorro, NM 87801*

PRECEDING PAGE BLANK NOT FILMED

PRECEDING PAGE BLANK NOT FILMED

Robert C. Reedy  
 Mail Stop J514  
 Los Alamos National Laboratory  
 Los Alamos, NM 87545

Serge Regnier  
 Université de Bordeaux I  
 Chimie Nucléaire, CENBG  
 Le Haut Vigneau  
 F-33170 Gradignan, France

Donald J. Rokop  
 Mail Stop J514  
 Los Alamos National Laboratory  
 Los Alamos, NM 87545

Rolf Sarafin  
 Institut für Kernchemie  
 Universität zu Köln  
 Zulpicher Str. 47  
 D-5000 Köln 1, Fed. Rep. Germany

Ludolf Schultz  
 Max-Planck-Institut für Chemie  
 Postfach 3060  
 D-6500 Mainz, Fed. Rep. Germany

Gabriel Simonoff  
 Université de Bordeaux I  
 Centre d'Etudes Nucléaires  
 de Bordeaux-Gradignan  
 Le Haut Vigneau  
 F-33170 Gradignan, France

Monique Simonoff  
 Université de Bordeaux I  
 Centre d'Etudes Nucléaires  
 de Bordeaux-Gradignan  
 Le Haut Vigneau  
 F-33170 Gradignan, France

Charles P. Sonett  
 Department of Planetary Sciences  
 University of Arizona  
 Tucson, AZ 85721

Martin S. Spergel  
 Department of Natural Sciences  
 York College, C. U. N. Y.  
 Jamaica, NY 11451

Tim Swindle  
 Department of Physics  
 Box 1105  
 Washington University  
 St. Louis, MO 63130

Yuji Tazawa  
 Department of Physics  
 Kyoto University  
 Kitashirakawa, Kyoto 606, Japan

Carol Velsko  
 L-396  
 Lawrence Livermore National Laboratory  
 Livermore, CA 94550

Rainer Wieler  
 Inst. for Crystallography  
 ETH-Zentrum, NOC61  
 Sonneggstr. 5  
 CH-8092 Zurich, Switzerland

Ronald D. Zwickl  
 Mail Stop D438  
 Los Alamos National Laboratory  
 Los Alamos, NM 87545